A bioinorganic investigation of some metal complexes of the Schiff base, *N*,*N*'-bis(3-methoxysalicylaldimine)propan-2-ol

A thesis submitted in fulfillment of the requirements for the degree of

Master of Science

of

Rhodes University

by

Estelle Mopp

February 2010

ABSTRACT

This thesis includes the synthesis, characterisation, antioxidant and antimicrobial activities of Cu(II)-, Co(II)- and Co(III) complexes with *N*,*N*'-bis(3-methoxysalicylaldimine)propan-2-ol, 2-OH-*o*VANPN. The Schiff base ligand, 2-OH-*o*VANPN, is derived from *o*-vanillin and 1,3-diaminopropan-2-ol. The *o*-vanillin condensed with 1,3-diaminopropan-2-ol in a 2:1 molar ratio yields this potential tetra- or pentadentate ligand. The complexes synthesized are tetra (or penta or hexa) coordinated. Formation of the complexes is symbolized as follows:-

MX_2 + 2-OH-*o*VANPN (2:1) → $[M(2\text{-OH-oVANPN})X_n]$ + H_nX

MX_2 + 2-OH-*o*VANPN (2:1) → $[M_n(2\text{-OH-oVANPN})OH] + H_2X_2$

MX_2 + (*o*-vanillin : diaminopropanol) (1:1) → $[M(1:1)X_2]$

MX_2 + (*o*-vanillin : diaminopropanol) (1:1) → $[M_3(1:1)X_4]$

M = Cu(II), Co(II) or Co(III); X = Cl; n = 1, 2. Their structural features have been deduced from their elemental analytical data, IR spectral data, and electronic spectral data. With the exception of $\{Cu_3(C_{11}H_{14}N_2O_3)\ (Cl)_4\ (H_2O)_6\}$**(A4)**, the Cu(II) complexes were monomeric with 2-OH-*o*VANPN acting as a tetradentate ligand. A binuclear Co(II) complex, $[Co_2(C_{19}H_{19}N_2O_5)(OH)]$ **(B1)**, was synthesised and the rest of the Co(II) and Co(III) complexes were monomeric with chloride ions coordinating to the metal centre in some cases. Electronic data suggest that the cobalt(II) complexes have octahedral geometries and the copper(II) complexes have square planar structures – Co(III) is likely to be octahedral.

Thermal analyses, which included the copper-block-method for determining sublimation temperatures, revealed that some copper(II) and cobalt(II) complexes are hygroscopic and sublime at 200 ^oC and below. DSC analyses of the Cu(II) complexes gave exotherms around 300 ^oC for complexes $K[Cu(C_{19}H_{20}N_2O_5)(OH)]\cdot 2H_2O$ **(A1)** and $[Cu(C_{11}H_{15}N_2O_3)(Cl)_2]\cdot 2H_2O$ **(A2)** and above 400 °C for $[Cu(C_{11}H_{16}N_2O_3)(Cl)_2]$ **(A3)** and $\{Cu_3(C_{11}H_{14}N_2O_3)(Cl)_4(H_2O)_6\}$ **(A4)**.

Antioxidant studies were carried out against the 2,2-diphenyl-1-picrylhydrazyl radical (DPPH·). The cobalt(II) complex, $[Co_2(C_{19}H_{19}N_2O_5)(OH)]$ **(B1)**, which was

synthesized in the presence of KOH, had no antioxidant activity, whilst the other cobalt(II) complexes, $[Co(C_{17}H_{17}N_2O_5(Cl))]\cdot 1½H_2O$ **(B2)**, $[Co(C_{19}H_{22}N_2O_5)(Cl)_2]\cdot 5½H_2O$ **(B3)** and $[Co(C_{19}H_{22}N_2O_5)(Cl)_2]\cdot 5½H_2O$ **(B4)**, which were synthesised in the absence of KOH, demonstrated antioxidant activity. The latter complexes are candidates for cancer cell line testing, while $[Cu(C_{11}H_{16}N_2O_3)(Cl)_2]$ **(A3)**, $\{Cu_3(C_{11}H_{14}N_2O_3)(Cl)_4(H_2O)_6\}$ **(A4)**, $[Co(C_{19}H_{21}N_2O_5)(Cl)_2]\cdot 5H_2O$ **(C2)** and $[Co(C_{19}H_{20}N_2O_5)(Cl)]\cdot 3H_2O$ **(C3)** may show anticancer activity through possible hydrolysis products.

Most of the complexes synthesized displayed antimicrobial activity against *Escherichia coli*, *Staphylococcus aureus*, *Pseudomonas aeruginosa*, *Aspergillus niger* and *Candida albicans*. The results indicated that complexes $[Cu(C_{11}H_{16}N_2O_3)(Cl)_2]$ **(A3)**, $[Co(C_{19}H_{22}N_2O_5)(Cl)_2]\cdot 5½H_2O$ **(B3)** and $[Co(C_{19}H_{21}N_2O_5)(Cl)_2]\cdot 5H_2O$ **(C2)** are active against the Gram-negative *Ps. aeruginosa* and that the ligand, 2-OH-*o*VANPN, did not have any activity. The same trend was observed with 2-OH-*o*VANPN, $\{Cu_3(C_{11}H_{14}N_2O_3)(Cl)_4(H_2O)_6\}$ **(A4)** and $[Co(C_{19}H_{20}N_2O_5)(Cl)]\cdot 3H_2O$ **(C3)** against the Gram-positive *S. aureus*. As for activity against *E. coli* and *C. albicans*, some complexes showed more activity than the ligand. There is an observed trend here that the metal complexes are more active (toxic) than the corresponding ligand, which is in agreement with Tweedy's chelation theory.

TABLE OF CONTENTS

LIST OF FIGURES

LIST OF TABLES

GLOSSARY

2-OH-*o*VANPN:	*N*,*N*'-bis(2-hydroxy, 3-methoxybenzylidene)-2-hydroxy-1,3-propanediamine or *N*,*N*′-bis(3-methoxysalicylaldimine)propan-2-ol or 1,3 bis(3-methoxysalicylideneimino)propan-2-ol
2-OHSALPN:	1,3-bis(salicylaldimine)propan-2-ol; 1,3-bis(salicylideneimino)propan-2-ol; *N*,*N*'-bis(2-hydroxybenzylidene)-2-hydroxy-1,3-propanediamine or HSALPN or H_3SalDpl
3MeOSALEN:	bis(3-methoxy salicylaldehyde)ethylenediimine
Acacen:	bis-acetylacetonateethylenediimine
Adaptive response:	Induction of a repair response (e.g. chromosomal repair mechanism) against the challenge (low) doses of mutagenic agent/ conditions (e.g. MNNG, UV light, etc.) to bacterial (or other living) cells. This response will result in increase of cell survival and a decrease of mutagenesis in the dozed cells
Antioxidant:	Any substance that, when present at low concentrations compared to those of an oxidisable substrate, significantly delays or prevents oxidation of that substrate (Fisch et al., 2003).
BACE1:	β-site APP-cleaving enzyme 1 (or β–secretase or memapepsin-2) is an aspartic acid protease important in the pathogenesis of Alzeimer's disease (APP = amyloid precursor protein). The pathogenesis is due to APP being cleaved (http://en.wikipedia.org/wiki/Beta_secretase/ Accessed 04-09-2008).
$[Co(acacen)L_2]^+$:	acetylacetonate ethylene diimine, L = Me imidazole
Cytochrome C:	Cytochrome C is a small heme protein which plays a role in respiration by carrying electrons from biological fuels to oxygen. The heme is associated with a copper ion, located close to the heme iron. Cytochromes undergo oxido-reduction through the complexed copper, which cycles between the +2 and +3 states of heme iron (Mathews and van Holde, 1990).
H_2SalDPT:	bis(salicylideneimino-3-propyl)amine

H_2SaltnOH:	*N*,*N*'-(2-hydroxypropane-1,3-diyl)bis(salicylideneamine)
H_2vanpa:	1-(3-methoxysalicylaldeneamino)-3-hydroxypropane
Invasion:	Cancer invasion is the process by which cells break away from a primary tumor and crawl through surrounding tissue. This enables the cells to move into a blood vessel and be transported through the body, possible establishing a secondary tumor at another site. {Invasion (cancer). http://www.ma.hw.ac.uk/ 28/07/2008}
IR:	Infrared
Metastasis:	The process by which cancer spreads from one organ (or part) at which it first arose as a primary tumor to a non-adjacent organ (or part) in the body. The cells have acquired increased mortality and the ability to invade another organ (or part of the same organ) {Metastasis (cancer), http://en.wikipedia.org/ 28/07/2008}
MNNG:	*N*-methyl-*N*'-nitro-N-nitrosoguanidine
MNU:	*N*-methyl-*N*-nitrosourea
NADH:	NADH is the reduced form of the coenzyme, Nicotinamide-adenine dinucleotide (NAD^+), which acts as an oxidizing agent in various biochemical reactions. NADH is a reducing agent in various biochemical reactions (Mathews and van Holde, 1990).
Oncogene:	An oncogene is a modified gene, or set of nucleotides that codes for a protein, which causes the malignancy of cancer (Oncogene, http://en.wikipedia.org/ 22/04/2004)
o-vanillin:	*o*-methoxysalicylaldehyde; 2-hydroxy-3-methoxybenzaldehyde; 2,3-(HO)(MeO)C_6H_3CHO
Q_4H_2:	Coenzyme Q_4H_2 is a reducing agent in various biochemical reactions oxidized (Vol'pin *et al.*, 1981)
salenH_2:	bis(salicylidene)ethylenediamine; *N*,*N*'-disalicylideneethylenediamine
SOS:	The synthesis of a whole set of DNA repair, recombination and replication proteins in bacteria containing severely damaged DNA.
umuC gene (*E. coli.*):	SOS mutagenesis and repair, subunit of DNA polymerase V

UV:	ultraviolet
Vanillin:	methoxysalicylaldehyde; 4-hydroxy-3-methoxybenzaldehyde

ACKNOWLEDGEMENTS

First and foremost, I would like to thank The Almighty Father.

A special thank you goes to my supervisor, Dr G. Watkins (Rhodes University), for his encouragement and support, especially in the field of UV/Vis and Infrared spectroscopy. "Having to supervise me, a part-time student, surely must have been even more challenging than it was for me to be a part-time research student. It is much appreciated that you always made time for consultations with me, even during hectic work periods."

I thank Walter Sisulu University (WSU) for financial support and acknowledge Rhodes University Microbiology Department for use of their laboratories and microbial cultures in carrying out the microbiological studies that formed part of this work. I also thank Dr D. Beukes, Dr E. Hosten and Ms B. Soko for the assistance with the DPPH test, ICP-MS and microanalysis, respectively.

A very special thank you goes to my husband, Arthur, and my daughters, Monique and Simone, for their unselfishness and for the numerous trips that they had to make to get me to adequate facilities required for carrying out my research and for consultation with my supervisor.

I would like to make use of this opportunity to thank my extended family (especially, my mom), friends and colleagues who have in any way contributed to making this journey of mine as stress free as possible.

Lastly, I hereby acknowledge all part-time postgraduate science students out there, but more especially women who are both mothers and wives. It is very difficult to be a diligent employee, parent and family person at the same time as acquiring, reporting and evaluating research data in this field of study.

1. INTRODUCTION TO DRUG DISCOVERY AND DRUG ACTION

As part of our investigation into possible anticancer and antimicrobial drugs, we report the synthesis, characterization, antimicrobial activity and antioxidant activity of 2-OH-*o*VANPN {*N*,*N*'-bis(2-hydroxy,3-methoxybenzylidene)-2-hydroxy-1,3-propanediamine}, a Schiff base ligand, and its Cu(II), Co(II), and Co(III) complexes. Accordingly, this chapter gives a short review of historical developments in the area of antimicrobial and anticancer drugs as well as a description of drug action and the mode of action of antimicrobial and anticancer drugs.

The multitude of discoveries and advances in the 20th century led to a massive increase in the life expectancy of humans for industrialized nations such that, with the exception of diseases such as cancer and AIDS, the focus is on morbidity rather than mortality, and the emphasis has changed from keeping people alive to keeping people fit (Britannica 23, 1990, p894). The death of humans from meningitis, tuberculosis, polio, smallpox and septicemia (septic wounds), once commonplace before the twentieth century is now almost unheard of.

A major problem associated with the use of antibacterial agents is that a microorganism can become resistant to a given drug (Britannica 17, 1990, p517). Despite all the developments of the 20th century, cancer is still the second (second to heart disease) highest killer disease in most modern Western countries (Britannica 23, 1990, p897). "Cancer is a tough problem. A cure will only come once all its facets are revealed, and the technology to manipulate the cancers is refined," said Dr William Tansey, a professor at Cold Spring Harbor Laboratory (Doting, 2008). The need for ongoing research and the development of new drugs, especially anticancer drugs and drugs to replace those that display microbial resistance cannot be overemphasized.

1.1 ADVANCES IN THE AREA OF ANTIMICROBIAL AGENTS

Since the beginning of time, potions and herbs were sources of medicine for various ailments (Britannica 23, 1990, p891). How these potions and herbs result in curing (or alleviating symptoms) of disease, were not necessarily fully understood.

Pharmacopoeia, the oldest existing catalogue of drugs, is a stone tablet from ancient Babylonia (*c*. 1700 BC) (Britannica 4, 1990, p233).

As early as 100 BC, the Roman encyclopaedist Varro expressed the idea that disease was caused by entry into the body of imperceptible particles (Britannica 23, 1990, p890). Fracastoro expressed this same theory in 1546, as did Athanasius Kircher a century later (Britannica 23, 1990, p890). In 1684, Francesco Redi wrote about "Observations on Living Animals Which Are to Be Found Within Other Living Animals", in which he sought to disprove the idea of spontaneous generation (Britannica 23, 1990, p891). "Everything must have a parent", he wrote; "only life produces life".

The 18th century marks a time when medical prescriptions were lengthy and doses were often large, and the search for a simple way of healing the sick continued (Britannica 23, 1990, p892). The writer and lecturer John Brown believed in only two types of diseases and two treatments, stimulant and sedative; his main remedies were alcohol and opium (opium contains morphine, a sedative used even in current times). On the other hand there was Samuel Hahnemann, the originator of homeopathy, a system of treatment involving administering very small doses of drug whose effects resemble the disease being treated. The science of modern pathology also had its beginnings in this century through the postmortem examinations of Giovanni Battista Morgagni. One highly significant advance, late in the century, was vaccination (e.g. material from cowpox was used as inoculations against smallpox). Around the same time, scientific thinking was making steady progress, and advances in physics, chemistry, and biological sciences were converging to form a rational scientific basis for every branch of clinical medicine.

Possibly the most outstanding advance of the 19th century was the conclusive evidence that certain diseases, as well as infections of surgical wounds, were directly caused by very small living organisms (Britannica 23, 1990, p893). This knowledge gave a whole new meaning to the area of pathology and resulted in an abrupt change in the practice of surgery. By the early 19th century, French and German chemists had isolated many active substances - morphine (opium), cocaine (cocoa leaves), quinine (bark of cinchona tree), and many others - from their crude plant sources (Britannica 9, 1990, p355). Agostino Bassi (Italy), who is regarded by some as the founder of the parasitic theory of infection, demonstrated that a disease of silkworms was caused by a fungus that could be destroyed by chemical agents (Britannica 23, 1990, p893). Louis Pasteur is the pioneer for the science of bacteriology by proving that the fermentation of wine and the souring of milk are caused by living microorganisms, and subsequently solved problems:- (1) of souring of milk; (2) in agriculture; (3) in industry, and (4) those of animal and human diseases (Franklin and Snow, 1975). Another pioneer in this field, Robert Koch, discovered the organisms for tuberculosis, in 1882, and cholera, in 1883 (Britannica 23, 1990, p893).

The phenomenal progress of medicine in the 20th century was further supported by improved communications (publications, conferences, computers and electronic media) amongst scientists worldwide, where teamwork became the norm. Subsequently, it has become more difficult to ascribe medical accomplishments to particular individuals (Britannica 23, 1990, p894). During the early 20th century, pharmacologists realized that a relation exists between the chemical structure of a compound and the effects it produces in the body of the patient (Britannica 9, 1990, p356). After 1930 pharmacological research underwent a rapid expansion (Britannica 9, 1990, 356). Constant testing was required for the routine control and standardization of drug products and their potency and purity (Britannica 23, 1990, 895) - this is currently common practice.

Due to the many technological advances of the 21st century, a rather easier systematic approach is employed for the discovery of new antimicrobial drugs; hence, many antimicrobial agents are available for bringing infectious diseases under control.

1.2 ADVANCES IN THE AREA OF CONTROL AND ELIMINATION OF MALIGNANT DISEASE (CANCER)

Drugs employed in cancer therapy are only among the more recent (20th century) advances in drug research (Britannica 4, 1990, p232).

Radium was discovered in 1898 and soon after that became useful in cancer treatments. High-voltage X-ray therapy and radioactive isotopes have largely replaced radium (Britannica 23, 1990, p897). Developments in radiation therapy include the use of radiopharmaceuticals (chemicals) that greatly sensitize tumor and not normal cells to the damaging effects of ionizing radiation, and the application of particle-beam (γ, β or α-particles) radiation therapy, using beams of protons, helium ions and heavy ions of such isotopes as carbon-12, neon-20, and argon-40 (Britannica 15, 1990, p563 and Dilworth and Parrott, 1998). The most effective of the isotopes is radioactive cobalt. Telecobalt machines (those that hold the cobalt at a distance) was invented during the 20th century and are still being developed for radiation therapy (Britannica 23, 1990, p897).

Since 1970, immunotherapy was developed for the control and elimination of cancer and may someday prove useful for manipulating the immunologic mechanisms of the cancer patient – Bacille Calmette-Guérin (BCG) (a vaccine against tuberculosis), for example, killed suspensions of several types of bacteria (Britannica 15, 1990, p563).

Another treatment involves the use of hyperthermia (Britannica 15, 1990, p563) because cancer cells have proved more sensitive to the killing effects of high temperature than normal cells, and specialized machines need still to be invented that can penetrate deep into the tissue to reach the tumor cells and to produce sufficient heat there to destroy these abnormal cells.

Transplantation of bone marrow cells also proved successful to cure acute leukemia of childhood (Britannica 15, 1990, p563).

Photodynamic therapy is frequently used for curing cancer (Dall'Acqua and Jori, 1995 and Dougherty *et al*., 1998).

There have been tremendous developments in the chemotherapy of cancer (Britannica 23, 1990, p897) and researchers are still developing new and more effective drugs to combat this disease. Combinations of chemotherapeutic agents that act on cells in different ways have been used simultaneously or in sequence (Britannica 15, 1990, p563 and Dilworth and Parrott, 1998), and have proved successful for childhood tumors and Hodgkin's Lymphoma as well as other localized neoplasm and in eradicating microscopic metastasis (Anonymous, 1978).

The use of inorganic metal complexes as chemotherapeutic agents dates back centuries, although organic, non-metal containing agents are most widely employed (Howard-Lock and Lock, 1987). Platinum drugs, for example Cisplatin, are proving effective against cancers of the ovaries and testes and a variety of solid tumors (Britannica 2, 1990, p796 and Howard-Lock and Lock, 1987). These platinum drugs are reported be toxic to the

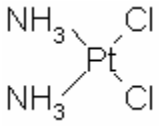

Figure 1.1: Structure of Cisplatin (Farrell, 1999 and Reedijk, 1996)

cancer patient and some cancers are resistant to the drugs (Reedijk, 1996); hence, a concerted effort is constantly made to prepare and screen drugs that have low toxicity and that can treat Cisplatin-resistant cancers (Keppler, 1993).

A variety of methods are currently available for destroying the malignant (cancer) cells from the host's body (Britannica 2, 1990, p796). Current cancer treatment depends on drugs and hormones, surgery, radiotherapy, or a combination of these (Britannica 2, 1990, p796 and Britannica 23, 1990, p897).

The most important discovery (Britannica 2, 1990, p796) regarding cancer has been that early detection of and prevention of this disease is of utmost importance. Examples of the latter are:- (1) prevention of inhaling cigarette smoke or asbestos to avoid lung cancer; (2) avoiding the use of cancer-causing substances in the manufacture of food and beverages; (3) avoiding exposure to ionizing radiation from sources such as X-rays, radioactive fallout, and ultraviolet light.

1.3 DISEASE AND CHEMOTHERAPY

Chemotherapy, in general, refers to the treatment of disease with chemicals (Britannica 17, 1990, p517). When used to refer to infectious diseases, the term is antimicrobial chemotherapy. Antimicrobial chemotherapy can be used either for prophylaxis (prevention) or treatment (cure) of disease caused by bacteria, fungi, viruses, protozoa, or worms (helminths) (Britannica 17, 1990, p517). Cancer chemotherapy uses synthetic chemicals and antibiotics that can differentiate to some degree between normal tissue cells and cancer cells. Chemotherapy is used in the treatment of cancer; no therapeutic agents are available for the prevention of cancer (Britannica 17, 1990, p517).

1.3.1 What is a drug?

A drug is any chemical agent that affects the function of living organisms (Britannica 4, 1990, p232). Drugs are used in treating, diagnosing, and preventing disease. Commonly used types of drugs include antibacterial, antifungal, stimulant, hormone, and so forth (Britannica 4, 1990, p232). Vaccines, which are preparations of killed or weakened bacteria or viruses used to stimulate resistance to subsequent infections are sometimes also considered drugs (Britannica 4, 1990, p232).

1.3.2 Drug action (general)

During the early 20th century, pharmacologists realized that a relationship exists between the chemical structure of a compound and the effects it produces in the body of the patient (Britannica 9, 1990, p356). In order for most drugs to be effective, an interaction

at the molecular level must occur between the drug and some target component of the cell (Britannica 17, 1990, p493). In most cases the interaction consists of a loose, reversible binding of the drug molecule. Three types of target molecules can be distinguished: (1) receptors; (2) macromolecules that have specific cellular functions, such as enzymes, transport molecules, and nucleic acids; (3) membrane lipids. Affinity is a term that describes the tendency of a drug to bind a receptor; efficacy describes the ability of a drug-receptor complex to produce a physiological response. Together, the affinity and efficacy of a drug determine its potency. A drug whose efficacy and affinity are sufficient for it to be able to bind to a receptor and affect cell function is said to be an agonist. A drug with the affinity to bind a receptor but without the efficacy to elicit a response is known as an antagonist because by binding to a receptor site, it can block the effect of an agonist. The binding of a drug to a receptor site requires an exact chemical fit, and a small change in a drug's chemical structure may alter its potency. The degree of binding can be measured directly by the use of radioactively labeled drugs or inferred indirectly from measurements of the biological effects of agonist and antagonist. These measurements have shown that the reaction

$$\text{Drug} + \text{receptor} \rightleftharpoons \text{drug-receptor complex}$$

mostly obeys the simplest form of law of mass action. Thus, there is a relationship between the concentration of drug and the amount of drug-receptor complex formed.

1.3.3 Antimicrobial chemotherapy

Antibacterial drugs:- Several factors determine whether an antibacterial agent will affect a microorganism (Britannica 17, 1990, p517). The drug must be delivered to a sensitive site in the cell, such as an enzyme that is involved in the synthesis of the cell wall or a protein/ enzyme involved in the synthesis of proteins or nucleic acids. Whether the antibacterial agent enters the microbial cell depends on the ability of the agent to penetrate the outer membrane of the cell, or on the presence or absence of transport systems for the antimicrobial agent, or on the availability of channels in the cell surface.

Antibiotics are substances produced by microorganisms that at low concentrations kill or inhibit other microorganisms (Britannica 17, 1990, p518). Natural penicillins, for example, are produced by fungi belonging to the species ***Penicillium***. Semisynthetic penicillin are produced by growing the fungus ***Penicillium*** under conditions whereby only the basic molecule (6-aminopenicillanic acid) is produced and then adding certain chemical groups to this molecule to give the different types of semisynthetic penicillins. Ampicillin, a broad-spectrum penicillin, is bactericidal (kills bacteria) for both Gram-positive and Gram-negative organisms because it interferes with the synthesis of the bacterial cell wall (Dollery, 1991). Ampicillin is ineffective against most staphylococcal infections and against ***Pseudomonas*** (Dollery, 1991). A major problem associated with the use of antibacterial drugs is that a microorganism that originally was sensitive to a given drug can become resistant (Britannica 17, 1990, p518).

Antifungal drugs:- Fungi appear in two morphological forms: a single cell that is round or oval (yeast**)**, and a filamentous form (mold). Bacteria differ from fungi in several ways, including chemical composition of the cell wall and cell membrane therefore different therapeutic agents are used for bacterial versus fungal infections (Britannica 17, 1990, p520). Antibiotics (e.g. Nystatin), synthetic chemical agents (e.g. Flucytosine) and antifungal agents (e.g. Miconazole) are all used to treat fungal infections (Britannica 17, 1990, p520).

Antiparasitic drugs:- The protozoans, unlike bacteria and fungi, do not have cell walls and antiprotozoal drugs act by breaking DNA (e.g. Metronidazole) or interfering with DNA replication (e.g. Quinacrine) or by inhibiting protozoan enzymes (e.g. Iodoquinol) (Britannica 17, 1990, p520)**.**

Antiviral drugs:- Viruses are among the most common and widespread causes of infectious disease and are also the most difficult of infectious organisms to control (Britannica 17, 1990, p521). Reasons (Britannica 17, 1990, p521) for the difficulty in developing chemotherapeutic agents to control this type of microorganism includes: (1) the structure of each virus differs; (2) periodic changes in antigenic proteins of a virus;

(3) the virus has to enter a cell of the host for it to be able to replicate and thus the chemotherapeutic agent must be able to inhibit the virus without affecting the host's cells. Viral vaccines, which are preparations of killed or weakened viruses used to stimulate resistance to subsequent viral infections, are considered antiviral drugs (Britannica 4, 1990, p232).

1.3.4 Cancer chemotherapy

1.3.4.1 What is cancer?

"Cancer" refers to malignant tumors, which can spread by invasion or metastases (The history of cancer, http://www.cancer.org/ 22/04/2004). This disease is characterized by the uncontrolled multiplication of abnormal cells in the body (Gupta, 1994 and Burck, *et al*., 1988). If this multiplication occurs in a vital organ or tissue, normal function will be impaired or halted, with possible fatal results.

1.3.4.2 Causes of cancer

The mechanism or groups of mechanisms responsible for cancer remain unknown (Britannica 2, 1990, p795). Two events (Kinzler and Vogelstein, 1997) possibly initiate the formation of a tumor. The first is when a proto-oncogene, which is a normal gene that can become an oncogene, is transformed into an oncogene (Oncogene, http://en.wikipedia.org/wiki/ 22/04/2004). The second possible event is the inactivation of a tumor suppressor gene.

Cancer lesions are probably influenced by the host's susceptibility and immunity to specific genetic mutations (Britannica 2, 1990, p796). Genetic mutations affect the factors controlling normal cell division (Burck *et al*., 1988). Certain cancers of the breast and prostate are considered dependant on various hormones; other cancers are dependant on the presence of certain viruses (Britannica 2, 1990, p796). X-rays, radioactive fallout, γ-rays and ultraviolet light were also identified as major causes of cancer (Britannica 2,

1990, p796). Chemical carcinogens (asbestos dust, food additives, some compounds contained in cigarette smoke, etc) have been implicated in cancer causing local changes in nucleotide sequences in DNA (Britannica 2, 1990, p796 and Howard-Lock and Lock, 1987). It is difficult to determine, however, what proportion of cancer is due to exposure to these agents, because the length of time between exposure and the appearance of cancer is usually prolonged (Britannica 2, 1990, p796).

1.3.4.3 Two recent advances in cancer research

A breakthrough in developing telomerase inhibitor drugs:- Emmanuel Skordalakes, a professor at the Wistar Institute, in Philadelphia, and co-workers have determined the structure of an enzyme, telomerase, which plays a key role in the growth of most tumors (Kim *et al*., 1994), opening the path to a decade-long search for telomerase inhibitors as a new class of anti-cancer drugs (Sapa-AFP, 2008). Jon Wilson, a scientist at The Institute of Cancer Research in London, described the research as a "major breakthrough" (Sapa-AFP, 2008).

According to Skordalakes (Sapa-AFP, 2008), the enzyme, telomerase, "is an ideal target for chemotherapy because it is active in almost all human cancer tumors but inactive in most normal cells". "That means that a drug that deactivates telomerase would most likely work against all cancers, with few side effects." Telomerase adds short sequences of DNA, known as telomerase, to the ends of chromosomes, to prevent damage and the loss of genetic information during cell division (Kim *et al*., 1994). The enzyme is active mainly in cells undergoing rapid cell division. In rapidly dividing cancer cells, telomerase allows the diseased cells to replicate endlessly and achieve "cellular immortality," the hallmark of all cancers (Kim *et al*., 1994). Skordalakes found that the red flour beetle produced large amounts of telomerase in a stable form needed to carry out research on the complicated structure of telomerase.

Turning down the Myc gene could shrink tumors:- US scientists are closer to finding a way to shrink tumors to their normal sizes, which may then cause the cells to self-destruct (Dotinga, 2008). Mother Nature programmed cells to commit suicide if they detect that they are damaged. Sometimes suicide does not take place; instead, proteins send signals

to tell the cells to keep growing (Dotinga, 2008). "As a result of this push, cancer can develop," said Dr. Dean Felsher, an associate professor of medicine and oncology at Stanford University School of Medicine. A gene known as Myc is considered important in the protein signaling process (Dotinga, 2008). By turning down the Myc gene, like using a dimmer switch on a lamp, the tumors could be shrunk to normal sizes and restore their ability to die as nature intended them to do (Dotinga, 2008). There is no treatment based on this approach yet, and fixing the genetic signals will not work for every type of cancer. However, scientists have implicated the Myc signal in cancers of the immune system and the lungs (Dotinga, 2008).

1.3.4.4 Drugs used in cancer chemotherapy

Every drug that has been developed to kill cancer cells, however, also affects rapidly dividing normal cells (Britannica 4, 1990, p232) because cancer cells demonstrate no biochemical differences to host (normal, healthy) cells (Range *et al.*, 1995). Microbial cells demonstrate biochemical differences to host (e.g. human cells); hence, antimicrobial therapy is comparably less problematic than chemotherapy of cancer (Range *et al.*, 1995).

There have been tremendous developments in the chemotherapy of cancer and researchers are still developing new and more effective drugs to combat this disease. Rapidly growing cancers i.e. childhood tumors and Hodgkin's lymphoma, respond very well to existing chemotherapy, and both disseminated and localized malignancies are frequently cured. On the other hand, there are the slow-growing tumors i.e. carcinomas of the lung, colon and breast, which are the predominant of the human cancers, and which respond poorly to existing chemotherapeutic agents (Anonymous, 1978).

A drawback with most therapeutic drugs is that they are designed to attack the genetic material - the DNA – of the tumor (cancer) cells in an attempt to stop them from multiplying and spreading the tumor, but these drugs can also kill normal cells (Britannica 2, 1990, p796). A major problem in cancer chemotherapy is that cancer cells

become resistant to drugs and drugs may have side effects that may result in toxicity to the cancer patient ((Britannica 15, 1990, p562 and Reedijk *et al*., 1996).

Another problem is that only a certain portion of the abnormal cells are dividing at any one time, and most cancer drugs can only destroy that part of the cancer cell population undergoing division. Each cancer drug exerts its effect at a different phase of the cell cycle (Britannica 4, 1990, p232).

To help with the afore-mentioned problems, combinations of chemotherapeutic agents that act on cells in different ways have been used simultaneously or in sequence (Britannica 15, 1990, p562). This allows cancer cells at different stages of division to be destroyed, causing less damage to normal cells, and diminishing the tendency of malignant cells to become resistant to a single drug.

Hormones:- Hormones as chemotherapeutics include steroids such as glucocorticoids and oestrogens (Range *et al*., 1995).

Photodynamic therapy:- Photodynamic therapy uses hematoporphyrin derivatives and specific dyes that diffuses slower from tumor cells than from normal cells due to slow lymphatic drainage in tumor tissue; thus, the dye (drug) selectively accumulates in the tumor cells (Dall'Acqua and Jori, 1995 and Dougherty *et al*., 1998). Red light from a tunable laser is directed at the tumor and leads to destruction of tumor cells when the dye generates singlet oxygen radicals (O·), which in turn destroy membranes, proteins, sterols and lipids.

Cytotoxic drugs:- Cytotoxic drugs (Range *et al*., 1995) as chemotherapeutic agents include:

- antimetabolites (e.g. methatrexate), which block DNA synthesis;
- alkylating agents (e.g. mechlorethamine), which prevent DNA replication;
- Cytotoxic antibiotics (e.g. mercaptopurine), which prevent cell division;
- Vinca alkaloids (e.g. vinblastine), which affect formation of mitotic spindle.

From examples (in brackets) above it can be seen that mostly organic, non-metal containing agents have chemotherapeutic activity (Howard-Lock and Lock, 1987).

Bioinorganic chemicals and metal complexes as drugs:- It is well known that some drugs have greater activity when administered as metal complexes than as free organic compounds (Golcu *et al*., 2005). Inorganic metal compounds are used as chemotherapeutic agents (Howard-Lock and Lock, 1987).

The search for antitumor activity among metal compounds have been greatly stimulated by the success of Cisplatin, which has cytotoxic effects on cancer cells due to formation of stable adducts of DNA which then block replication or inhibit DNA transcription (Guo and Sadler, 2000).

Copper(II) complexes of salicylaldehyde derivatives are active against a variety of tumor cell lines (Guo and Sadler, 2000). It is possible that a Cu(II) amino acid phenanthroline complex will soon enter clinical trials (Guo and Sadler, 2000). At the Chemotherapy National Service Center, Co(II) derivatives of Schiff bases of salicylaldehyde showed activity against one form of Walker Sarcoma of the rat (Hodnett *et al*., 1970). Strong anticancer activity against Ehrlich ascites carcinoma (EAC) was observed with complexes derived from the Schiff base, hydroxysalicylaldehyde, and its amine analogues (Golcu *et al*., 2005). A Zn(II), a Ni(II) and a Cu(I) complex with the Schiff base derived from 2,4-dihydroxybenzaldehyde and L-arginine gave 32.2%, 51.7% and 53.3% inhibition rates, respectively, to EAC (Chunhua *et al*., 1993). Co(III) complexes with tetradentate ligands have displayed selective anticancer activity (Osinsky *et al*., 2000). Di-pyridyl ketone thiosemicarbazone series of iron chelators showed marked and selective antitumor activity *in vitro* and *in vivo* (Richardson *et al*., 2006).

Transition metal complexes capable of cleaving DNA are of importance for their potential use as new structural probes in nucleic acids chemistry and as therapeutic agents (Reddy, *et al*., 2004). The complexes showing visible light-induced DNA cleavage are of particular interest as they can be made effective in highly targeted therapeutic

applications (Reddy, *et al*., 2004). The DNA-binding and photocleavage properties of ruthenium(II) polypyridyl and related class of transition metal complexes have been studied. Alkylcobalt(III) complexes generate alkyl radicals, which are known to damage biological targets (e.g. cancer cells) and especially to cleave nucleic acids (Sykes, 2000).

Radical scavenging behaviour of the polyphenolic Schiff bases is affected by coordination to a metal ion; this mechanism has possible relevance to the design of antioxidants for use in cancer therapeutics and in food preservation (Golcu *et al*., 2005).

The above discoveries among bioinorganic chemicals and metal complexes as drugs support the present work, which is research in the area of metal-based chemistry in an attempt to discover drugs that have low toxicity to the cancer patient and that can treat Cisplatin-resistant cancers.

1.4 REFERENCES

1. Anonymous. *Cancer Facts and Figures*. **1979**. American Cancer Society. New York. 1978.
2. Burck, K.B.; Liu, E.T. and Larrick, J.W. *Oncogenes: An introduction to the concept of cancer genes*. **1988**. Springer-Verlag, New York. 350.
3. Chunhua, C.; Zishen, W. and Zhenhuan, Y. *Synthesis and Reactivity in Inorganic and Metal-Organic Chemistry*. **1993**. 23. 1725-33.
4. Dall'Acqua, F. and Jori, G. *Principle of Medicinal Chemistry*, 4th Edition. **1995**. Foye, W.O.; Lemke, T.L.; William, D.A. (Eds). Williams and Wilkins. Baltimore. Chapter 41.
5. Dilworth, J.R. and Parrott, S.J. *Chem. Soc. Rev.* **1998**. 27. 43-55.
6. Dollery, C. *Therapeutic Drugs*. **1991**. Boobis, A.R.; Burley, D.; Davies, D.M.; Harrison, P.I. (Editorial board). Churchill Livingstone. A117.

7. Doting, R. (HealthDay News © 2008 New York Times Partner Publications) "*A* Dimmer switch could stop tumour signals" In: *Business Day*. 03 September **2008**. AVUSA Group. Johannesburg. South Africa.
8. Dougherty, B.W.; Gomer, C.J.; Henderson, B.W.; Jori, G.; Kekkel, D.; Korbelik, M; Moan, J. and Pen, Q. ***J. Natl. Cancer Institute***. **1998**. 90. 889-96.
9. Farrell, N. ***Coord. Chem. Rev.*** **1999**. 99. 2201-3.
10. Franklin, T.J. and Snow, G.A. "Antiseptics, antibiotics and the cell membrane" In: *Biochemistry of antimicrobial action*. 2nd ed. **1975**. Chapman and Hall.
11. Golcu, A.; Tumer, M.; Demirelli, H. and Wheatley, R.A. *Inorganica Chimica Acta*. **2005**. 358. 1785-97.
12. Gupta, S.P. *Chemistry Revelations*. **1994**. 94. 1507-51.
13. Hodnett, E.M. and Dunn, W.J., III. Journal of Medicinal Chemistry. **1970**. 13. 768-70.
14. Howard-Lock, H.H. and Lock, C.J.L. "Medicinal properties of organometallic compounds" In: *Comprehensive Coordination Chemistry*. **1987**. Wilkinson, G. (ed.). Pergamon. Oxford.
15. Keppler, B.K. *Metal complexes in cancer chemotherapy*. **1993**. VCH. New York. 436.
16. Kinzler, K. and Vogelstein, B. *Nature*. **1997**. 386. 761-3.
17. Oncogene. http://en.wikipedia.org/ Accessed 22/04/2004.
18. Osinsky, S.P.; Levitin, T.; Bubnovskaya, L.; Sigan, A.; Ganusevich, I.; Michailenko, V. and Kovelskaya, T. *6th Internet World Congress for Biomedical Sciences*. **2000**. Inabis Poster #3.
19. Rang, H.P.; Dale, M.M. and Ritter, J.M. *Pharmacology*. 3rd edition. **1995**. Churchill Livingstone. Edinburgh. 835.
20. Reddy, P.A.N.; Santra, B.K.; Nethaji, M. and Chakravarty, A.R. *Journal of Inorganic Biochemistry*. **2004**. 98. 377-86.
21. Reedijk, T. *Chemistry Communications*. **1996**. 801-6.
22. Richardson, D.R.; Sharpe, P.; Lovejoy, D.B.; Senaratne, D.; Kalinowski, D.S.; Islam, M. and Bernhardt, P.V. *Journal of Medicinal Chemistry*. **2006**. 49. 6510-21.

23. Sapa-AFP. "Cancer on the run at last" published in *The Times*, 02 September **2008**. Avusa Group, Johannesburg, South Africa.
24. Guo, Z. and Sadler, P.J. "*Medicinal Inorganic Chemistry*" In: *Advances in Inorganic Chemistry*. **2000**. Sykes, A.G. (ed.). Academic Press. New York. 183-303.
25. The history of cancer. http://www.cancer.org/ Accessed 22/04/2004.
26. *The New Encyclopaedia. Britannica*. 15th Edition. 1990. Encyclopaedia Britannica, Inc., Chicago, Robert P. Gwinn, R.P. (Chairman), Board of Directors:- Norton, P.B.(President); Goetz, P.W. (Editor in Chief): Britannica 2. 795-6.
27. *The New Encyclopaedia*. *Britannica*. 15th Edition. **1990**. Encyclopaedia Britannica, Inc., Chicago, Robert P. Gwinn, R.P. (Chairman), Board of Directors:- Norton, P.B.(President); Goetz, P.W. (Editor in Chief): Britannica 4. 232-3.
28. *The New Encyclopaedia. Britannica*. 15th Edition. **1990**. Encyclopaedia Britannica, Inc., Chicago, Robert P. Gwinn, R.P. (Chairman), Board of Directors:- Norton, P.B.(President); Goetz, P.W. (Editor in Chief): Britannica 9. 355-6.
29. *The New Encyclopaedia. Britannica*. 15th Edition. **1990**. Encyclopaedia Britannica, Inc., Chicago, Robert P. Gwinn, R.P. (Chairman), Board of Directors:- Norton, P.B.(President); Goetz, P.W. (Editor in Chief): Britannica 15. 562-3.
30. *The New Encyclopaedia. Britannica*. 15th Edition. **1990**. Encyclopaedia Britannica, Inc., Chicago, Robert P. Gwinn, R.P. (Chairman), Board of Directors:- Norton, P.B.(President); Goetz, P.W. (Editor in Chief): Britannica 17. 493-521.
31. *The New Encyclopaedia. Britannica*. 15th Edition. **1990**. Encyclopaedia Britannica, Inc., Chicago, Robert P. Gwinn, R.P. (Chairman), Board of Directors:- Norton, P.B.(President); Goetz, P.W. (Editor in Chief): Britannica 23. 890-7.

2. GENERAL INTRODUCTION

As mentioned before, the focus of this thesis is to report the synthesis, characterization and biological (antioxidant and antimicrobial) activities of a Schiff base ligand, *N,N'*-bis(2-hydroxy,3-methoxybenzylidene)-2-hydroxy-1,3-propanediamine, and its Cu(II), Co(II), and Co(III) complexes.

Bioinorganic chemistry, which involves the interaction of metal complexes with biological systems, draws increasing interest. Some authors have shown the anticancer activity of a number of cobalt-containing compounds *in vitro* and *in vivo* (Osinsky *et al.*, 2000 and Sergej *et al.*, 2000). Such data warrants investigations with cobalt complexes and similar compounds.

A considerable amount of research has been done on the chemistry of the metal complexes of Schiff bases containing nitrogen donors. Some reasons reported are: their stability, biological activity and potential application in many fields such as oxidation, catalysis, electrochemistry, and so forth (Tai *et al.*, 2003).

The study of metal complexes with Schiff bases is by far too large to be fully reviewed in the present work. Potential biological activity could be displayed by the hydrolysis products of the Shiff base i.e. the Shiff base precursors, by the labilized Shiff-base ligand or by the Schiff base complex.

This literature review highlights some areas of interest to this thesis, in particular, *biological activity*, *synthesis* and *structure determination* of:

- Schiff base precursors,
- Schiff bases, and
- Transition metal complexes of Schiff bases, including those [Mn(II), Fe(II), Ni(II) and Zn(II)] other than the Cu(II), Co(II) and Co(III) studied in this work so that the variety of possible binding modes of Schiff base ligands of similar structure are examined.

2.1 SCHIFF BASE PRECURSORS

The biological activities of the Schiff base precursors have been widely examined.

2.1.1 Biological activity of the aldehyde unit

Effect on mutagenesis:- Vanillin (4-hydroxy-3-methoxybenzaldehyde) (Figure 2.1) and its isomer *o*-vanillin (2-hydroxy-3-methoxybenzaldehyde or 3-methoxysalicylaldehyde) (Figure 2.2), which is one of the ligand constituents in the present work, have an effect on the adaptive and SOS responses induced in *Escherichia coli* by *N*-methyl-*N*-nitrosourea (MNU) and UV irradiation (Takashi *et al*., 1990). These vanillins also had an effect on mutagenesis (Takashi *et al*., 1990). The effects were either potentiating or suppressing. *o*-Vanillin markedly inhibited the MNU-induced adaptive response, while both vanillins potentiated the UV-induced SOS response (Takashi *et al*., 1990). These phenomena appear to be responsible for the comutagenic or antimutagenic role of these chemicals in MNU and UV mutagenesis (Takashi *et al*., 1990), hence, indicating that compounds of both vanillins are worth investigating for biological activity, but moreover, for anti-cancer activity.

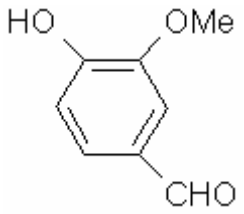

Figure 2.1: Structure of vanillin (Takashi *et al*., 1990)

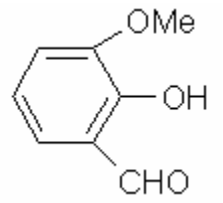

Figure 2.2: Structure of *o*-vanillin (Takashi *et al*., 1990)

Effect on mutations induced by MNNG:- Mutations induced by *N*-methyl-*N'*-nitro-*N*-nitrosoguanidine (MNNG) were strongly enhanced in the presence of *o*-vanillin in

Escherichia coli B (Watanabe *et al*., 1990). It was necessary to add simultaneously MNNG and *o*-vanillin to the bacterial growth medium. The results suggested that *o*-vanillin had inhibited induction of the adaptive response (Vericat and Barbé, 1988), and consequently, the MNNG-induced mutation frequency was increased (Watanabe *et al*., 1990). These suggestions are in contrast to the antimutagenic roles (UV mutagenises) of both vanillins outlined in the previous paragraph, which seem to suggest that activity is not linked to the hydroxy group because its position is different in the two vanillins.

Genotoxic activity:- The genotoxic effect of vanillin and other phenolic compounds on the DNA of *Escherichia coli* was determined, and gave negative results (Mikulasova and Bohovicova, 2000). The negative results obtained were confirmed by the assessment of the number of revertants via the Ames test. The ability of vanillin and *o*-vanillin to increase the viability of cells and to decrease the number of mutations in bacteria pre-treated with 4-nitroquinoline-1-oxide was verified (Mikulasova and Bohovicova, 2000), and serve once again as a reason for anti-cancer-testing of compounds containing these moeities.

2.1.2 Spectroscopic considerations for the aldehyde unit

UV data:- The band at 400 nm in the near UV spectrum of *o*-vanillin was found to be intense in ethanol, but almost absent in hexane; thus, indicating solvent-dependence of the absorption maxima (Wilkinson *et al*., 1987). The presence of this band has been attributed to the enol-keto tautomeric equilibrium of the kind shown in Figure 2.3, the keto-amine tautomer (Figure 2.3(b)) being responsible for that absorption (Wilkinson *et al*., 1987).

Figure 2.3: Keto-amine tautomeric equilibrium for *o*-vanillin

NMR data of the OH proton on salicylaldehyde and its derivatives:- Proton NMR data of *o*-vanillin showed coupling between the aldehydic and the hydroxyl proton on the molecule (Schaefer *et al*., 1984). In salicylaldehyde derivatives that contain sufficiently large substituents ortho to another functional group, this positive spin-spin coupling is observed between the two side-chain protons, that is, the aldehyde-proton and the OH-proton. This coupling, formally over 5 bonds, correlates with the chemical shift of the OH proton (Schaefer *et al*., 1984).

2.1.3 Biological activity of the diaminopropanol unit and related compounds

BACE1 inhibitors containing 3-aminopropanol for the treatment of Alzheimer's disease:- Alzheimer's disease (AD) is a debilitating neurodegenerative disorder which imparts tremendous suffering to more than 20 million people worldwide (Baxter and Reitz, 2005). β-amyloids (peptides consisting of 40-42 amino acids) accumulate in the brain of the AD patient and are involved in progression of the disease (Demont *et al*., 2004 and Beta_secretase, http://en.wikipedia.org/wiki/ 04/09/2008). Levels of BACE1 mRNA and protein expression are higher in the brains of sporadic AD patients. BACE1 leads to formation of β-amyloids and thus build-up thereof (Demont *et al*., 2004 and Beta_secretase, http://en.wikipedia.org/wiki/ 04/09/2008). Drugs to block BACE1 in theory would prevent the build-up of β-amyloids and could provide improvements in the cognitive symptoms of AD as well as alter the course of the disease. 3-Aminopropanol incorporated into BACE inhibitors had some biological activity (Demont *et al*., 2004).

Converting aminoalcohol to imine to facilitate transport to tumour site for anti-tumour action:- The reactivity of an amino group in a potential anti-tumour agent, such as 2-amino-2-methyl-1-propanol, results in a very small percentage of the applied dose reaching the tumor site (Billman *et al*., 1969). This is why converting it to a blocking group, by reacting it with an aldehyde to produce an imine, usually protects the amino group:-

$$\underset{\text{(aldehyde)}}{ArCHO} + \underset{\text{(aminoalcohol)}}{H_2N\text{-}C(CH_3)_2\text{-}CH_2OH} \rightarrow \underset{\text{(Schiff base)}}{ArC(H)=N\text{-}C(CH_3)_2\text{-}CH_2OH}$$

The blocking group can be removed selectively at the tumor site through hydrolysis of the imine to generate the active amine (Billman *et al*., 1969).

Inhibitors of the enzyme involved in replication of herpes virus:- Dunnick and co-workers found that functionalised 1, 2-diamines, when incorporated into the Schiff base backbone of inhibitors, lead to increased inhibitor specificity for the enzyme involved in replication of the herpes virus, and therefore inhibits replication of the herpes virus (Dunnick *et al*., 1999). Cobalt(III) Schiff base complexes $[Co(acacen)L_2]^+$ (acacen = bisacetylacetonateethylenediimine, L = methyl imidazole) (Figure 2.4) have been shown to inhibit the replication of the herpes virus (Dunnick *et al*., 1999). The N_2O_2-core of these complexes are the same as for complexes in the present work.

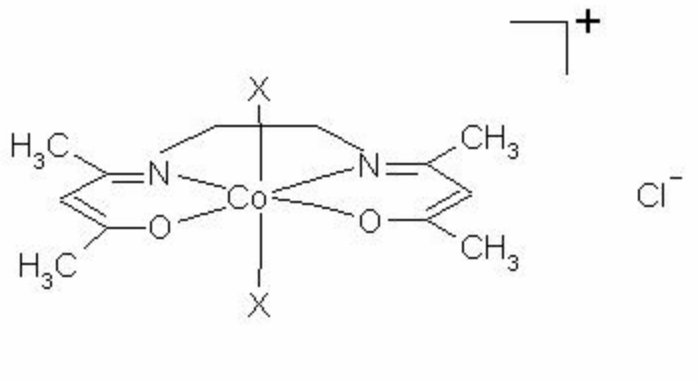

Figure 2.4: Structure of $\{Co(acacen)X_2\}$: X = NH_3 or 2-Methyl imidazole

Ability to complex and retard DNA migration:- *N*,*N*'-diacyl-1,2-diaminopropyl-3-carbamoyl-(dimethylaminoethane) cationic lipids were screened for ***in vitro*** transfection activity at different charge ratios in the presence and absence of helper lipids. Gel electrophoresis showed that one of the tested lipids was found to complex and retard DNA migration (Aljaberi *et al*., 2005).

Antibacterial activity:- Brown and co-workers conducted a study on the correlation between heterocyclic compound structure and biological activity (Brown *et al*., 1976). They found that if a compound had a long lipophilic end (a long hydrocarbon chain such as propanol, for example), which could interact with the cellular components and thus enhance transport of the compound to the active site, it would show greater biological

activity (e.g. antibiotic activity, antibacterial activity, etc). They also found that the presence of an amino group, which could readily interact with cell membrane components, also enhances biological activity.

Effect of poly(alcohol) on DNA transfection:- Nantz and co-workers tested a series of lipidic ammonium tetrafluoroborate salts for DNA transfection activity involving DNA phosphate of a reporter gene (Nantz *et al*., 1998). They found that poly(alcohol) substituted headgroups improve DNA transfection and the mechanism is not based on activation of the ammonium ion.

Use of N,N' –dibenzoyl-1,3-diaminopropan-2-ol as a radioactive compound:- *N*,*N*'–dibenzoyl-1,3-diaminopropan-2-ol was initiated to form tritiated *N*,*N*'–dibenzoyl-1,3-diaminopropan-2-ol, which mimics a natural lipid drug carrier (Lambert and Gallez, 1996). Five minutes after intravenous administration of the tritiated analog into mice, 9% of the injected dose per g organ was found in the brain, which decreased to 1% after 3 hours while in the same time radioactive levels measured in the urine increased.

Use of 1,3-diaminopropan-2-ol for synthesis of building blocks for lipophilicity and other biological testing:- In the light of the need for building blocks libraries by combinatorials chemists, Marmillon and co-workers developed a library of 1,3 propanediamines as follows: With correct synthesis conditions, 1,3-diaminopropan-2-ol leads to formation of 2-alkoxypropanediamines and 2-alkylpropanediamines (Marmillon *et al*., 1998).

2.2 SCHIFF BASES

Shiff bases, of which the ligand used in the present work belong to, even when not coordinated to metals, are known to have slight antitumor activities (Hodnett *et al*., 1970). Some Schiff bases were screened at the Cancer Chemotherapy National Service Center against lymphoid leukemia in mice and intramuscular Walker sarcoma in rats, and

were found to be inactive against leukemia and to significantly slow down the tumor growth in rats (Hodnett *et al*., 1970).

2.2.1 General structure and synthesis

Ligands with an O, N donor set are the most commonly used as ligands to transition metals (Wilkinson *et al*., 1987), and are also the type of ligand used in the present work. The condensation of primary amines with aldehydes and ketones yields Schiff bases (imines), which are characterised by the presence of a C=N double bond (Wilkinson *et al*., 1987). To prevent these from rapidly decomposing or polymerising, an aryl group (this is the minimal requirement) must be bonded to the nitrogen or to the carbon. Therefore, a Schiff base is a ligand that contains an imine (or C=N) group, which in turn is bound to an aryl group via the nitrogen or the carbon (Wilkinson *et al*., 1987). Such a ligand is named after the researcher Schiff who first reported their synthesis over one hundred years ago (Wilkinson *et al*., 1987).

The most commonly used method of obtaining a Schiff base is by the condensation reaction (Figure 2.5) between (a) and (b) with the formation of an intermediate hemiaminal (c). It must be noted that very few Schiff bases commonly used as ligands have been prepared and characterised in the uncomplexed state, since the corresponding metal complexes have been directly obtained by other procedures, such as direct reaction between metal ions and constituents of the Schiff base ligand (Wilkinson *et al*., 1987).

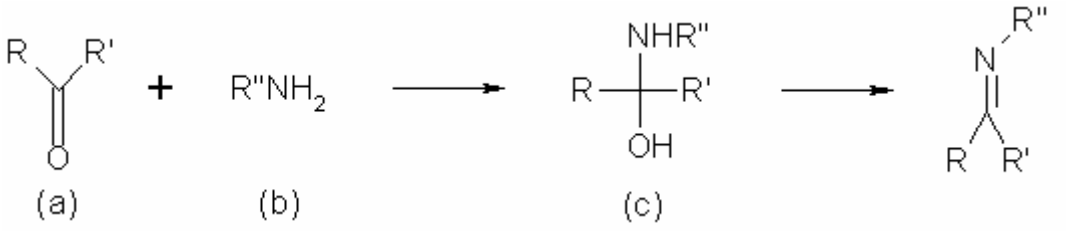

Figure 2.5: The most common method for synthesising a Schiff base

2-OHSALPN [*N*,*N*'-bis(2-hydroxybenzylidene)-2-hydroxy-1,3-propanediamine] (Figure 2.6) was prepared by the condensation reaction between salicylaldehyde and 1,3-diamino-2-propanol, and its single crystals obtained (Liang *et al*., 1997). The crystal structure showed that two molecules of 2-OHSALPN are linked together centro-

symmetrical by hydrogen bonds. It is classified as a pentadentate ligand and is capable of forming, in addition to mononuclear complexes, binuclear complexes with exogenous or endogenous bridging groups (Liang *et al*., 1997).

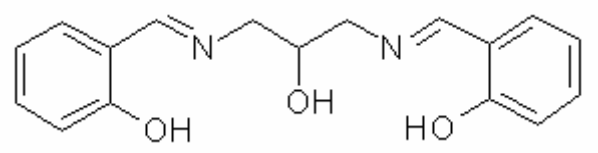

Figure 2.6: Structure of 2-OHSALPN

2OH-*o*VANPN {*N*,*N*'-bis(2-hydroxy,3-methoxybenzylidene)-2-hydroxy-1,3-propanediamine} (Figure 2.7) is the ligand used in the present work. It is similar in structure to 2-OHSALPN and is also classified as a pentadentate ligand that is capable of forming in addition to mononuclear complexes, binuclear complexes with exogenous or endogenous bridging groups (Liang *et al*., 1997).

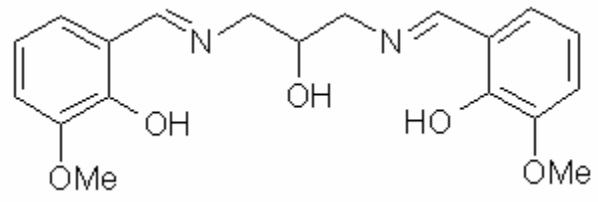

Figure 2.7: Structure of 2OH-*o*VANPN

Ghose prepared some Schiff bases. The reaction of $H_2NCH_2CH_2NH_2$ with *o*-vanillin resulted in a ligand similar to 2OH-*o*VANPN, except a diamine instead of a diamino alcohol was used (Ghose, 1983). In another similar system, *N*,*N*'-bis(4-alkoxysalicylaldimine)propan-2-ol, which is similar to the ligand in the present investigation, was found to give 78-92% yields (Ku *et al*., 2000).

Nishida and Kida synthesised 2-OH-*o*VANPN as well as a similar ligand that incorporated acetyl acetone instead of 1,3-diaminopropan-2-ol (Nishida and Kida, 1986). They have also reported crystal structures and magnetism data for binuclear Cu(II) complexes, which were derived from their (OH-SALPN) ligand and a coligand. The H_3SalDpl-Schiff base formed by the condensation of salicylaldehyde and 1,3-

diaminopropan-2-ol, was prepared and some nickel complexes prepared from this ligand and other co-ligands (Brezina et al., 1997). Schiff base complexes with derivatives of the pentadentate ligand bis(salicylideneimino-3-propyl)amine were prepared, and the 1:1 dioxygen adduct of Co[sal(*n*-propyltrimethylsilyl)DPT] was isolated and its X-ray molecular structure determined (Carré *et al.*, 2003). H_3L, a pentadentate ligand derived from the condensation of acetylacetone or salicylaldehyde with 1,3-diaminopropan-2-ol or 1,5-diaminopentan-3-ol and which is similar to the ligand in the present work, was used to synthesize Cu_2LL' and Ni_2LL' (HL' = exogenous 2-atom bridge between the 2 metal centers consisting of pyrazole and related species) (Mazurek *et al.*, 1986). The imine group, which is typical of Schiff base ligands, was observed in the latter complexes (Mazurek *et al.*, 1986). It has already been mentioned before that the acacen (acacen = bisacetylacetonateethylenediimine) ligand (Figure 2.4) has been used in synthesis of cobalt(III) complexes (Dunnick *et al.*, 1999). This ligand has many similarities to the ligand in the present study.

2.2.2 Spectroscopic considerations

IR data:- The C=N stretching frequencies of Schiff base ligands occur in the region between 1680 and 1603 cm^{-1} when H, alkyl or aromatic (Ar) groups are bonded to the C and N atoms (Wilkinson *et al.*, 1987). Aromatic groups on the C and N atoms cause a shift of the frequency towards the lower part of the range. The presence of an OH group at the 2-position of the phenyl ring on either side of the C=N bond, as was the case with the ligand in the present work, causes a bathochromic (to lower frequencies) shift as shown in Table 2:1 (Wilkinson *et al.*, 1987). Upon coordination to metal ions through both O and N, a decrease of the C=N frequency is generally observed (Wilkinson *et al.*, 1987).

Table 2:1: Typical C=N stretching frequencies for some $R'C_6H_4CH{=}NR''$ derivatives in $CHCl_3$ solutions

R′	R″	ν (cm^{-1})
H	2-OHC_6H_4	1657
2-OH	2-OHC_6H_4	1634
2-OH	$CH_2N{=}CHC_6H_4$-2-OH	1634

In these compounds the phenolic C-O stretching vibration occurs between 1288 and 1265 cm^{-1} (Wilkinson *et al*., 1987).

For complexes of the type Cu_2LL' and Ni_2LL' (HL' = exogenous 2-atom bridge between the 2 metal centers consisting of pyrazole and related species; H_3L is derived from the condensation of salicylaldehyde with 1,3-diaminopropan-2-ol or 1,5-diaminopentan-3-ol), an IR band in the range 1610 - 1630 cm^{-1} was ascribed to νC=N, and another in the range 1580 - 1590 cm^{-1} ascribed to νC=C (Mazurek *et al*., 1986). Carré and co-workers reported IR (cm^{-1}; CCl_4) data for cobalt complexes of derivatives of bis(salicylideneimino-3-propyl)amine to be 1633 cm^{-1} (νC=N) and 1582 cm^{-1} (νC=C) (Carré *et al*., 2003).

UV data:- Schiff bases derived from substituted salicylaldehyde (SAL) and alkylamines, exhibit four bands in the near UV that are solvent dependent. The band in the region of 240 nm, attributed to the $n \rightarrow \pi$ transition of the C=N chromophore, is optically active if the chromophore is asymmetrical about the C=N bond (Wilkinson *et al*., 1987), such as is the case with the ligand used in the present work. Data for the ultraviolet absorption maxima of 2-OHSALPN [bis(salicylidene)-1,3-diaminopropan-2-ol], which is similar to 2OH-*o*VANPN used as ligand in the present work, in various solvents are summarised in Table 2:2 (Alexander and Sleet, 1970). The UV absorption spectra, in absolute ethanol of 2-OHSALPN, gave the maxima (nm) as shown in Table 2:1 (Alexander and Sleet, 1970).

Table 2:2 (Alexander and Sleet, 1970)**:** The UV maxima of bis(salicylidene)-1,3-diaminopropan-2-ol in various solvents.

UV ABSORPTION MAXIMA (nm)			
Water	Ethanol	Dioxan	Cyclohexane
-	257, 282, 318, 404	258, 318, 404	280, 322

2.3 TRANSITION METAL COMPLEXES OF SCHIFF BASES

Transition metal complexes of Schiff bases have been known from as early as 1840, when a dark green crystalline solid, bis(salicylaldimino)Cu(II), had been isolated from the reaction of cupric acetate, salicylaldehyde, and aqueous ammonia (Holm *et al*., 1966).

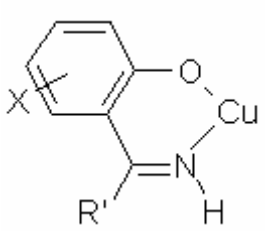

Figure 2.8: Structure of bis(salicylaldimino)Cu(II)

Metal complexes of Schiff bases have occupied a central role in the development of coordination chemistry (Holm *et al*., 1966). Evidence of this is given by the vast number of publications ranging from synthesis to biological activity of these complexes.

In recent years, there has been considerable interest in the chemistry of transition metal complexes of Schiff bases (Golcu *et al*., 2005). This is due to the fact that Schiff bases offer opportunities for inducing substrate chirality, tuning the metal centred electronic factor, and enhancing the solubility and stability of either homogeneous or heterogeneous catalysts (Golcu *et al*., 2005). Schiff base complexes have been amongst the most widely studied coordination compounds in the past few years, since they are becoming increasingly important as biochemical, analytical and antimicrobial reagents (Golcu *et al*., 2005).

Schiff base complexes are known to offer (i) ease and flexibility of the synthetic procedure; (ii) diverse properties; and (iii) use as biological models or biologically active compounds.

2.3.1 Biological activity

Catalysts for regulation of cellular processes:- Metal complexes synthesised by Volpin and co-workers, for example, could be used as catalysts for regulation of certain

processes in living cells because they show catalytic activity in model chemical reactions such as the autooxidation of NADH (Mathews and van Holde, 1990) and cytochrome C (Vol'pin *et al*., 1981).

Anticancer activity:- It has been shown that Schiff base complexes derived from 4-hydroxysalicylaldehyde and amines have strong anticancer activity, e.g., against ***Ehrlich ascites carcinoma*** (EAC) (Golcu *et al*., 2005). Good antitumor activities were observed with some metal chelates (Hodnett *et al*., 1972). Tumor cells are generally more acidic than normal cells, and Schiff base compounds are readily hydrolysed in acidic medium; hence, Schiff base compounds are preferentially hydrolysed at the tumor site (Billman *et al*., 1969). The activity of these compounds could be due to the molecule as a whole or due to liberation of aldehydes at the tumor site (Billman *et al*., 1969).

2.3.2 Synthesis and characterisation

From all the Schiff base complexes, those derived from salicylaldimines have been by far the most thoroughly studied and have played an important role in revealing the preferred co-ordination geometries of metal complexes (Holm *et al*., 1966). Of particular interest have been those involved in forming copper(II) complexes since they reveal surprising molecular diversity (Marinovich *et* al., 1999). It seems like a sensible choice then in the present work to investigate metal complexes of 2OH-*o*VANPN, which is a salicylaldimine.

Structural types and naming of salicylaldimine complexes:- Currently the most significant complexes of the salicylaldimines are of the structural types (**a**) and (**b**) in Figure 2.9 in which R, X, and B are generalised nitrogen, ring, and bridging group substituents, respectively (Holm *et al*., 1966). Type (**a**) in Figure 2.9 corresponds to the 1 : 1 salicylaldehyde-alkylamine stoichiometry of the ligand and type (**b**) in the same figure, to the 1 : 2 salicylaldehyde-alkylamine mole ratio. Furthermore, these two structures represent mononuclear complexes, but bi-and trinuclear complexes with this ligand have also been synthesized (Holm *et al*., 1966). According to the numbering of the salicylaldimine structural types, if in Figure 2.9 (a), X = 3-Me, R = *n*-Pr, and *n* = 2, the

name of the complex is bis-(3-methyl-*N*-*n*-propyl-salicylaldimino)M(II) or M(X-R-sal)$_n$. If in Figure 2.9 (b) B = CH_2CH_2 and X = H, the complex is named *N*,*N*′-bis(salicylidene)ethylenediaminoM(II) or M(H-sal)$_2CH_2CH_2$ (Holm *et al*., 1966). This method avoids cumbersome systematic naming of these complexes.

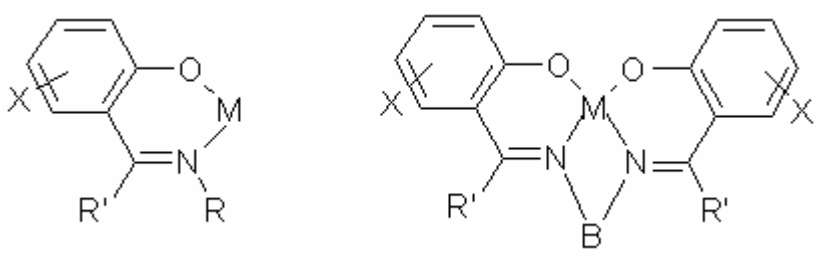

(a) **(b)**

Figure 2.9: The most significant structural types of the salicylaldimine complexes

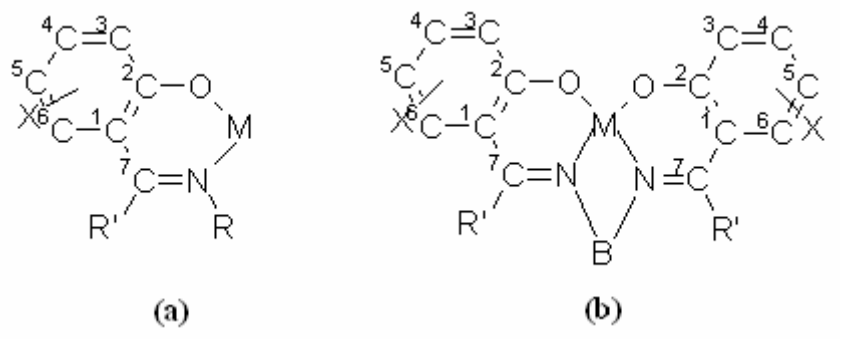

(a) **(b)**

Figure 2.10: Systematic numbering of the most significant structural types of the salicylaldimine complexes

Synthetic methods for salicylaldimine complexes:- The following three synthetic methods have been employed for salicylaldimine complexes (Holm *et al*., 1966 and Kruger *et al*., 2000).

(*i*) The self-assembly or aggregation of metal centres and preformed ligand species in the presence of base. These reactions are usually carried out homogeneously in alcohol or aqueous alcohol solution with a base such as acetate or hydroxide, but occasionally fail for *N*-alkylsalicylaldimines due to hydrolysis of the Schiff base.

(*ii*) The direct reaction of primary amine into preformed bis- or tris(salicylaldehyde) metal complex. This reaction, originally discovered by Schiff, is the most important general preparative method.

(*iii*) The reaction of salicylaldehyde with the amino group(s) already bound to the metal. The reaction has been applied to a variety of ring substituted complexes (See Figure 2.9 or 2.10 above) with B = en and pn.

The present work employed predominantly method (i) for salicylaldimine complex synthesis because this method is known to offer the advantage of more stringent control over the course of the reaction and upon the products that form over the other two routes (Kruger *et al*., 2000).

Use of visible absorption spectra to determine structural geometry of chelates:- The determination of the geometry of a chelate by use of visible absorption spectra is easily achieved by comparing the chelate spectrum with that of its unidentate analog. This direct comparison is not expected to be exact because it has definitely been shown that a chelating ligand and its unidentate analog are not necessarily in the same position in the spectrochemical series (Hare, 1968).

Geometrical forms of Schiff base complexes of transition metal ions:- Most chelates that are formed with transition metal ions have pseudo-octahedral geometry; that is, they are six-coordinate, and if the donor atoms were the same and if the spanning chelate moiety were neglected, they would be geometrically regular octahedral (Hare, 1968). Tetrahedral geometry is not common in chelates, but the divalent metal ions of Mn, Fe, Co, Ni, Cu, and Zn and trivalent Fe have all been shown to form tetrahedral complexes, and chelate examples exist for most of these ions (Hare, 1968). In addition, various salicylaldimine Schiff bases have shown (Holm *et al*., 1966) to form five-coordinate chelates with many metals including Cu(II) and Co(II).

Geometrical forms of N-alkylsalicylaldimines chelates of transition metal ions:- A large variety of *N*-alkylsalicylaldimines chelates (Figure 2.11) of Co(II), Ni(II), Cu(II), and Zn(II) have been prepared, and they constitute the best examples of pseudo-tetrahedral chelates with mixed donor atoms (Hare, 1968).

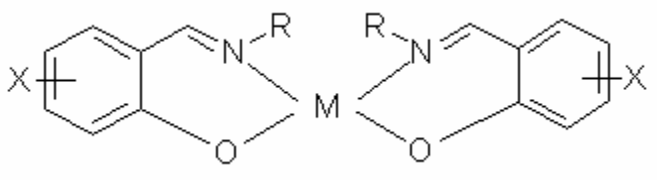

Figure 2.11: *N*-alkylsalicylaldimine chelates, M = Co(II), Ni(II), Cu(II) and Zn(II)

These complexes may exist in associated polymeric (octahedral), square-planar, and tetrahedral forms (Hare, 1968). The ligand used in the present work belongs to the *N*-alkylsalicylaldimine class of ligands. Mikuriya and co-workers, for example, when attempted to prepare a tetranuclear species with 1.3 bis(salicylideneamino)-2-propanol (L), isolated a binuclear complex $\{Mn_2(L)_2(H_2O)\}.\ 3CH_3OH$ (Mikuriya *et al*., 1992a). The diffuse reflectance spectrum of the complex showed three absorption bands at 372, 525 (shoulder) and 725 nm (shoulder). These bands may be due to the splitting of the ground ^5E_g and the excited $^3T_{2g}$ states of the octahedral Mn(III) ion, which has a ^5D ground term. Co(II) chelates of the *N*-alkylsalicylaldimines are totally indicative of tetrahedral geometry in the solid state and in solution. {Bis(*N*-isopropylsalicylaldimine copper(II)} is a flattened tetrahedron with bands at 1124, 714 and 488 nm (van Wyk *et al*. 2008). Co(II) complexes from *N*-(aryl) salicylaldimine ligands have a distorted tetrahedral geometries (van Wyk *et al*. 2008).

A list of definitely characterised transition metal-salicyladimine complexes derived from N,N'-bis(salicylaldimine):- A fraction from the list of definitely characterised transition metal-salicyladimine complexes is set out in Tables 2:3 and 2:4 (Holm *et al*., 1966). The transition metals, namely, Co(II), Co(III) and Cu(II), used in the present work, are listed, together with the possibilities for X and R.

Table 2:3: Characterisation of bis-and tris-salicylaldimine complexes derived from bi-and tridentate ligands (Holm *et al*., 1966)

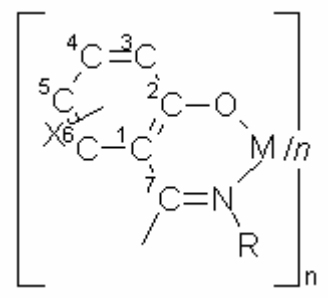

cobalt(II)-, cobalt(III)- and copper(II) complexes

M	R	X
Co(II)	H	H
Co(II)	Me (or Et)	H
Co(II)	*n*-Pr	H, 3-Cl
Co(III)	H	H
Co(III)	Me (or Et)	H
Co(III)	*n*-Pr	H, 3-Cl
Cu(II)	H	H
Cu(II)	Me (or Et)	H
Cu(II)	*n*-Pr	H, 3-Me, 3-Cl
Cu(II)	*i*-Pr	3-OMe, 3-Cl

Table 2:4: Characterisation of *N,N'*- bis (salicylaldimine) complexes (Holm *et al*., 1966)

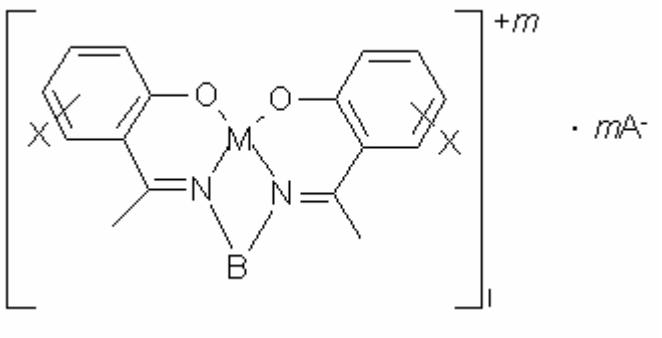

cobalt(II)- (m = 0), cobalt(III)- (m = 1) and copper(II) (m = 0) complexes

M	B	X	A^-
Co(II)	CH_2CH_2	H, 3-OMe, 3-OEt; 3-Me, 3-Et	
Co(II)	$CH_2CH_2CH_2$	H	
Co(II)	CH_2CHMe	H, 3-MeO	
Co(III)	CH_2CH_2	H	OH^-, Cl^-
Co(III)	$(CH_2)_2NH(CH_2)_2NH(CH_2)_2$	H	Cl^-, $½S^{-2}$
Cu(II)	$CH_2CH_2CH_2$	H	
Cu(II)	CH_2CHMe	H	
Cu(II)	$(CH_2)_2NH(CH_2)_2$	H	
Cu(II)	$(CH_2)_4COR'$: R'= OMe; OEt	H	

2.3.3 Manganese

Manganese (II), (III) and (IV) are of biological importance. Enzymes containing Mn(III) in at least one of their catalytic forms, like manganese superoxide dismutase, use manganese in redox roles at their catalytic center (Bonadies *et al*., 1989).

2.3.3.1 Biological activity

Mn^{2+} in enzyme catalysis:- The effects of divalent metal ions (M^{2+}) on the catalase-like activities of mononuclear Schiff base Mn(III) complexes, such as [Mn(salen)Cl], [Mn(saltn)Cl], [Mn(saltnOH)Cl], and [Mn(saltnOCOPh)Cl], in dimethylformamide (DMF) have been reported (Uehara, *et al*., 1998). In the presence of M^{2+}, $[Mn(salen)]^+$ reacted with M^{2+} (M^{2+} = Mn^{2+}, Co^{2+}, Ni^{2+}, Cu^{2+}, and Zn^{2+} ions) to give dinuclear Mn(III)-M(II) and trinuclear $Mn(III)_2$-M(II) complexes are inactive toward H_2O_2 in DMF. For the Cu^{2+} ion, the dinuclear Mn(III)-Cu(II) complexes with the salen and saltnOCOPh ligands showed high catalase-like activities, although the trinuclear complexes were inactive (Uehara *et al*., 1998).

Dinuclear Mn(III) complexes oxidize water to dioxygen:- The pentadentate ligand, 2-OHSALPN, used in the synthesis of dinuclear Mn(III) complexes, formed an attractive model for modelling the structure and activity of enzymes containing manganese(III) at their active sites (Bonadies *et al*., 1989). Such dinuclear Mn(III) complexes were able to photochemically oxidize water to form dioxygen (Bonadies *et al*., 1989).

Salen (and salicylideamino)-type Cu(II) complexes for reduction of H_2O_2:- The effects of Cu^{2+} on the catalase-like (redox) activities of Schiff base Mn(II) complexes such as [Mn(salen)Cl] and [Mn(saltnOCOPh)Cl] were reported (Uehara *et al*., 1998). In the presence of Cu^{2+}, the manganese(II) complex reacts with the copper ion to give Mn(III) complexes highly active towards H_2O_2 in dimethylformamide (DMF) (Uehara *et al*., 1998).

2.3.3.2 Synthesis and characterisation

Ligand exchange interactions involving Mn(III) complexes of N-alkylsalicylaldimine:- Reaction of 1,3-bis(salicylideneamino)-2-propanol (H_3L), which is very similar to the ligand used in the present work, with $Mn(OAc)_2.4H_2O$ in the presence of ethylenediamine and NaSCN resulted in [Mn(salen)(NCS)], while in the presence of H_2O and Et_3N gave $[Mn_2(L)_2(H_2O)]\cdot 3CH_3OH$ (Mikuriya *et al*., 1992a). The manganese ion in [Mn(salen)(NCS)] is coordinated by two nitrogen atoms and two oxygen atoms forming a square pyramid, with the manganese(III) ion displaced from the O1, N1, N2, O2 plane by a 0.20 Å toward an axially coordinated thiocyanate ion. For $[Mn_2(L)_2(H_2O)]\cdot CH_3OH$, both manganese ions, as expected for high-spin Mn(III), have severely distorted octahedral geometries. The first product was unexpected and was a result of ligand exchange interactions and incorporation of the precipitating agent (NaSCN) into the manganese complex structure (Mikuriya *et al*., 1992a). It is for this reason that metal complex syntheses in this work predominantly involved synthesizing the complexes from the corresponding pre-formed ligand and a metal salt (that is, in the absence of ligand constituents or other possible ligands) instead of the other synthetic methods mentioned for salicylaldimine complexes under section 2.3.2.

Geometrical arrangement of a Mn(III)-N-alkylsalicylaldimine:- The Mn complexes, $[Mn(III)(Hvanpa)_2(NCS)]$ and $[Mn(III)(Hvanpa)_2]Cl\cdot H_2O$ {H_2vanpa = 1-(3-methoxysalicylaldeneamino)-3-hydroxypropane}, which has much structural similarity to the ligand (2OH-*o*VANPN) in the present work, were previously prepared and the crystal structure of the latter complex determined using X-ray crystallography (Zhang *et al*., 2000). This monomeric complex had a six-coordinate octahedral geometry. The Mn-O and Mn-N distances in the equatorial plane were in agreement with those found for other Mn(III)-Schiff-base complexes of this type. In the axial direction, the Mn-O distances were found to be measurably longer than those in the equatorial plane due to Jahn-Teller distortion at the d^4 Mn(III) center. The lattice H_2O molecules, which form part of the structure of the Mn complex, were found to interact with the phenolic O atoms through H bonding (Zhang *et al*., 2000).

2.3.4 Iron

The iron ion is of particular importance in biological systems. For example, a microorganism like ***E. coli*** devotes almost 50 genes to proteins involved in iron uptake, while the potential for mammalian tumors to develop can be estimated by the density of their transferrin receptors, which is required for iron uptake and which is therefore essential for cell growth (Cortés-Cortés *et al*., 2008).

2.3.4.1 Biological activity

Iron chelators for the treatment of cancer:- There has been much interest in the development of iron (Fe) chelators for the treatment of cancer (Richardson *et al*., 2006). Richardson and co-workers developed a series of di-2-pyridyl ketone thiosemicarbazone (HDpT) ligands which showed marked and selective antitumor activity in vitro and in vivo. The higher antiproliferating efficacy of the HDpT series of chelators relative to the related di-2-pyridyl ketone isonicotinoyl hydrazone (HPKIH) analogues can be ascribed in part, to the redox potentials of their Fe complexes which lead to the generation of reactive oxygen species. The most effective HDpT ligands as antiproliferative agents possess considerable lipophilicity and were shown to be charge neutral at physiological pH, allowing access to intracellular Fe pools, where the Fe complexes would be formed (Richardson *et al*., 2006).

Antibacterial activities *of* $Fe_3O(CH_3COO)_6(CH_3COOH)(H_2O)Cl(MeImid)\cdot H_2O$:- The complex, $[Fe_3O(CH_3COO)_6(CH_3COOH)(H_2O)]Cl(MeImid)\cdot H_2O$, where MeImid is 2-methyl-imidazole, was tested for antibacterial activity against different bacterial strains and was found to display activity over Gram-negative bacteria, but not Gram-positive strains (Cortés-Cortés *et al*., 2008). These complexes have a bacteriostatic (prevents cell replication) effect on bacterial targets.

Diiron complexes for oxygen transport and hydroxylation of alkanes:- Oxo and hydroxo-bridged diiron units are known to perform activities such as oxygen transport and hydroxylation of alkanes in biology (Cortés-Cortés *et al*., 2008).

2.3.4.2 Synthesis and characterisation

Electron transfer and ligand exchange involving Fe(salen):- The heterogeneous reaction of Fe(salen) (Figure 2.12) with ligands ($L^- = F^-$, Cl^-, OH^-, NCS^-, CN^-, SH^-, and SR^-) in MeCN afforded the purplish complexes $[Fe(salen)L]^-$, isolated as Na^+ or Et_4N^+ salts (Mukherjee *et al*., 1988). Also generated *in situ* was $[Fe(salen)(OC_6H_4\text{-p-Me})]^-$. The complexes contained high-spin Fe(II) in a square-pyramidal coordination unit with an axial L^- ligand, exhibited isotropically shifted ^1H NMR spectra of good resolution, and are electrochemically oxidizable to Fe(salen)L in chemical reversible processes. Absorption and NMR spectra clearly indicate the similarity in structure of the complexes. In this investigation by Mukherjee and co-workers fresh insight was gained into how coordinatively unsaturated complexes of this type may undergo electron transfer and ligand exchange (Mukherjee *et al*., 1988).

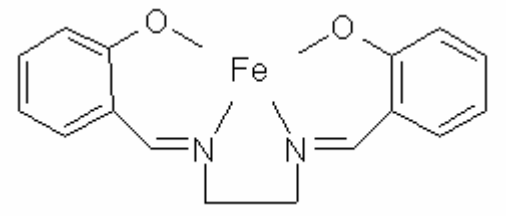

Figure 2.12: Structure of Fe(salen)

N-alkylsalicylaldimine complexes of Fe(II) and Fe(III):- Mononuclear Fe(II) and Fe(III) complexes of type (b) in Figure 2.9 have been prepared from *N*-alkylsalicylaldimine and the corresponding iron ion. The ultraviolet and visible spectra of a large number of salts of the type $[Fe(X\text{-sal})_2B]Cl$ (B = Lewis base), which is of structural type (b) in Figure 2.9, have been recorded, but no substantive interpretations have been offered (Holm *et al*., 1966).

2.3.5 Cobalt(II)

2.3.5.1 Biological activity

Co(II) complexes as anticancer agents:- Co(II) derivatives of Schiff bases of salicylaldehyde was found to be active against one form of Walker sarcoma of the rat at the Chemotherapy National Service Center (Hodnett *et al*., 1970 and Hodnett *et al*.,

1972). Vol'pin and Novodarova investigated the possibility of using cobalt chelates as catalytic generators of active oxygen radicals aimed at various cell targets, especially DNA and RNA (Vol'pin and Novodarova, 1992).

Antifungal activity of cobalt complexes:- Cobalt complexes investigated by Vol'pin and Novodarova had demonstrated high fungicide activity toward rice blast disease (Vol'pin and Novodarova, 1992).

Oxidation of phenol by Co(II) complexes:- Cobalt(II) complexes derived from *N*-(aryl) salicylaldimines ligands were found to be active for the oxidation of phenol, producing catechol and hydroquinone as the major products (van Wyk *et al*., 2008).

Cobalt(II) complexes as catalysts for biochemical processes:- Cobalt(II) complexes proved to be active catalysts for influencing some biochemical processes. Vol'pin and co-workers selected the complexes on the basis of their catalytic activity in model chemical reactions such as autooxidation of NADH (Mathews and van Holde, 1990), Q_4H_2 and cytochrome C (Vol'pin *et al*., 1981). Cobalt(II) complexes with *N*,*N'*-bis-(salycilidene)ethylenediamine and other chelates proved to be active catalysts (Vol'pin *et al*., 1981). Cobalt(II) tris-*o*-phenanthroline perchlorate was found to stimulate energization in chromatophores of purple bacteria (Vol'pin *et al*., 1981).

Co(II) complexes inactive as oxygen carriers:- A hemocyanin (Figure 2.13) is a copper(II)-containing oxygen-carrying protein in the hemolymph of molluscs and arthropods, which bind one molecule of dioxygen per two copper atoms (Lorösch and Haase, 1986).

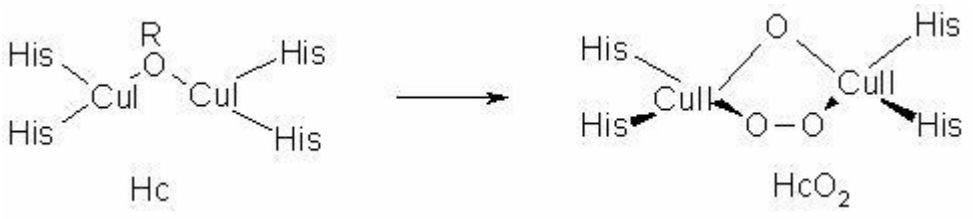

Figure 2.13: Possible structures for deoxygenated and oxygenated hemocyanin (McKee *et al*., 1984)

The hemocyanin active site was assigned as an antiferromagnetically spin-coupled copper pair. The Cu(II) pair in the hemocyanin of ***Limulus polyphemus*** was substituted with cobalt(II) (Lorösch and Haase, 1986). The absorption spectrum of the Co(II)-hemocyanin was exclusively due to the Co(II) ions and near-infrared results indicated tetrahedral coordination around the Co(II) center, which was in contrast to the tetragonal cupric site in unsubstituted Cu(II)-hemocyanin. Reaction of the Co(II)-substituted-hemocyanin with peroxide did not give rise to spectral changes that indicates the formation of a peroxo-bridged dimer. This demonstrates that the oxy-form, which is analogous to the oxygenated form of Cu(II)-hemocyanin, was not possible. Therefore, Co(II)-hemocyanin served as a model for the deoxy form of the Cu(II)- hemocyanin protein (Lorösch and Haase, 1986).

Co(II) complexes of SALEN and 3MeOHSALEN as potential dioxygen and oxygen carriers:- The cobalt(II) complexes of Schiff bases, such as SALEN (and its analogues), which is similar to the ligand and subsequently, the cobalt complexes, in the present work, have been the first and most studied of the dioxygen carriers as potential reagents for oxygen separation and transport (Chen *et al*., 1989). The O-active forms of cobalt(salen) (see Figure 2.14) derived from solvated forms such as $[Co(salen)]\cdot C_6H_6$, $[Co(salen)]\cdot CHCl_3$ and $[Co(salen)]\cdot(C_5H_5N)$, have long been known to bind dioxygen reversibly in the solid state (Murray *et al*., 1986). It has generally been accepted that the product of oxygenation is the diamagnetic peroxo-bridged species $[Co(salen)]_2O_2$ (Murray *et al*., 1986). However, a detailed study (Murray *et al*., 1986) showed that this

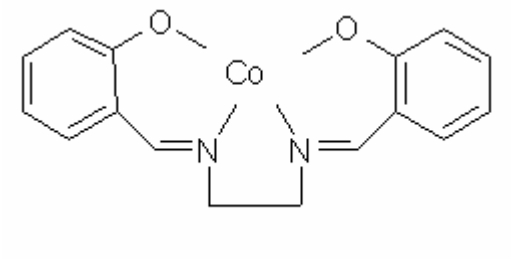

Figure 2.14: Structure of Co(salen)

was an oversimplification. The oxygenated species also contained the paramagnetic superoxo-like species [O_2Co(salen)] as well as dimer "inactive" [Co(salen)]$_2$ centers. The magnetic properties of the O-active Co(salen) samples were compatible with ferromagnetically coupled pairs of Co(salen) molecules, with further weak antiferromagnetic coupling between such sets of pairs. These magnetostructure features appeared to be related to the solid-state O reactivity (Murray *et al*., 1986). Two cobalt complexes, one with SALEN (Figure 2.14) and the other with MeOSALEN (Figure 2.15), were two of 18 complexes investigated for dioxygen affinities and oxygen-carrying properties (Chen *et al*., 1989). SALEN and 3MeOHSALEN are similar to the ligand in the present work. Co3MeOSALEN was prepared by Bailes and Calvin by having reacted the Schiff base and sodium hydroxide (1:2) followed by a hot aqueous solution of cobaltous acetate and the air removed from the reaction flask (Bailes and

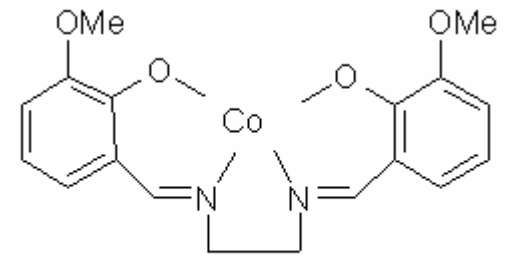

Figure 2.15: Structure of Co3MeOSALEN

Calvin, 1947). Cobalt(II) complexes of tetradentate Schiff bases such as CoSALEN and 3MeOHSALEN do not bind dioxygen sufficiently without a basic monodentate ligand that coordinates the Co(II) in the position *trans* to the dioxygen (Chen *et al*., 1989). 4-

Methylpyridine (4-picoline) was employed as the axial ligand for this investigation (Chen *et al*., 1989). There has not yet been a sufficiently broad study of cobalt Schiff base complexes to establish structure-activity guidelines that may be used to design oxygen-carriers having the most suitable properties for removal of oxygen from a mixture of inert gases without the oxygen-carriers (complexes) undergoing degradation reactions to unreactive carriers (complexes) (Chen *et al*., 1989).

Heterogenous Co(II) and Cu(II) complexes as potential oxygen carriers:- Cobalt(II) Schiff base complexes that are able to reversibly coordinate the dioxygen ligand in solution, are known to undergo oxidative degradation to inert compounds incapable of carrying oxygen (Carré *et al*., 2003). Therefore, in the search for dioxygen carriers that are immune against oxidative degradation, Carré and co-workers investigated heterogenous Co(II) and Cu(II)complexes.

Reasons for investigating Co(II) complexes in the present work:- The above-mentioned approaches provide new possibilities for the regulation of biochemical processes and should promote the creation of new such cobalt compounds with high biological activity (Vol'pin and Novodarova, 1992); hence, the present investigation into Co(II) and Co(III) complexes of salicylaldimines.

2.3.5.2 Synthesis and characterisation

Geometrical structure of N,N′-bis(salicylidene)ethylenediaminocobalt(II):-

Cell dimensions and packing considerations revealed that *N,N′*-bis(salicylidene)ethylenediaminocobalt(II) had a planar structure (Holm *et al*., 1966).

Structure and geometry of cobalt(II) complexes of salicylaldimines:- Salicylaldimine complexes of Co(II) are well known and appear to be confined to types (a) and (b) in Figure 2.9. The UV spectra of the Co(II) chelates of the *N*-alkylsalicylaldimines are totally indicative of tetrahedral geometry in the solid state and in solution (Hare, 1968).

2.3.6 Cobalt(III)

2.3.6.1 Biological activity

Anticancer activities of alkylcobalt(III) complexes:- Alkylcobalt(III) complexes generate alkyl radicals, which are known to damage biological targets (e.g. cancer cells) and are especially able to cleave nucleic acids (Sykes, 2000).

Anticancer activity of [Co(acacen$_2$en)(NH$_3$)$_2$]Cl:- Some authors have shown that inorganic cobalt(III) complexes, which contain no metal-carbon bond, can be reduced in tumors due to the reductive nature of many tumors (Osinsky *et al*., 2000). Tumors contain significant regions of low oxygen tensions; thus, can kickstart a catalytic autooxidation process involving generation of very reactive oxygen species, which in turn could start catalytic oxidation of substrates and thereby show antitumor action (Osinsky *et al*., 2000). Osinsky and co-workers conducted *in vivo* anti-cancer tests on complexes with the basic structure [Co(acacen$_2$en)(NH$_3$)$_2$]Cl and their analogs. Local hyperthermia (1h; 43 or 41℃) was performed using a microwave unit. The tumors were irradiated by 190 kV X-rays (RT). All cobalt complexes showed anticancer, in particular, antimetastatic activity (Osinsky *et al*., 2000).

Anticancer activity of Co(III) complexes of Schiff bases:- Osinsky and co-workers have shown that cobalt(III) complexes with tetradentate Schiff bases have been shown to display selective anticancer activity, in particular, antimetastatic activity (Osinsky *et al*., 2000).

Antiviral activity of [Co(III)(acacen)L$_2$]$^+$:- The complex [Co(acacen)L$_2$]$^+$ (Figure 2.16), where L = ammonia or methylimidazole, has also been shown to inhibit the replication of the herpes virus. A possible mechanism for the observed inhibition involved the inactivation of an enzyme by irreversible binding of the cobalt complex to histidine residues (Dunnick *et al*., 1999). This kind of research aims to increase inhibitor specificity by attaching short peptides that are known to have a high affininity for target enzymes. Functionalised 1,2-diamines, such as the 1,3-diaminopropan-2-ol that is used in

the present work, are incorporated into the Schiff base backbone of such inhibitors (Dunnick *et al*., 1999).

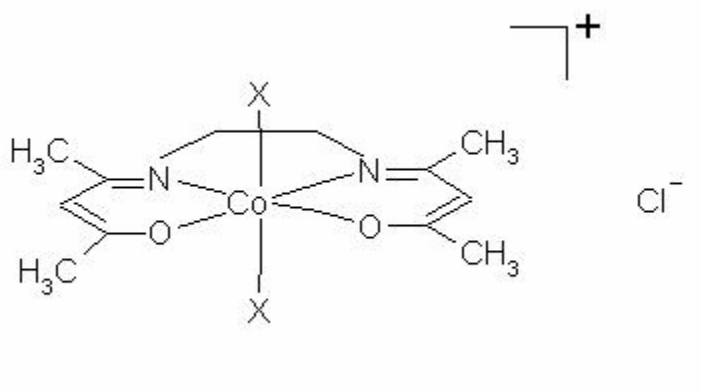

Figure 2.16: Structure of cobalt(III) Schiff base complexes of acacen (acacen = bis-acetylacetonate ethylene diimine), where X = NH_3 or 2-MeIm (Dunnick *et al*., 1999)

Reduction of activity of human α-thrombin by Co(III) complexes of acacen:- α-Thrombin is an enzyme associated with the blood coagulation cascade in humans. It converts fibrinogen into fibrin and ultimately results in the formation of blood clots (Takeuchi *et al*., 1998). This ultimate effect of α-thrombin can be unwanted in a patient who had undergone thrombolytic therapy following a heart attack as the enzyme's activity has been linked to reocclusion of coronary arteries; hence Tacheuchi and co-workers' interest in cobalt(III) Schiff base complexes of acacen (Figure 2.16). The latter complexes, which each have an N_2O_2 donor set around the metal, reduce enzymatic activity by binding to histidine residues in enzyme active sites and on enzyme surfaces in a random fashion. It was found that binding of these complexes is controlled by axial ligand substitution. To increase inhibitor specificity and potency, a short peptide (-dFPR-) that is known to have a high affinity for the human α-thrombin active site was attached to the chelate. The targeting peptide, linked to a cobalt chelate lead to selective, irreversible inhibition of thrombin. Further work on such peptide-chelate conjugates could yield powerful and highly selective inhibitors toward a variety of enzyme targets (Takeuchi *et al*., 1998).

2.3.6.2 Synthesis and characterisation

Structure and geometry of salicylaldimine complexes of Co(III):- Salicylaldimine complexes of Co(III) are well known. Just as Co(II), Co(III) complexes appear to be

confined to types (a) and (b) in Figure 2.9 (Holm *et al*., 1966). Nearly all Co(III) complexes of type (b) in Figure 2.9 permit the formation of quasi-octahedral complexes (Holm *et al*., 1966).

2.3.7 Nickel

Much of the interest in salicyladimine complexes rests within this group (Holm *et al*., 1966). Here, the effects of ligand structure on the stereochemical and electronic properties of complexes have been dramatically illustrated and most thoroughly investigated (Holm *et al*., 1966).

2.3.7.1 Biological activity

Anticancer activity of a nickel(I) complex with the Schiff base derived from 2,4-dihydroxybenzaldehyde and L-arginine:- A nickel(I) complex with the Schiff base derived from 2,4-dihydroxybenzaldehyde and L-arginine has been synthesized and characterized by elemental analyses, TG-DTA, IR, electronic spectra and conductivity measurements (Chunhua *et al*., 1993). The results suggest that the Schiff base acts as a tridentate ligand. Electronic and fluoresence spectroscopy indicated that the nickel(I) complex intercalate DNA (Chunhua *et al*., 1993). This nickel complex gave 51.7% inhibition rates to EAC (Ehrlich ascites carcinoma) during a test for anticancer activity (Chunhua *et al*., 1993).

Antibacterial activity and structure of metal complexes of 2-(N-salicylideneamino)-3-carboxyethyl-4,5-dimethylthiophene:- Mn(II), Fe(II), Co(II), Ni(II), Cu(II) and Zn(II) complexes with a potentially tridentate Schiff base, formed by condensation of 2-amino-3-carboxyethyl-4,5-dimethylthiophene with salicylaldehyde were synthesized and characterized on the basis of elemental analyses, molar conductance values, magnetic susceptibility measurements, UV–vis, IR, EPR and NMR spectral data, wherever possible and applicable (Daniel *et al*. 2008). Spectral studies reveal that the free ligand exists in a bifunctionally hydrogen bonded manner and coordinates to the metal ion in a tridentate fashion through the deprotonated phenolate oxygen, azomethine nitrogen and ester carbonyl group. The ligand and the complexes were subjected to antibacterial screening

using two pathogenic bacteria (***Staphylococcus aureus*** and ***Alpha-haemolytic streptococci***). It has been observed that the ligand has been physiologically active and chelation enhanced its activity. The mode of action of the complexes indulge in the formation of hydrogen bonded interaction through the coordinated anion, azomethine group etc with the active centers of the cell constituents resulting in interference with the normal cell processes (Daniel, *et al*. 2008).

Antimicrobial activity of salicylidene-based mixed-ligand Ni(II) complexes:- A few mixed-ligand complexes of the types $\{M(SB^1)_2$ bipy-amine$\}$ and $\{M(SB^2)_2$ bipy-amine$\}$ (M = Mn(II), Co(II), Ni(II) and Cu(II), HSB^1 = 5-chlorosalicylidene analine, HSB^2 = 5-bromosalicylidene analine and bipy-amine = 2,2′-bipyridalamine) showed antimicrobial activities against bacteria, yeasts and fungi (Dholakhiya and Patel, 2002).

2.3.7.2 Synthesis and characterization

Electrochemical oxidation of N,N′-polymethylenebis(3,5-di-tert-butylsalicylaldiminato)nickel(II) complexes:- Several *N*,*N*′-polymethylenebis(3,5-di-*tert*-butylsalicylaldiminato)nickel(II) complexes, $Ni(L_x)$ (x = 1 – 4) (Figure 2.17), have been studied by cyclic voltammetry under nitrogen atmosphere and in situ UV–Vis spectroscopy in DMF (Özalp-Yaman *et al*., 2005). The first oxidation peak potential for all the Ni(II) complexes corresponds to the reversible one-electron oxidation process of the metal center, yielding Ni(III) species. The second oxidation peak of the complexes was assigned as the ligand based oxidation, generating a coordinated phenoxy radical species (Özalp-Yaman *et al*., 2005). This second oxidation could be an important aspect

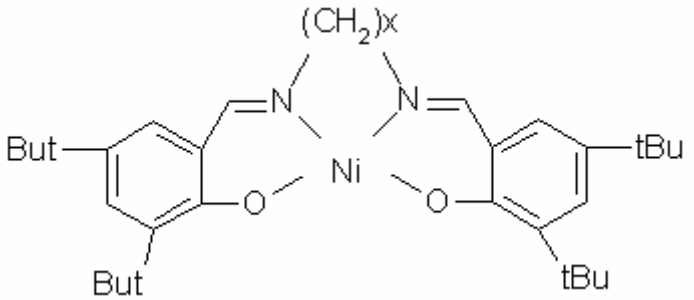

Figure 2.17: *N*,*N*′-polymethylenebis(3,5-di-*tert*-butylsalicylaldiminato)nickel(II) complexes (Özalp-Yaman *et al*., 2005)

in developing anticancer drugs.

Geometry of Ni(II) chelates of N-alkylsalicylaldimines:- Interest in Ni(II) salicylaldimine complexes was initiated by the fact that in noncoordinating solvent, Ni(Me-sal) was paramagnetic, which was initially proposed to be due to planar (diamagnetic) and tetrahedral (paramagnetic) species that existed in solution (Holm *et al.*, 1966). Later it was suggested that weak axial perturbation by solvent molecules of the planar complexes stabilised a triplet ground state (that is, the triplet state was lowered to within thermal range), which in turn required a five coordinate structure of the Ni(II) complex (Holm *et al.*, 1966). Spectra of Ni(II) chelates of *N*-alkylsalicylaldimines were found to be characteristic of tetrahedral Ni(II) with transitions $^3T_1 \rightarrow {}^3A_2$ (ν_2), $^3T_1 \rightarrow {}^3T_1$ (ν_3), and $^3T_1 \rightarrow {}^1T_2$ (or ^1E), respectively, assigned to bands at 1492, ~ 667 and 9174 nm (Hare, 1968). Structure studies of *N*,*N'*-bis(salicylidenethylenediamino)Ni(II) revealed that the entire molecule was not planar but twisted about the C-C bond with bridging groups in the gauche configuration (Holm *et al.*, 1966).

Dinucleur Ni(II) complexes of 2-OHSALPN:- The Schiff base ligand, H_3SalDpl (or 2-OHSALPN), was formed by the condensation of salicylaldehyde and 1,3-diamino-2-propanol (Brezina et al., 1997). Three dinuclear compounds, Ni_2(SalDpl)N(CN)$_2$·2H_2O, Ni_2(HSalDpl)PhA·2MeOH and Ni_2(HSalDpl)Pc·2MeOH (where H_2PhA = phthalic acid and H_2Pc = pyrocatechol) were prepared and characterized by elemental analyses, IR and visible spectroscopies and magnetochemical measurements (Brezina *et al.*, 1997).

IR data of dinuclear Ni(II) complex of 2-OHSALPN, with the pyrazolate anion as coligand:- A nickel(II) complex, Ni_2(L)(pz), was synthesised (L = 2-OHSALPN and pz = pyrazolate anion) (Mikuriya *et al.*, 1992b). The ligand, L, is very similar to the ligand (2OH-*o*VANPN) in the present studies. IR data revealed a broad band in the range 3250 - 3420 cm^{-1} for the alcohol and phenol OH in the free ligand, but absent in the complex, which indicates that the alcoholic and phenolic protons are lost upon complexation. The νC=N band appeared at 1630 cm^{-1} in the free ligand and at 1620 cm^{-1} upon complexation, suggesting that the imino nitrogen is coordinated to the nickel ion.

The molecular structures of these complexes were determined by single-crystal X-ray structure analyses (Mikuriya *et al*., 1992b).

Mono- and dinuclear Ni(II) complexes of 2-OHSALPN-type ligand and pyrazole-type coligand:- Redox processes in DMF at mercury and platinum electrodes were examined for Cu_2LL' and Ni_2LL' (H_3L = pentadentate ligand derived from the condensation of acetylacetone or salicylaldehyde with 1,3-diaminopropan-2-ol or 1,5-diaminopentan-3-ol; HL' = exogenous 2-atom bridge between the 2 metal centers consisting of pyrazole and related species) (Mazurek *et al*., 1986). Evidence for structurally different forms of the complexes was provided in this investigation. Amongst the complexes synthesised was a mononuclear complex of 1,3-bis(salicylideneamino)-2-propanol with Ni(II) and Cu(II), respectively, which is similar to what was synthesised in the present work. For complexes of this type, a IR band in the range 1610 - 1630 cm^{-1} was ascribed to *ν*C=N, and 1580 - 1590 cm^{-1} ascribed to *ν*C=C (Mazurek *et al*., 1986).

2.3.8 Copper

Copper is an essential trace element and its concentration in the cytoplasm of cells is regulated by different mechanisms (that is, pumps, exchangers and by proteins expression, which use copper in their active sites) (Fernandes *et al*., 2006). The development of mimic systems for copper metalloenzymes has proved of importance to understand the processes of natural biomolecules as well as to extend this knowledge to systems other than those of natural occurrence, for example, the use of copper compounds for mechanistic studies, drug design or as biotechnological tools. Copper synthetic compounds are able to promote nucleic acid (especially DNA) cleavage and are therefore worth investigating both *in vitro* and *in vivo* against cancer cells.

The chemistry of copper-based pseudonucleases in photodynamic therapy has received little attention (Reddy *et al*., 2004). Copper being a bio-essential transition metal ion, its complexes showing photocleavage activity could find better application at the cellular level in comparison to the 4d- or 5d metal analogues (Reddy *et al*., 2004). The first copper complex showing efficient DNA cleavage activity was bis(1,10-

phenanthroline)copper(I) (Reddy *et al*., 2004).

2.3.8.1 Biological activity

Light-induced photocleavage of DNA by bis(1,10-phenanthroline)copper(I), [CuL(phen)](ClO_4), [CuL(dpq)](ClO_4) and [CuL(dmp)](ClO_4) for possible use as photodynamic therapeutic agents:- The first copper complex showing efficient DNA cleavage activity was bis(1,10-phenanthroline)copper(I) (Reddy *et al*., 2004). Copper(II) complexes [CuLL′](ClO_4), where HL is a NSO-donor Schiff base {2-(methylthio)phenyl}salicylaldimine and L′ is a NN-donor base like 1,10-phenanthroline (phen), dipyridoquinoxaline (dpq) and 2,9-dimethyl-1,10-phenanthroline (dmp), were prepared in high yield from the reactions of copper(II) acetate hydrate with the NN-donor heterocyclic bases and the NSO-donor Schiff base in methanol and isolated as perchlorate salts (Reddy *et al*., 2004). The infrared band at 1612 cm^{-1} is assignable to the C=N functional group (Reddy *et al*., 2004). The complexes have a distorted square-pyramidal (4 + 1) CuN_3OS coordination geometry. Relative binding of the complexes to calf thymus (CT) DNA with respect to the bis-phen copper(II) complex was studied by fluorescence spectral method (Reddy *et al*., 2004). The cleavage of supercoiled DNA was monitored by agarose gel electrophoresis. Photocleavage experiments were conducted at different complex concentrations (50–300 μM) and exposure times (Reddy *et al*., 2004). The phen and dpq complexes showed photocleavage activities. The dpq complex with its high DNA binding propensity exhibited efficient photocleavage activity under aerobic conditions on visible or UV light irradiation (Reddy, *et al*., 2004). Mechanistic studies revealed oxygen sensitization in the photocleavage reactions (Reddy, *et al*., 2004). The role of the heterocyclic base in the complexes is primarily binding to the DNA minor groove while the Schiff base containing thiomethyl group and dpq with a quinoxaline moiety act as photosensitizers. The results showing red light-induced photocleavage activity are of importance in the development of the chemistry of copper-based reagents for photodynamic therapy (PDT) for which the basic requirements are the presence of a photosensitizer (drug), oxygen and a light source of wavelength >650 nm (Reddy *et al*., 2004).

Anticancer activity of salicylaldehyde-based Cu(II) complexes:- Copper(II) complexes of salicylaldehyde derivatives are active against a variety of tumor cell lines (Sykes, 2000). A complex from the mixed-ligand Cu(II) amino acid phenanthroline complexes may soon enter clinical trials because of the success of $[Cu(L\text{-}Ser)(phen)(H_2O)]^+$ as an effective anticancer agent (Sykes, 2000).

Anticancer activity of a copper(I) complex with the Schiff base derived from 2,4-dihydroxybenzaldehyde and L-arginine:- A copper(I) complex with the Schiff base derived from 2,4-dihydroxybenzaldehyde and L-arginine has been synthesized and characterized by elemental anlyses, TG-DTA, IR, electronic spectra and conductivity measurements (Chunhua *et al*., 1993). The results suggest that the Schiff base acts as a tridentate ligand. Electronic and fluoresence spectroscopy indicated that the Cu(I) complex intercalate DNA (Chunhua *et al*., 1993). This complex gave 53.3% inhibition rates to EAC (Ehrlich ascites carcinoma) during a test for anticancer activity (Chunhua *et al*., 1993).

$[Cu(HPCINOL)Cl]Cl{\cdot}MeOH$ and $[Cu_2(Hbtppnol)(\mu\text{-}CH_3COO)](ClO_4)_2$ promote cleavage of DNA:- Fernandes and co-workers demonstrated that near physiological conditions [Cu(HPCINOL)Cl]Cl·MeOH {HPCINOL = 1-(bis-pyridin-2-ylmethyl-amino)3-chloropropan-2-ol} promoted the cleavage of plasmid DNA of human myeloid leukemia cells, THP-1, through hydrolytic cleavage of the DNA phosphate ester groups, which remain coordinated to the copper(II) center (Fernandes *et al*., 2006). Rossi and co-workers, supported by structural and kinetic data, have shown that the copper complex, $[Cu_2(Hbtppnol)(\mu\text{-}CH_3COO)](ClO_4)_2$ {H_2btppnol = *N*-(2-hydroxybenzyl)-*N*,*N*′,*N*′-tris(2-pyridylmethyl)-1,3-diaminopropanol}, can promote stoichiometric hydrolysis of the bis(2,4-dinitrophenyl)phosphate (a DNA mimic), promoting the cleavage of only one 2,4-dinitrophenyl group, while the 2,4-dinitrophenylphosphate group remained bonded to the copper centres after the hydrolysis process, forming a phosphate bridge (Rossi *et al*., 2005).

Antimicrobial activity of Cu(II) and Cd(II) complexes of bidentate Schiff base ligands:- Cd(II) and Cu(II) complexes of bidentate Schiff base ligands (Figure 2.18) were synthesized and characterized (Golcu *et al*., 2005). In the ligands, the bands in the 3500 – 3420 cm^{-1} range may be assigned to *v*O–H stretching (Golcu *et al*., 2005) . For the free ligands, the broad bands in the 2800 – 2700 cm^{-1} range are assigned to the OH group vibration (*ortho* position) associated intramolecularly with the nitrogen atom of the imine group (Golcu *et al*., 2005).

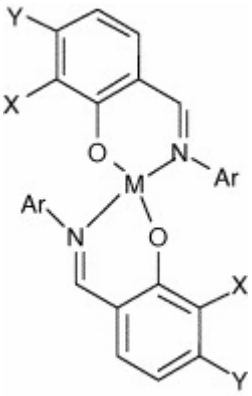

Figure 2.18: Cu(II) and Cd(II) complexes of bidentate Schiff base ligands

Fifteen compounds (in $CHCl_3$) were evaluated for their *in vitro* antibacterial activity against *Bacillus megaterium* DSM 32 and antifungal activity against *Candida tropicalis* FMC 23 by the agar-well diffusion method (Golcu *et al*., 2005). It was observed that all the compounds tested showed antibacterial and antifungal activity.

Antimicrobial activities of Cu(II) complexes derived from N-salicylideneglycinato aquacopper(II) hemihydrate parent compound:- The reaction of an equimolar ratio of *N*-salicylideneglycinatoaquacopper(II) hemihydrate (the parent compound) with urea, pyridine, 2,4-dimethylpyridine, 3,5-dimethylpyridine, quinoline, 4-methylquinoline, isoquinoline, or 3-methylisoquinoline, respectively, resulted in solid products containing complexes of the type Cu(salgly)L with distorted square pyramidal coordination polyhedra (Valent *et al*., 2005). Using the resulting solid products as test material, tests in

vitro were run on various strains of bacteria, yeasts and filamentous fungi. Some of these complexes were found to have antimicrobial activity (Valent *et al*., 2005). Single crystal X-ray diffraction methods performed on the *N*-salicylidene glycinatoureacopper(II) dimer revealed that the copper(II) atoms were bridged by two phenolic oxygen atoms with a Cu---Cu distance of 3.1093(11) Å and Cu---O---Cu angle of 94.47(12)°(Valent *et al*., 2005).

2.3.8.2 Synthesis and characterisation

Spectroscopic data of salicylideneamino-based Cu(II) complexes as structural models for active site of hemocyanin:- Dinuclear complexes containing copper(II) centers are being investigated because of their relevance as structural models for the active sites in the dioxygen-binding protein hemocyanin (see Figure 2.13) and various multicopper oxidases (Mazurek *et al*., 1985). The preparation of a pentadentate binucleating ligand, 2,6-bis(salicylideneamino)methyl)-4-methylphenol (H_3L), together with the corresponding pyrazolate-bridged copper(II) complex, Cu_2LL' (HL' = pyrazole) were synthesised by Mazurek and co-workers (Mazurek *et al*., 1985). Spectroscopic evidence suggested square-planar coordination of the Cu ions in their Cu(II) complex. The complex had unusual stereochemical flexibility. The latter property generally enables one to study reactions coupled with reduction in some detail. IR data of the prepared Cu(II) complex revealed an absorption band at 1632 cm^{-1} compared to 1640 cm^{-1} for the free ligand and which was assigned to *ν*C=N. A UV absorption maximum in the solid state of this complex was observed at 560 nm. In chloroform solution, the UV absorption maximum occurred at 612 nm which is consistent with a square-planar coordination of the copper(II) centers (Mazurek *et al*., 1985).

Spectral data for copper(II) complexes of Schiff bases derived from amino acids and o-vanillin (Guangbin, 1994):- A broad infrared band around 3400 cm^{-1} indicated a coordinated water molecule and this was supported by thermogravimetric analysis. Also, infrared bands at 925 and 775 cm^{-1} was found to be due to rocking and wagging modes of coordinated water. A strong band at 1640 cm^{-1} was due to the imino group and bands in

the range 529 - 553 cm^{-1} and 425 - 504 cm^{-1} assigned to *ν*M-N and *ν*M-O vibrations. A single d-d band between 651 and 652 nm (or 15 360 and 15 336 cm^{-1}) was said to indicate a square planar coordination of two Cu(II) centres, which is further confirmed by solid state maximum at 560 nm and a shoulder at 605 nm (Guangbin, 1994). Cu(II) complexes derived from L-phenyl-alanine and *o*-vanillin were synthesised and characterised (Wang and Chang, 1994). IR data revealed a broad band at 3400 and 3460 cm^{-1} due to the coordinated water in the Cu(II) complex. Bands at 925 and 775 cm^{-1} were due, respectively, to rocking and wagging vibrations of the coordinated water. A strong band at 1640 and 1649 cm^{-1} was observed due to *ν*C=N. The *ν*M-N was observed at 549 cm^{-1} (Cu), while *ν*M-O (phenolic oxygen) were observed between 425 and 480 cm^{-1} (Wang and Chang, 1994). UV data (Wang and Chang, 1994) of the Cu(II) complex gave λ_{max} (ε 104 - 142 $M^{-1}. cm^{-1}$) in the range 651-652 nm, ascribed to a single d-d band. The ^2D band is known to split to the $^2E_g \rightarrow {}^2T_{2g}$ (octahedral complex) and $^2T_2 \rightarrow {}^2E$ (tetrahedral complex). The Cu(II) complex was found to be square planar. It was concluded that the Schiff bases were probably bivalent anions with tridentate ONO donors derived from the carboxylate O, imino N, and phenolic O (Wang and Chang, 1994).

Spectroscopic data of Cu(II) complexes of 2-OHSALPN and 2-OHSALPN-type ligands:- A binuclear Cu(II) complex of the ligand formed by condensation of salicylaldehyde, and 1,5-diaminopentan-3-ol were reported (Mazurek *et al.*, 1982). The binuclear Cu(II) compound (compound 2a) (Figure 2.19) featured a bridging ligand alkoxide group and an additional single-atom-bridging ligand X (X = OH, OR, Cl, Br). The N_2O_2-donor atom set around this compound was found to be essentially planar. The UV absorption spectra for this compound in MeCN and DMF revealed λ_{max} of 605 and 600 nm, respectively. The solid complex gave λ_{max} at 620 nm (Mazurek *et al.*, 1982). Another compound reported by the same team of researchers [Figure 2.20] was mononuclear and had none of these features. The mononucleating nature of the ligand used for synthesis of the latter was thus established and was attributed to the shorter chain ligand backbone 1,3-diaminopropan-2-ol in which the steric strain is too great for formation of binuclear compounds. This suggests that the ligand investigated in the present work would produce

only the mononuclear complex. However, a mixed metal dinuclear complex (metal: Ni, Zn) has been reported (Arici *et al*., 2001).

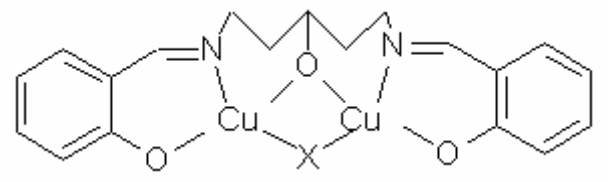

Figure 2.19: Structure of binuclear compound (compd. 2a) (Mazurek *et al*., 1982)

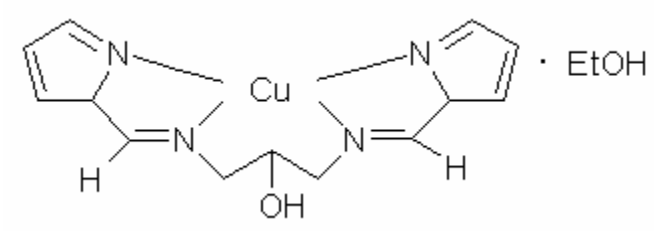

Figure 2.20: Structure of mononuclear compound (compd. 8) (Mazurek *et al*., 1982)

The compound shown in Figure 2.20 was reported to have a broad absorption in the region of OH stretching at 3500 - 3300 cm^{-1} due to the uncoordinated secondary OH of the diamine, but may also be due to the solvated EtOH. The UV absorption spectra for this compound in $CHCl_3$, MeCN and DMF revealed λ_{max} of 560, 555 and 555 nm, respectively. The solid complex gave λ_{max} of 554 nm (Mazurek *et al*., 1982). A separate team of researchers synthesised a mononuclear complex of 1,3-bis(salicylideneamino)-2-propanol with Cu(II), which is similar to that shown in Figure 2.20 and to the complexes synthesised in the present work. For these complexes an IR band in the range 1610 - 1630 cm^{-1} was ascribed to *ν*C=N, and 1580 - 1590 cm^{-1} ascribed to *ν*C=C (Mazurek *et al*., 1986).

Geometrical structure of 2-OHSALPN-based Cu(II) complexes as models for the active site structure of multicopper oxidases:- Mukherjee and co-workers attempted to prepare mimics to model the active site structure of multicopper oxidases such as ascorbate oxidase, which shows a triangular arrangement of the copper centers (Mukherjee *et al*., 2003). Two angular trinuclear copper(II) complexes, **1** and **2** (Figure 2.21), with the formula $[Cu_3(HL)LL'](ClO_4)$ were synthesized (Mukherjee *et al*., 2003). L' is imidazole (Him, **1**) or 1-methylimidazole (1-MeIm, **2**) and H_3L is a Schiff base

obtained from the condensation of salicylaldehyde and 1,3-diaminopropan-2-ol (2:1 mole ratio). **1** and **2** were prepared from the reaction of **I** (Figure 2.21) and **II** (Figure 2.21) in the presence of L' and were isolated as perchlorate salts. The crystal structures of **1** and **2** revealed an angular arrangement of the metal atoms in the trinuclear core that can model the active site structure of multicopper oxidases (Mukherjee *et al*., 2003). **I** is the monomeric copper(II) complex that is known to model galactose oxidase (type-2 copper

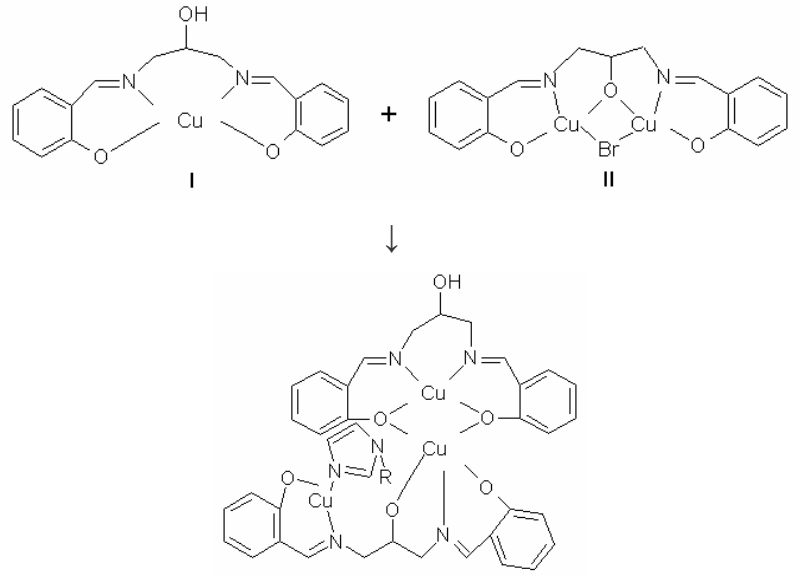

Figure 2.21: [{Cu_3(HL)LL'}(ClO_4)] (R = H, **1**; Me, **2)** (Mukherjee *et al*., 2003)

protein) activity by effectively catalyzing oxidation of primary alcohols in the presence of KOH and O_2 (Mukherjee *et al*., 2003). **II**, a dinuclear copper(II) complex, serves as a structural and functional model for the type-3 copper protein and is used for NLO applications (Mukherjee *et al*., 2003). **I (**and in one case, **II)** have similar structure to copper and cobalt complexes in the present work. In the trinuclear complexes, **1** and **2**, the coordination geometry of two terminal copper atoms is distorted square-planar (Mukherjee *et al*., 2003). The central copper has a distorted square-pyramidal (4 + 1) geometry. The mean Cu···Cu distance is ~3.3 Å. The complex has a diphenoxo-bridged dicopper(II) unit with the phenoxo oxygen atoms showing a planar geometry. In addition, the complex has an endogenous alkoxo-bridged dicopper(II) unit showing a pyramidal geometry for the oxygen atom (Mukherjee *et al*., 2003).

Geometrical structure of 2,2'-bis(salicylideneamino)-diphenylcopper(II):- 2,2'-bis(salicylideneamino)-diphenylcopper(II) (Figure 2.9 (a): M = Cu, n = 2 and R = phenyl) was reported to be a flattened tetrahedral complex (Holm *et al*., 1966).

UV data and geometry of copper(II) complexes of salicylaldimine:- Shifts of the 375 nm band, observed in those solvents with which bis-salicylaldehydeethylene diiminecopper(II) is able to form addition compounds, in addition to solvent effect, were suggested to be due to a shift from tetracoordinate planar structure to pentacoordinate pyramidal structure (Tanaka, 1958). The X-ray structure of bis(*N*-propylsalicylaldimine)copper(II), which is similar to that in the present work, shows the chelate to be a flattened tetrahedron with bands at 1124, 714, and 487 nm, respectively (Hare, 1968). Cu(II) chelates with Schiff bases derived from ethylenediamine, 1,2-diphenylethylenediamine and 5-X-salicylaldehyde (X = OCH_3, H, Br, NO_2) were synthesised and characterised by elemental analysis and IR and UV-visible spectroscopies (Zolezzi *et al*., 1999). The absorption spectra of these metal complexes in the visible region were consistent with near square planar coordination geometries. Trends in absorption spectra were correlated with electronic effects of the substituents at position 5 of salicylaldehyde (Zolezzi *et al*., 1999).

Ultraviolet photochemistry of N,N'-bis(salicylidene)ethylenediaminecopper(II):- The ultraviolet photochemistry of *N,N*'-bis(salicylidene)ethylenediaminecopper(II) was studied (Byung-Tae, 1995). Spectral changes on 254 nm irradiation was observed in the solvents chloroform, dichloromethane, and 1,2-dichloroethane, but not in ethanol, methanol, and acetonitrile. The latter may have been an indication that solvent binding to the 5th and 6th coordination site of the copper center inhibited photochemical reaction (Byung-Tae, 1995).

2.3.9 Zinc

The Zn^{2+} ion is important in many biological processes (Uhlenbrock *et al*., 1996). Zinc is an essential metalloelement required by all cells for activation of a large number of Zn-dependent enzymes which have roles in normal metabolic processes involved in the

multifaceted biochemical-mediated function and maintenance of all tissues(Uhlenbrock *et al*., 1996). In addition, Zn-dependent enzymes have many specific key roles in overcoming tissue injury or inflammatory disease states (Uhlenbrock *et al*., 1996). The use of small molecular mass chelates or complexes of Zn then constitutes the most propitious forms of Zn for the delivery of this metalloelement to required cellular sites enabling Zn-dependent enzyme syntheses and facilitation of Zn-dependent biochemical processes (Boghaei and Gharagozlou, 2007).

2.3.9.1 Biological activity

Anticancer activity of a zinc(II) complex with the Schiff base derived from 2,4-dihydroxybenzaldehyde and L-arginine:- A zinc(II) complex with the Schiff base derived from 2,4-dihydroxybenzaldehyde and L-arginine has been synthesized and characterized by elemental anlyses, TG-DTA, IR, electronic spectra and conductivity measurements (Chunhua *et al*., 1993). The results suggest that the Schiff base acts as a tridentate ligand. Electronic and fluoresence spectroscopy indicated that the Zn(II) complex intercalates DNA (Chunhua *et al*., 1993). This complex gave 32.2% inhibition rates to EAC (Ehrlich ascites carcinoma) during a test for anticancer activity (Chunhua *et al*., 1993).

Antimicrobial activity of complexes of Zn(II), Cu(II), Ni(II), Co(II) and Mn(II) with the Schiff bases derived from acetoacetanilido-4-aminoantipyrine and 2-aminophenol/2-aminothiophenol:- Neutral tetradentate chelate complexes of Cu(II), Ni(II), Co(II), Mn(II), Zn(II) and VO^{II} have been prepared in EtOH using Schiff bases derived from acetoacetanilido-4-aminoantipyrine and 2-aminophenol/2-aminothiophenol (Raman *et al*., 2003). The Schiff base structures (Figure 2.22) gave Zn(II) complexes, structures of which were confirmed by microanalytical data, magnetic susceptibility, infrared,

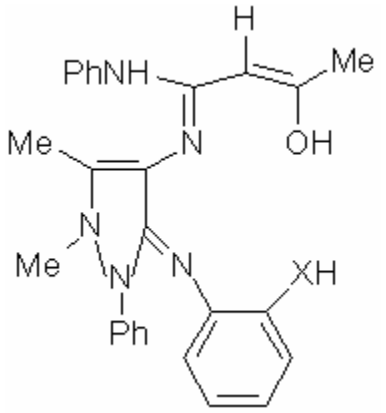

Figure 2.22: The Schiff base structures for formation of Zn(II) complexes (Raman *et al*., 2003)

ultraviolet–visible, ^{1}H-NMR and ESR spectral techniques. Electronic absorption and infrared spectra of the complexes suggest a square-planar geometry around the central metal ion, except for VO^{II} and Mn(II) complexes which have square-pyramidal and octahedral geometry, respectively (Raman *et al*., 2003). The in vitro antimicrobial activity of these complexes was tested against ***Salmonella typhi***, ***Staphylococcus aureus***, ***Klebsiella pneumoniae***, ***Bacillus subtilis***, ***Shigella flexneri***, ***Pseudomonas aeruginosa***, ***Aspergillus niger*** and ***Rhizoctonia bataicola***. Most of the metal chelates have higher antimicrobial activity than the free ligands (Raman *et al*., 2003).

Antimicrobial activities of a Zn(II), Cu(II) and Ni(II) complexes with Schiff base derived from 2-hydroxy-1-naphthaldehyde, 2,4-pentanedione and p-phenylenediamine:- A zinc(II) complex of the unsymmetrical Schiff base derived from 2-hydroxy-1-naphthaldehyde, 2,4-pentanedione and ***p***-phenylenediamine of the general formula $[Zn(C_{10}H_6OCH{:}N(C_6H_4)N{:}C(CH_3)CH{:}C(CH_3)O]$, [ZnL], and its adducts with 2,2′-bipyridine (bipy) and 1,10-phenanthroline (phen) have been synthesized and characterized by elemental analyses, conductance, room temperature magnetic susceptibility, and infrared and electronic spectral measurements (Osowole *et al*., 2005). The ligand was found to be tetradentate, coordinating via the imine N and enolic O atoms (Osowole *et al*., 2005). The magnetic moments (***sic***) and electronic spectra for the Zn(II) Schiff base complex indicated 4-coordinate and the adduct 6-coordinate (Osowole *et al*., 2005), whilst the Cu(II) and Ni(II) complexes indicated octahedral geometry. The antimicrobial properties of the ligand and compounds against ***Staphylococcus aureus***,

Streptococcus faecalis, *Escherichia coli*, *Pseudomonas aeruginosa*, *Salmonella typhi*, *Klebsiella pneumoniae*, *Enterococcus faecalis* and *Candida albicans* are reported (Osowole *et al*., 2005). The compounds generally exhibited good activity against the selected organisms (Osowole *et al*., 2005). [CuLphen] gave comparable antimicrobial activity to Gentamycin (Osowole *et al*., 2005), which is a well established antibiotic. The minimum inhibitory concentrations (MICs) of the sensitive compounds are between 1.0 – 12.0 mg/mL (Osowole *et al*., 2005).

2.3.9.2 Synthesis and characterisation

Spectroscopic data of Zn(II) and Cu(II) complexes of o-vanillin and L-phenyl-alanine:- Zn(II) complexes derived from *o*-vanillin and L-phenyl-alanine were synthesised and characterised (Wang and Chang, 1994). IR data revealed a broad band at 3400 and 3460 cm^{-1} due to the coordinated water in the Zn(II) complex. Bands at 925 and 775 cm^{-1} were due, respectively, to rocking and wagging vibrations of the coordinated water. A strong band at 1640 and 1649 cm^{-1} was observed due to *ν*C=N. The *ν*M-N were observed between 529 and 553 cm^{-1}, while *ν*M-O (phenolic oxygen) were observed between 425 and 504 cm^{-1} (Wang and Chang, 1994). It was concluded that the Schiff bases were probably bivalent anions with tridentate ONO donors derived from the carboxylate O, imino N, and phenolic O (Wang and Chang, 1994).

IR data of trinuclear Zn complex of 2-OHSALPN:- Trinuclear $[Zn_3(O_2CPh)_2(hsalpn)_2]\cdot 2MeOH$, where hsalpn = 1,3-bis(salicylideneamino)-2-propanol (2-OHSALPN), was synthesized (Uhlenbrock *et al*., 1996). No significant shift of the *ν*C=N band of free H_2hsalpn is observed upon complexation. In each spectrum the absorption is at ***ca.*** 1630 cm^{-1} for this band (Uhlenbrock *et al*., 1996). There are two bands in the far IR spectrum of the complex at 330 and 225 cm^{-1}, which this team of researchers assigned to *ν*M-O and *ν*M-N vibrations, respectively. Single-crystal X-ray diffraction analysis revealed the following structural features: one central zinc ion is octahedrally co-ordinated and two terminal zinc ions are surrounded by five donor atoms in the form of a square pyramid (Uhlenbrock *et al*., 1996). The left and right wing zinc ions are connected to the central metal atom ***via*** two phenolate oxygens of the

dinucleating ligand and the oxygens (2 x O^-) of the benzoate ion ($PhCOO^-$) (Uhlenbrock *et al*., 1996).

Geometrical structure of dinuclear mixed metal complexes of 2OH-oVANPN:- The crystal structure of {Bis(*N*,*N*-dimethylformamide)[μ-*N*,*N*'-bis(salicylidene)-1,3-propane-diaminato]nickel(II)}dibromozinc(II) was reported (Arici *et al*., 2001); thus, indicating that the ligand (2OH-*o*VANPN) in the present work can act as a bridging ligand in monodinuclear and heterodinuclear complexes. This compound, represented as $\{NiZnBr_2(C_3H_7NO)_2(C_{17}H_{16}N_2O_2)\}$, showed that the Ni atom had an irregular octahedral environment involving two O and two N atoms from the bis(salicylidene)-1,3-propanediaminate ligand in the equatorial plane, and two O atoms from the dimethylformamide groups (Arici *et al*., 2001). Zn-O-Ni, O-Zn-O, Ni-O-Zn and O-Ni-O angles in the bridged plane were reported (Arici *et al*., 2001).

2.4 THE PRESENT INVESTIGATION: RESEARCH RATIONALE

The aim of this thesis is to present newly synthesized copper(II), cobalt(II) and cobalt(III) complexes of the ligand, 2-OH-*o*VANPN, as potential anticancer and antimicrobial drugs.

2.4.1 Specific objectives of this research:-

- to synthesize 2-OH-*o*VANPN, *N*,*N*′-bis(3-methoxysalicylaldimine)propan-2-ol, which was previously synthesized by Nishida and Kida (Nishida and Kida, 1986);
- to use this 2-OH-*o*VANPN or its precursors to synthesize copper(II), cobalt(II) and cobalt(III) complexes using four synthetic methods found in the literature for similar compounds;
- to establish the structures and some properties of the synthesized ligand and complexes using microanalysis, metal-titration, ICP-MS, far-infrared, mid-infrared, electronic spectroscopy and thermal analytical method;
- to perform some preliminary biological (antioxidant and antimicrobial) tests to

establish which of the ligand and complexes are eligible for cancer cell-line testing at the National Cancer Institute (NCI).

2.4.2 Choice of ligand for this investigation

2-OH-*o*VANPN, a Schiff base, was chosen as the ligand in this work because Schiff bases are known to have slight antitumor activities (Hodnett *et al*., 1970) and the precursors of this ligand are known to have anticancer (Takashi *et al*., 1990; Watanabe *et al*., 1990; Aljaberi *et al*., 2005 and Lambert and Galez, 1996) and antimicrobial (Mikulosova and Bohovicova, 2000; Dunnick et al., 1999 and Brown *et al*., 1976) activities.

2.4.3 Choice of metals for this investigation

Copper(II), Cobalt(II) and Cobalt(III) were chosen to produce the complexes because complexes of these metals are known to destroy cancer cells (Reddy et al., 2004; Sykes, 2000; Vol′pin and Novodarova, 1992 and Osinski et al., 2000) and are also known to have antimicrobial activity (Vol′pin and Novodarova, 1992 and Dunnick et al., 1999).

2.4.4 Choice of methods for synthesizing the complexes during this investigation

The literature revealed four synthetic methods (Mazurek *et al*., 1982; Mazurek *et al*., 1986 and Zolezzi *et al*., 1999) for the synthesis of complexes, from salicylaldimine ligands, of the type that has no metal-carbon bonds. The absence of metal-carbon bonds has been linked to anticancer activity in some complexes; hence, these methods were chosen for the present work. All four methods were attempted as the outcome of the synthesis could not be predicted for the specific combinations of metal ion and ligand in this work and because structure determinations are usually done collectively on all the newly synthesized compounds in order to save time on instrument calibration and optimization.

2.4.5 Choice of biological tests for this investigation

A free radical scavenging assay, which employs the 2,2-Diphenyl-1-picrylhydrazyl (DPPH) radical, was peformed on the synthetic compounds in this work to establish their free radical scavenging (quenching) properties. The reason for this test is that cancer is usually spread (and initiated) by free radicals that attack healthy tissue; hence, if the synthetic compound is able to scavenge these free radicals, the cancer could be prevented from spreading or from being initiated by these free radicals. A second reason is that if the synthetic compound is able to quench free radicals, it may also be able to oxidize other sustrates, such as DNA and RNA of cancer cells, and thereby destroy cancer cells (tumors). The ligand in this work and the ligand precursors, *o*-vanillin and 1,3-diaminopropan-2-ol, was synthesized by other researchers and had not been tested for antioxidant activity before; thus, these were included in the antioxidant test.

The reason for antimicrobial testing of the synthetic compounds in this work was to establish whether these had biological activity before possibly sending them for cancer cell-line testing at the National Cancer Institute (NCI). The disk-plate method that was used in the present work is a common qualitative antibacterial and antimycotic test and was therefore used as a quick test for activity. After having established antimicrobial activity and that sample concentration had an effect on activity, dimethylformamide (DMF) was used as solvent for the sample to ensure complete dissolution of the sample in a repeat of the disk-plate method and in the quantitative tube dilution method of antimicrobial testing. The disk-plate and tube-dilution method may have given false negative results for antifungal testing of the ligand and complexes in the present work. The reason for false negative results may lie in the fact that fungal spores, which were used in these antifungal tests, are morphologically more resistant to penetration by antifungal agents than the fungus that produces them; thus, the radial growth method was employed so that the test samples could better penetrate the test organism, *Aspergillus niger*, and thereby display true antifungal activity results. The ligand in this work, although synthesized by other researchers, was included in all the antimicrobial tests mentioned above because its antimicrobial activity was not known by the time this investigation had started.

2.5 REFERENCES

1. Alexander, P.W. and Sleet, R.J. *Aust. J. Chem*. **1970**. 23. 1183-90.
2. Aljaberi, A.; Chen, P. and Savva, M. *Chemistry and Physics of Lipids*. **2005**. 133. 135-49.
3. Arici, C.; Svoboda, I.; Musa, S.; Atakol, O. and Fuess, H. *Acta crystallographica*. **2001**. 57. 31-2.
4. Bailes, R.H. and Calvin, M. *J. Am. Chem. Soc.* **1947**. 69. 1886-93
5. Baxter, E.W. and Reitz, A.B. "BACE Inhibitors for the treatment of Alzeimer's disease" In: *Annual Reports in Medicinal Chemistry*. 40. **2005**. 35-48.
6. Beta secretase. http://en.wikipedia.org/wiki/ Accessed 04-09-2008.
7. Billman, J.H.; Koehler, F. and May, R. *Journal of Medicinal Chemistry*. **1969**. 58. 767-9.
8. Boghaei, D.M. and Gharagozlou M. *Spectrochimica Acta Part A: Molecular and biomolecular spectroscopy*. **2007**. 67. 944-9.
9. Bonadies, J.A.; Kirk, M.L.; Lah, M.S.; Kessissoglou, D.P.; Hatfield, W.E. and Pecoraro, V.L. *Inorganic Chemistry*. **1989**. 28. 2037-44.
10. Brezina, F.; Sindelar, Z. and Pastorek, R. *Chemica*. **1997**. 36. 7-10.
11. Brown, R.; Fischer, R.; Blunk, J.; Berlin, K.D.; Ramalingam, K. and Durham, N.N. *Proc. Okla. Acad. Sci.* **1976**. 56. 15-17.
12. Byung-Tae, A. *Bulletin of the Korean Chemical Society*. **1995**. 16. 200-1
13. Carré, F.; Corriu, R.J.P; Emmanuelle, L-B; Mehdi, A.; Reyé, C; Guilard, R.; Sýkora, J. and van der Lee, A. *The Royal Society of Chemistry: Dalton Transactions*. **2003**. 3211-5.
14. Chen, D.; Martell, A.E. and Sun, Y. *Inorganic Chemistry*. **1989**. 28. 2647-7.
15. Chunhua, C.; Zishen, W. and Zhenhuan, Y. *Synthesis and Reactivity in Inorganic and Metal-Organic Chemistry*. **1993**. 23. 1725-33.
16. Cortés-Cortés, P.; Atria, A.M.; Cotreras, M.; Fernandéz, O.P. and Corsini, G. *Journal of Chilean Chemical Society*. **2008**. 53. 1527-32.
17. Daniel, V.D.; Murukan, B.; SindhuKumari, B. and Mohanan, K. *Spectrochimica Acta Part A: Molecular and Biomolecular Spectroscopy*. **2008**. 70. 403-10.

18. Demont, E.H.; Redshaw, S. and Walter, D.S. *WO Patent 111022-AL*. **2004**. Publication no. WO/2004/111022.
19. Dholakhiya, P.P. and Patel, M.N. *Synthesis and Reactivity in Inorganic, Metal-Organic, and Nano-Metal Chemistry*. **2002**. 32. 753-62.
20. Dunnick, A.L.; Baker, T.; Yang, C.; Goodman, M.; Gray, H.B.; Meade, T.J. *Book of Abstracts. 217th ACS National Meeting*. California. **1999**. 21-25.
21. Fernandes, C.; Parrilha, G.L.; Lessa, J.A.; Santiago, L.J.M.; Kanashiro, M.M.; Boniolo, F.S.; Bortoluzzi, A,J,; Vugman, N.V.; Herbst, M.H. and Horn, A. *Inorganica Chimica Acta*. **2006**. 359. 3167-76.
22. Ghose, B.N. *Revista Portuguesa de Quimica*. **1983**. 25. 147-50.
23. Golcu, A.; Tumer, M.; Demirelli, H. and Wheatley, R.A. *Inorganica Chimica Acta*. **2005**. 358. 1785-97.
24. Guangbin, W. *Synthesis, reaction, inorganic metal-organic chemistry*. **1994**. 24. 623-30.
25. Hare, C.R. "Visible and Ultraviolet Spectroscopy" In: *Spectroscopy and Structure of Metal Chelate Compounds*. John Wiley and Sons. New York. **1968**. 112-55.
26. Hodnett, E.M. and Dunn, W.J., III. *Journal of Medicinal Chemistry*. **1970**. 13. 768-70.
27. Hodnett, E.M. and Dunn, W.J., III. *Journal of Medicinal Chemistry*. **1972**. 15. 339-40.
28. Holm, R.H.; Everett, G.W, JR.; Chakravorty, A. *Progress in Inorganic Chemistry*. **1966**. 7. 83-203.
29. Kruger, P.E.; Moubaraki, B.; Fallon, G.D. and Murray, K.S. *J. Chem. Soc. Dalton Trans.* **2000**. 713-8.
30. Ku, S-M.; Wu, C-Y. and Lai, C.K. *J. Chem. Soc. Dalton Trans*. **2000**. 3491-2.
31. Lambert, D.M. and Gallez, B. *Journal of Labelled Compounds and Radiopharmaceuticals*. **1996**. 38(10). 873-953.
32. Liang, H.; Wang, X-J.; Cong, Y-L.; Li, S-T. and Zeng, J-Q. *Journal of Structural Chemistry -China-*. **1997**. 16. 141-3.
33. Lorösh, J. and Haase, W. *Biochemistry*. **1986**. 25. 5850-7.

34. Marinovich, A.F.; O'Mahony, R.S.; Waters, J.M. and Waters, T.N.M. *Croatica Chemica Acta*. **1999**. 72. 685-703.

35. Marmillon, C.; Jerosch, H.; Calas, M.; Bonnet, P.A. and Escale R. *Tetrahedron Letters*. **1998**. 39. 6179-80.

36. Mathews, C.K. and van Holde, K.E. *Biochemistry*. **1990**. The Benjamin/ Cummings Publishing Company, Inc. California.

37. Mazurek, W; Berry, K.J.; Murray, K.S.; O'Connor, M.J.; Rodgers, J.R.; Snow, M.R. and Wedd, A.G. *Inorganic Chemistry*. **1982**. 21. 3071-80.

38. Mazurek, W; Bond, A.M.; Murray, K.S.; O'Connor, M.J. and Wedd, A.G. *Inorganic Chemistry*. **1985**. 24. 2484-90.

39. Mazurek, W; Bond, A. M.; O'Connor, M.J. and Wedd, A.G. *Inorg. Chem*. **1986**. 25. 906-15.

40. McKee, V.; Zvagulis, M.; Dagdigia, J.V.; Patch, M.G. and Reed, C.A. *Journal of the American Chemical Society*. **1984**. 106. 4765-72.

41. Mikulasova, M. and Bohovicova, I. *Biologia (Bratislava)*. **2000**. 55. 229-34.

42. Mikuriya, M.; Yamato, Y. and Tokii, T. *Bulletin of the Chemical Society of Japan*. **1992a**. 65. 1466-8.

43. Mikuriya, M.; Sasaki, T.; Anjiki, A.; Ikenoue, S. and Tokii, T. *Bulletin of the Chemical Society of Japan*. **1992b**. 65. 334-39.

44. Mukherjee, R.N.; Abrahamson, A.J.; Patterson, G.S.; Stack, T.D. and Holm, R.H. *Inorganic Chemistry*. **1988**. 27. 2137-44.

45. Mukherjee, A.; Rudra, I.; Naik, S.G.; Ramasesha, S.; Nethaji, M. and Chakravarty, A.R. *Inorganic Chemistry*. **2003**. 42. 5660-8.

46. Murray, K.S.; Van den Bergen, A.; Kennedy, B.J. and West, B.O. *Australian Journal of Chemistry*. **1986**. 39. 1479-93.

47. Nantz, M.H.; Li, L.; Zhu, J.; Aho-Sharon, K.L.; Lim, D. and Erickson, K.L. *Biochimica et Biophysica Acta*. **1998**. 1394. 219-23.

48. Nishida, Y and Kida, S, *J. Chem. Soc. Dalton Trans*. **1986**. Issue 1. 2633.

49. Osinsky, S.P.; Levitin, T.; Bubnovskaya, L.; Sigan, A.; Ganusevich, I.; Michailenko, V. and Kovelskaya, T. *6th Internet World Congress for Biomedical Sciences*. **2000**. Inabis Poster #3.

50. Osowole, A.; Kolawole, G. and Fagade, O. *Synthesis and Reactivity in Inorganic, Metal-Organic, and Nano-Metal Chemistry*. **2005**. 35. 829-36.
51. Özalp-Yaman, Ş; Veli T. Kasumov, V.T. and Önal, A.M. *Polyhedron*. **2005**. 24. 1821-8.
52. Raman, N.; Kulandaisamy, A.; Thangaraja, C. and Jeyasubramanian, K. *Transition Metal Chemistry*. **2003**. 28. 36-9.
53. Reddy, P.A.N.; Santra, B.K.; Nethaji, M. and Chakravarty, A.R. *Journal of Inorganic Biochemistry*. **2004**. 98. 377-86.
54. Richardson, D.R.; Sharpe, P.; Lovejoy, D.B.; Senaratne, D.; Kalinowski, D.S.; Islam, M. and Bernhardt, P.V. *Journal of Medicinal Chemistry*. **2006**. 49. 6510-21.
55. Rossi, L.M.; Neves, A.; Bortoluzzi, A.J.; Hörner, R.; Szpganicz, B.; Terenzi, H.; Mangrich, A.S.; Periera-Maia, E.; Castellano, E.E. and Haase, W. *Inorganica Chimica Acta*. **2005**. 358. 1807-22.
56. Schaefer, T.; Sebastian, R.; Laaitikainen, R. and Salman, S.R. *Canadian Journal of Chemistry*. **1984**. 62. 326-31.
57. Sergej, M.D.; Levitin, I.; Bubnovskaya, L.; Sigan, A.; Ganusevich, I.; Michailenko, V. and Kovelskaya, T. *6th Internet World Congress for Biomedical Science*. **2000**.
58. Guo, Z. and Sadler, P.J. "*Medicinal Inorganic Chemistry*" In: *Advances in Inorganic Chemistry*. **2000**. Sykes, A.G. (ed.). Academic Press. New York. 183-303.
59. Tai, X.; Yin, X.; Chen, Q. and Tan, M. *Molecules*. **2003**. 8. 439-43.
60. Takahashi, K; Sekiguchi, M. and Kawazoe, Y. *Mutation Research*. **1990**. 230. 127-34.
61. Takeuchi, T.; Bötcher, A.; Quezada, C.M.; Simon, M.I.; Meade, T.J. and Gray, H.B. *Journal of the American Chemical Society*. **1998**. 120. 8555-6.
62. Tanaka, T. **1958**. 80. 4108-10.
63. Uehara, M.; Urade, M.; Ueda, A.; Sakagami, N. and Abe, Y. *Bulletin of the Chemical Society of Japan*. **1998**. 71. 1081-88.

64. Uhlenbrock, S.; Wegner, R. and Krebs, B. *J. Chem. Soc. Dalton Trans*. **1996**. 3731-6.

65. Valent, A.; Melník, M.; Hudecová, D.; Dudová, B.; Kivekäs, R. and Sundberg, M.R. *Inorganica Chimica Acta*. **2005**. 358. 1785-97.

66. van Wyk, J.L.; Mapolie, S.F.; Lennartson, A.; Hakansson, M. and Jagner, S. *Inorganica Chimica Acta*. **2008**. 361. 2094-100.

67. Vericat, J.-A and Barbé, J. *Mutagenesis*. **1988**. 3. 165-8.

68. Vol'pin, M.E.; Novodarova, G.N. and Kolosova, E.M. *Inorganica Chimica Acta*. **1981**. 50. 21-31.

69. Vol'pin, M.E. and Novodarova, G.N. *Journal of Molecular Catalysis*. **1992**. 74. 153-62.

70. Wang, G. and Chang, J.C. *Synthesis and reactivity in Inorganic and Metal-Organic Chemistry*. **1994**. 24. 623-30.

71. Watanabe, Kazuko.; Ohta, T.; Watanabe, M.; Kato, T. and Shirasu, Y. *Mutation Research*. **1990**. 243. 273-80.

72. Wilkinson, G.; Gillard, R.D. and McCleverty, J.A. *Comprehensive Coordination Chemistry: The Synthesis, Reactions, Properties & Applications of Coordination Compounds*. 2. Pergamon Press. **1987**. 716-21.

73. Zhang, C-G.; Sun, J.; Kong, X-F. and Zhao, C-X. *Journal of Coordination Chemistry*. **2000**. 50. 353-62.

74. Zolezzi, S.; Decinci, A. and Spodine, E. *Polyhedron*. **1999**. 18. 897-904.

3. SYNTHESIS AND PHYSICOCHEMICAL CHARACTERIZATION

This chapter reports the synthesis and characterization of Cu(II), Co(II) and Co(III) complexes of the Schiff base ligand, (2-hydroxy, 3-methoxysalicylaldimine)propan-2-ol. Mainly methods of Mazurek and co-workers (Mazurek *et al*., 1986) were employed and involved the self-assembly of metal centers and preformed ligand in the presence (or absence) of the base, KOH. These reactions were carried out in alcohol. An alternative solvent, dichloromethane was used by Zolezzi and co-workers (Zolezzi *et al*., 1999). Another method reported by Mazurek and co-workers involved quantitatively adding an ethanolic solution consisting of the ligand constituents, 2-hydroxy, 3-methoxysalicylaldehyde and diaminopropan-2-ol, to a solution (in ethanol) of the metal salt (Mazurek *et al*., 1982). All metal complexes were synthesized in stoichiometric (1:1) molar proportions to yield mononuclear complexes, although a binuclear cobalt complex and a trinuclear copper complex were also formed from these reactions.

Structure determination and characterisation studies included microanalysis, metal (copper and cobalt) analysis, thermal analysis, electronic (UV-Vis) spectroscopy and infrared (IR) spectroscopy.

3.1 A REVIEW OF PHYSICAL AND CHEMICAL CHARACTERIZATION

Structure determination is one of the fundamental operations in chemistry, and spectroscopy has proved to be a powerful tool for structure determination. The collective information provided by each spectroscopic technique is often sufficient to elucidate even the most complex structures.

Methods of assigning ligand to metal (L-M) vibrations in the IR spectra of transition metal complexes:- Among the many vibrations M-L are the most important since they provide direct information regarding the structure of the complex and the nature of the metal-ligand bond. The vibrations appear below 600 cm^{-1} and are linked to the high mass of the metal ion and the comparative weak nature of the M-L bond. These assignments are often difficult to interpret because the IR spectrum is complicated by intermolecular

interactions, lattice modes, lowering of symmetry, vibrational coupling and the appearance of ligand vibrations activated by complex formation (Ferraro, 1971 and Adams, 1964). Methods that have been used to assign M-L vibrations and that are applicable to metal complexes in the present work are as follows:-

- Since M-L vibrations are absent from the free ligands a comparison of the spectra of the free ligands and its metal complex yield assignments of the M-L modes. This method often fails to give unambiguous assignments because some ligand vibrations activated by complex formation may appear in the same region as the M-L vibrations (Nakamoto, 1963).
- The metal-ligand vibrations are expected to appear in the same region for complexes of identical metals with similar substituted ligands (Nakamoto, 1963).
- The M-L vibrations of a series of isostructural complexes are metal sensitive and shift according to the properties of the metals. Hence, the IR bands which follow the order of the CFSE's of the metals can be attributed to M-L modes (Hulett and Thornton, 1971 and Shephard and Thornton, 1971).

3.1.1 Structure and electronic spectra of Schiff bases

The structures of Schiff bases and their analogues have been thoroughly studied and summarized (Calligaris and Randaccio, 1987 and Costamanga *et al*., 1992). The structure of Schiff bases is related to the possibilities for tautomeric transformation, formation of hydrogen bonds and conformational effects (Garnovskii *et al*., 1993).

Bands reported (Sanmartín *et al*., 2000) for *N*,*N′*-bis(3-hydroxysalicylidene)-1,3-diaminopropan-2-ol, which is very similar in structure to the ligand in the present work, gave λ_{max} at 225, 270, 290, 330 and 425 nm in methanol. OH-SALPN, which is also very similar in structure to the ligand in the present work, is known to exhibit bands at 260, 318 and 415 nm in ethanol (Alexander and Sleet, 1970 and Mazurek *et al*., 1982). A λ_{max} range of 229 - 239 nm is indicative of π-π_3^* transitions and a λ_{max} range of 255 – 265 nm is reported to be due to π-π_2^* transitions (Zolezzi *et al*., 1999). The Schiff base synthesized by Ramesh and Maheswaran gave bands in the range 295 - 249 and 330 - 346 nm, which were assigned to $\pi \rightarrow \pi^*$ and $n \rightarrow \pi^*$ transitions to the C=N group of the

Schiff base ligand (Ramesh and Maheswaran, 2003). Zhou and co-workers, in turn, assigned the bands in the range 212 – 281 nm to the benzene $\pi \rightarrow \pi^*$ transition and the lower energy band at 334 nm to the chromophore $\pi \rightarrow \pi^*$ of the imine (Zhou *et al.*, 1999).

2-OH-Schiff bases (in MeOH) that show any band equal or greater than 400 nm is an indication of the keto-amine tautomeric form of the Schiff base (Yildiz *et al.*, 1998 and Popovic *et al.*, 2004).

3.1.2 Geometrical structure and electronic spectra of copper(II) complexes

The +2 oxidation state of copper is by far the commonest state in which the copper ion has nine *d*-electrons, and most of the divalent compounds are four-coordinate (Nicholls, 1973). There are a number of quite stable, five-coordinate complexes of Cu^{2+}, all involving ligands that are considered to be π-acceptors.

Copper(II) complexes are generally blue or green (Jorgenson *et al.*, 1962; Cotton and Wilkinson, 1980 and Hartfield and Whyman, 1969). The origin of the colour is due to the maximum of four electronic transitions; d-d transitions; charge transfer transitions (both metal to ligand and ligand to metal), and internal ligand transitions. Such transitions occur between the ground state and the excited states of the crystal field levels (Nakamoto, 1978).

The d^9 ion is associated with large distortions; thus, electronic spectroscopy can not be used on its own as a tool for identification of structure. There is a large number of copper(II) electronic spectra in the literature where the structure is known but the assignment is not certain (Ferguson, 1964).

An example of this uncertainty can be found in the $^2T_{2g} \rightarrow {}^2E_g$ transition for octahedral copper(II) complexes in which the $t_{2g} - e_g$ separations are from approximately 769 nm for CuO_2 to about 556 nm for CuN_6. Several absorption bands may be expected in this region for a tetragonally distorted octahedral copper(II) complex. These bands correspond to

transitions from sublevels (d_{xz}, d_{yz} and d_{xy}) of $^2T_{2g}$ to $d_{x^2-y^2}$ and d_{z^2}; this is due to splitting (Figure 3.2) of the ^2E_g and $^2T_{2g}$ ground terms of an octahedron as the result of Jahn-Teller distortion and in turn results in overlapping of bands and a more complex spectrum, with the appearance of a low energy shoulder. For a tetracoordinated copper(II) complex square planar geometry is more favoured. The distortion of this system commonly leads to four transitions, namely from the ground state $^2B_2$ to $^2A_2$, to $^2A_2$, to $^2B_1$ and to $^2A_1$ (Ferguson, 1964). Absorptions above 500 nm have been observed (Lever, 1978) for distorted tetrahedral square planar $[CuBr_4]^{2-}$ and $[CuCl_4]^{2-}$ while the tetra-coordinated copper(II) ion with stronger field ligands such as imines will appear blue shifted (Lever, 1978). Copper(II) ion complexes are susceptible to ligand-solvent exchange or the possibility of more than one species in equilibrium, depending on coordination number involved (Ali and Livingstone, 1974 and Battistoni *et al.*, 1971).

It is established that copper(II) complexes with *N*-alkylsalicyladimines can occur in square planar or tetrahedral configuration, depending on the bulkiness of the alkyl group and the ring constituents. However, only a few examples of tetrahedral distortion from square planar are known. In the case of tetra- or penta-dentate Schiff base copper(II) complexes like 1,3-bis(salicylaldimine)propan-2-olcopper(II), the co-ordination geometry of the copper is regular square planar significantly distorted toward tetrahedral with two oxygens and two nitrogens from salicylaldimine moieties. The Cu(II) complex in DMF (dark green) gave an electronic spectrum with two absorption bands at 370 and 611 nm. The former band being as a result of $\pi \rightarrow \pi^*$ (imine) and the latter band due to internal charge transfer or d-d transitions (Kitajima *et al.*, 1986).

To understand the preferential formation of square planar Cu(II) complexes of this kind, it is necessary to consider the crystal field splitting of the various geometries, see Figure 3.1 and 3.2 (Nicholls, 1973). The essence of this crystal field theory (CFT) is that the five *d*-orbitals, which are degenerate and equal in energy in the gaseous metal ion, become differentiated in the presence of the electrostatic field due to the ligands. Those orbitals lying in the direction of the ligands are raised in energy with respect to those lying away

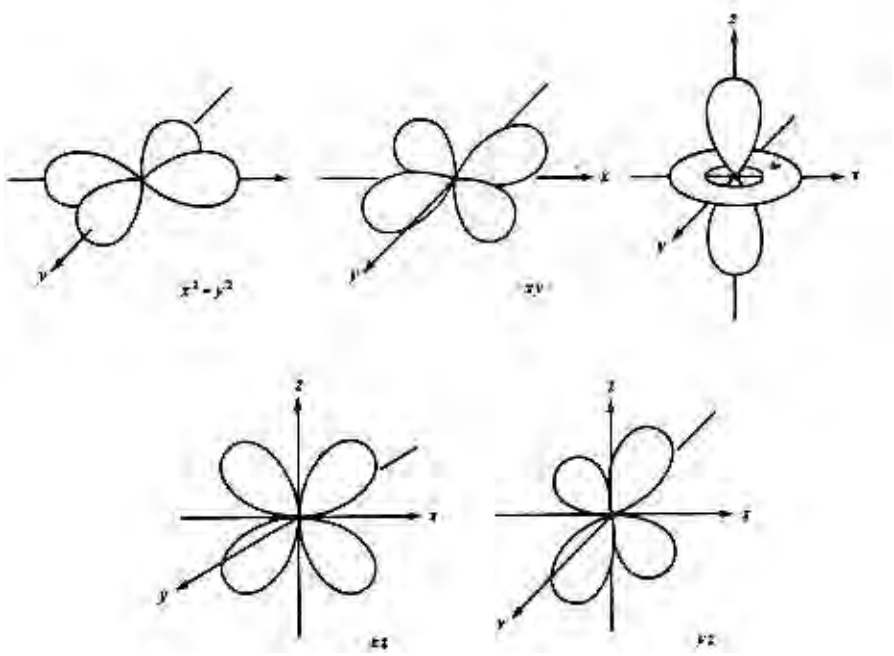

Figure 3.1: Spatial arrangement of the five *d*-orbitals (Hall, 1983)

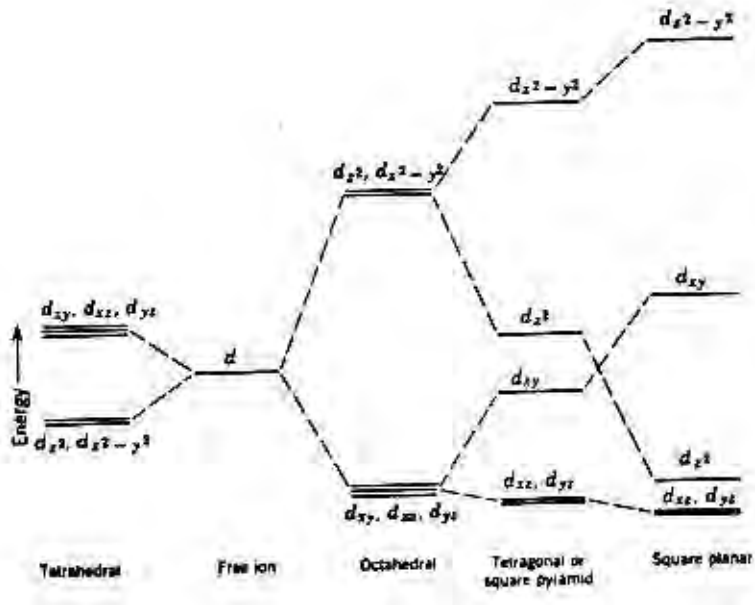

Figure 3.2: Crystal field splittings of the *d*-orbitals of a central ion in complexes of various geometrical structures (Hall, 1983)

from the ligands. By preferentially filling the low-lying levels, the *d*-electrons can stabilise the system as compared to the case of random filling of the *d*-orbitals. The gain in bonding energy achieved in this way may be called the crystal field stabilisation energy (CFSE). With the afore-mentioned in mind, the fact that Cu^{2+} has nine *d*-

electrons, it is easy to see why square planar geometry would be favoured, since it is possible to leave the $d_{x^2-y^2}$ orbital half-empty. For strong tetragonal (or square planar) geometry, ligand orbitals along the z-orbitals are absent; therefore, the energy of the *d*-orbitals along the z^2-axis drops to below d_{xy}, and d_{xz} and d_{yz} becomes doubly degenerate. In the case of weak tetragonal (or square pyramidal) geometry, imagine the ligand orbitals being pulled away along the z-axis such that those lying on the z-axis become lower in energy than those on the (x^2-y^2)-axis, and d_{xz} and d_{yz} are at lower energy than d_{xy} (Hall, 1983)

Many examples of the general structural types depicted by Figure 3.4 for Cu(II) complexes are known. There appears to be no evidence of the existence of Cu(I) salicyaldimines.

The dicopper(II) complex, $[Cu_2LBr]_n \cdot 6H_2O$ (Figure 3.3) of trianionic pentadentate Schiff base ligands gave a d-d band at 620 nm in methanol in its electronic spectrum (Naik *et al.*, 2006). The complex was found to have 5-coordinate square-pyramidal geometry in which the nitrogen, alkoxo and phenoxo oxygen atoms are in the basal plane and it was observed that the loss of water ($-6H_2O$) occurred in the range 30-140 ^oC (Naik *et al.*, 2006).

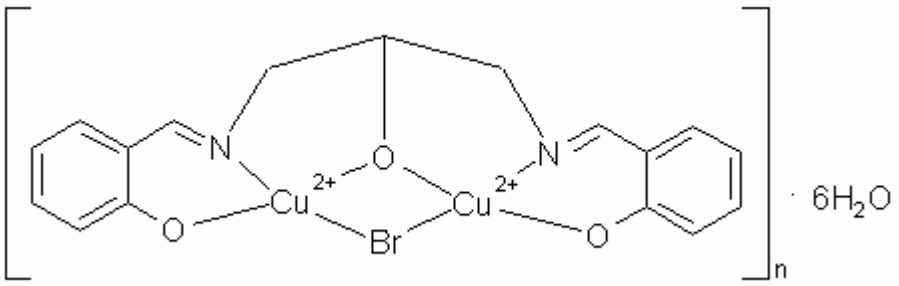

Figure 3.3: Structure of $[Cu_2LBr].6H_2O$ (Naik *et al.*, 2006 and Mukherjee *et al.*, 2003)

[Cu(2-OH-SALPN)] and [Cu(*o*VANPN)] were found to have distorted tetrahedral geometries (Nishida *et al.*, 1991). [Cu_2SalDpl.carboxylate] (SalDpl = 2-OH-SALPN), in which the copper atoms were square-planar, gave a solid-state electronic spectrum with a band at 620 nm and a solution (CH_2Cl_2) electronic spectrum also at 620 nm, but gave a shift in the spectral band to 640 nm when DMF was the solvent (Butcher *et al.*, 1995).

$[Cu_2SalDpe(OH)\cdot H_2O]$ (SalDpe is almost identical to 2-OHSALPN, but has 1,5-diaminopropan-3-ol instead of 1,3-diaminopropan-2-ol) is a hydroxyl-bridged complex that gave a band at 610 nm in solid state and 585 nm in CH_2Cl_2 and DMF (Butcher *et al.*, 1995). This suggests that the compound has one 4-coordinate and one 5-coordinate copper atom in the solid state and two 4-coordinate copper atoms in solution. The water molecule was observed to be present in the crystal lattice (Butcher *et al.*, 1995).

$[Cu_2(HL)(H_2O)_2]_n$ (L = *N*,*N*′-bis(3-hydroxysalicylidene)-1,3-diamino-2-propanol) was observed as a green solid with solid-state electronic spectrum showing a band at 620 nm, and a solution (MeOH) spectrum with a band at 630 nm (Sanmartín *et al.*, 2000).

Mn^{II}(2-OHSALPN) gave UV-Vis-spectrum (MeOH) with the following bands: 216, 235, 290 and 692 nm (Bertoncello *et al.*, 1991).

3.1.3 Geometrical structure and electronic spectra of cobalt(II) complexes

Co^{2+}, with its seven *d* electrons, is usually found in four-coordinate tetrahedral and six-coordinate octahedral geometrical arrangements (Carlin *et al.*, 1965 and Nicholls, 1973). This is due to the relatively low difference in crystal field stabilization energies between octahedral and tetrahedral cobalt(II) (d^7) complexes (Nicholls, 1973). It is known that the spectrum of tetrahedral cobalt is more intense than that of octahedral cobalt; strongly structured peaks are characteristic in the visible region (Carlin *et al.*, 1965). The differences in band positions (Kuzniarska-Biernacka *et al.*, 2003) can be regarded as characteristic of the stereochemistry of the cobalt(II) complexes. Unfortunately both are known to give rise to bands near 500 nm although tetrahedral complexes more frequently exhibit maxima near 667 nm. If the spectrum is not complicated by overlap with a strong UV (charge transfer) tail, intensity is the best spectral indicator of stereochemistry (Carlin *et al.*, 1965).

Colour is not a useful indicator of stereochemistry: Many tetrahedral complexes are "blue" and octahedral compounds are "pink" or "brick red" (Carlin *et al.*, 1965), but

"purple" octahedral Co_2SiO_4 (Goodgame and Cotton, 1961) and "pink" tetrahedral cobalt dipivaloylmethanide (Cotton and Soderberg, 1962) had been isolated.

According to the simplified energy level diagram, high spin octahedral Co(II) complexes have three electronic transitions (Nicholls, 1973). The spectra have a band in the near infrared which is assigned to the lowest energy transition $^4T_{1g} \rightarrow {}^4T_{1g}(P)$ transitions. The $^4T_{1g} \rightarrow {}^4A_{2g}$ transition is frequently not observed. The first two transitions have normal intensities of octahedral spin-allowed Laporte forbidden bands (Nicholls, 1973). The fine structure or shoulder in the visible region has been attributable to the $^4T_{1g} \rightarrow {}^4A_{2g}$ transition, but it may also have originated from spin-orbit coupling, vibrational broadening, low symmetry components to the ligand field or transitions to doublet states (Nicholls, 1973).

The simplified energy level diagram of tetrahedral Co(II) also has three electronic transitions (Nicholls, 1973). The first transition, ν_1 [$^4T_2 \rightarrow {}^4A_2$], occurs in the 3000 - 5000 cm^{-1} (3333 - 2000 nm) region and has rarely been observed. Goodgame and Goodgame reported the near infrared spectra of tetrahedral cobalt(II) (Goodgame and Goodgame, 1965). The second transition ν_2 [$^4A_2 \rightarrow {}^4T_1(F)$], has a broad band appearing in the near infrared; ν_3 [$^4A_2 \rightarrow {}^4T_1(P)$] is intense, broad and is known to exhibit a great deal of structure (Nicholls, 1973).

Salicylaldimine complexes of Co(II), such as is investigated in the present work, are well known and are confined to two structural types, as depicted by Figure 3.4 (Holm *et al.*, 1966).

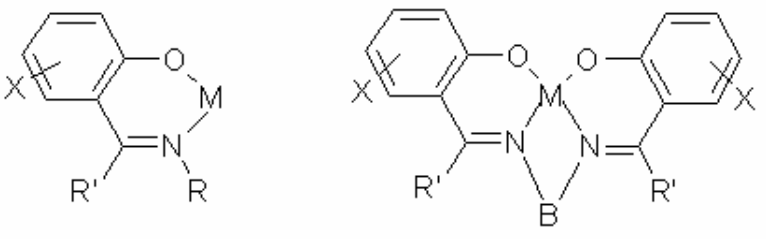

(a) **(b)**

Figure 3.4: The most significant structural types of the salicylaldimine complexes

These complexes are found to be uniformly pseudotetrahedral irrespective of the nature of R (Figure 3.4). The complexes are red to brown crystalline solids. Co(*n*Bu-sal)$_2$ was found to be tetrahedral. Co(R-sal)$_2$ complexes in solution (benzene) for R = C_6H_5 were shown to be the same as the reflectance spectra of the R = *i*-Pr, *s*-Bu, and *n*-Bu complexes (Holm *et al.*, 1966). Three spin-allowed crystal field bands are expected in tetrahedral Co(II), viz., $^4A_2(F) \rightarrow {}^4T_2(F)$ (ν_1), $\rightarrow {}^4T_1(F)$ (ν_2) $\rightarrow {}^4T_1(P)$ (ν_3). ν_1 is generally too far in the infrared to be easily observed. Co(R-sal)$_2$ complexes show two bands at 1298 nm and 892 nm, which may be assigned to components of ν_2; a shoulder at 588 nm due to ν_3. Charge transfer bands are found at 400 nm, 357 nm and 294 nm (Holm *et al.*, 1966).

The ligand field spectra of several Co(sal)$_2$en complexes have been recorded and an absorption near 8330 cm^{-1} suggested, and therefore not yet given as a definite assignment, as characteristic of low-spin planar Co(II) complexes (Holm *et al.*, 1966).

$[Co_2(HL)(H_2O)_2]_n$ (L = *N*,*N*′-bis(3-hydroxysalicylidene)-1,3-diamino-2-propanol or 2-OHSALPN) was observed as a brown solid with solid-state electronic spectrum showing broad bands with λ (nm) at 500, 640 and 1300 (Sanmartín *et al.*, 2000). The corresponding purple complex, Co(H_3L)(H_2O), gave a solid-state electronic spectrum with bands at 490, 620 and 1300 nm, and a solution (EtOH) spectrum with bands at 480 and 610 nm.

3.1.4 Geometrical structure and electronic spectra of cobalt(III) complexes

From Figure 3.2 it is easy to see that the cobalt(III) ion with its six *d* electrons will favour octahedral geometry since it is possible to leave the highest energy d_{z^2} and $d_{x^2-y^2}$ orbitals unoccupied. Tetragonal and square-planar geometries are less favoured since d_{z^2} orbitals are lower lying and there would be less crystal field stabilization energy than for octahedral complexes (Nicholls, 1973).

Comparison of the crystal field splitting and corresponding crystal field stabilization energy for hexa aqua complexes of Co(II), Cu(II) and Co(III) give values of 9300 cm^{-1}

(111 kJ. mol^{-1}), 12 600 cm^{-1} (151 kJ. mol^{-1}) and 18 600 cm^{-1} (222 kJ. mol^{-1}), respectively (Lee, 1991). Co^{3+}, with its larger crystal field stabilization energy of 222 kJ. mol^{-1}, is likely to be octahedral and is also more likely to be low spin (i.e. diamagnetic) with the imine ligand, especially as $Co(en)_3^{3+}$ is low spin (Lee, 1991) and an imine is higher in the spectrochemical series than an amine. The d-d UV transitions (Lee, 1991) will thus be:-

$^1A_{1g} \rightarrow {}^1T_{1g}$; $^1A_{1g} \rightarrow {}^2T_{2g}$ (Visible)

$^1A_{1g} \rightarrow {}^1E_g$; $^1A_{1g} \rightarrow {}^1A_{2g}(G)$; $^1A_{1g} \rightarrow {}^1A_{2g}(F)$ (Vaccuum UV below 200 nm)

Salicylaldimine complexes of Co(III) are well known and appear to be confined to structural types (a) and (b) in Figures 2.9 and 2.10 (Holm *et al*., 1966). For R = *n*-Pr in Figure 3.4, the stereochemistry of the Co(III) salicylaldimine complex was found to be octahedral. For tris-chelate metal complexes of Co(II) and Co(III) containing three identical unsymmetrical bidentate ligands, the electronic spectra show only one ligand field band ($^1A_{1g} \rightarrow {}^1T_{1g}$) (Holm *et al*., 1966).

3.2 EXPERIMENTAL (PHYSICAL AND CHEMICAL CHARACTERIZATION)

Reagents used:- All reagents used were analytical grade from Sigma-Aldrich Chemical Company Inc., USA. The solvents were dried and distilled before use according to standard procedures.

3.2.1 Microanalysis (C, H and N)

Carbon, hydrogen and nitrogen combustion microanalyses were carried out using a Fisons Elemental Analyzer 1108 CHNS-O, University of Kwazulu-Natal, South Africa.

3.2.2 Metal analysis

ICP-MS:- The quantity of copper or cobalt in some of the isolated complexes were determined using inductively coupled plasma – mass spectrometry, on a Perkin-Elmer Sciex Elan 6100 ICP-MS, Nelson Mandela Metropolitan University, South Africa.

Direct titration:- The method of Schwarzenbach (Schwarzenbach, 1955) was used for some of the synthesized complexes. Between 0.03 g and 0.05 g (accurately weighed) of the metal complex was transferred into a 50 ml beaker. A small amount of concentrated acid mixture (3 : 1 HNO_3 : H_2SO_4) was used to cover the weighed complex and a watch glass placed on the beaker. The mixture was gently boiled until the brownish fumes ceased. The clear solution was quantitatively transferred to a 100 ml volumetric flask, made up to volume, and mixed thoroughly. A 25.00-ml aliquot was neutralized to about pH 6 and a tip of a spatula murexide indicator (1 part murexide : 100 parts NaCl) added. The metal-murexide complex formed just before titration served as an acid-base indicator for the subsequent neutralization, which was carried out by adding NH_3 until the solution just turned yellow. Titration with standard, approximately 0.01 M (or lower concentration) ethylene diamine tetraacetic acid (EDTA) was then conducted until a sharp colour from yellow to violet (or purple) was observed. If during titration, an orange (due to the formation of an orange metal-murexide complex instead of a yellow cobalt-murexide complex) colour was observed, a few drops of NH_3 were added to give a yellow colour again, and the titration with EDTA continued. The colour change is greenish to purple with the Cu(II) complexes. From the titration results, the % metal was determined.

Back-titration:- The method of Schwarzenbach (Schwarzenbach, 1955) was used for some of the isolated cobalt complexes. The cobalt complex was dissolved in 15 ml of 1 : 5 nitric acid and after having added more than the equivalent amount of standard, approximately 0.01 M EDTA, neutralized with 1.0 M NaOH (and with 0.1 M NaOH close to neutralization). The resulting solution was diluted to around 100 ml and 2 ml of pH 10 ammonia-ammonia chloride buffer added. The resulting solution was titrated with standard Mn^{2+} to the wine red end point. The titration results was used to determine the % metal [To prepare pH 10 buffer: Dissolve 70 g of solid NH_4Cl in 600 ml of concentrated reagent-grade (15 M) NH_3 and dilute the mixture to 1 Liter with deionised water. Adjust pH with NH_3 or HCl if necessary to reach pH 10].

3.2.3 Melting point

Melting temperatures were recorded from a Gallenkamp Melting point apparatus. Temperatures were uncorrected.

3.2.4 Thermal analysis

Differential Scanning Calorimetry (DSC):- DSC curves for the ligand and all copper(II) complexes synthesized in this work, were recorded on a Perkin-Elmer instrument (10 ^{o}C. min^{-1}) in air and N_2 atmospheres, respectively, over the temperature range 50 – 600 ^{o}C. The other complexes were not exposed to this form of thermal analysis as it was found that copper complexes sublimed and their sublimates had accumulated in the purge line of the closed DSC furnace.

Sublimation temperatures (copper block):- Sublimation temperatures were determined for all the metal complexes using a specially designed copper block, with bored holes for sample tube and thermometer, heated on a hot plate. Sublimation temperatures were recorded from the thermometer, which was fitted inside a copper block and located directly above the sample tube, which was also fitted into the same copper block such that the depth, into the copper block, of the thermometer mercury tip and the sample was the same. The latter ensured that both thermometer tip and sample experienced the same temperature inside the copper block. Temperatures were uncorrected.

Thermal Gravimetric analysis (TGA) was not done on any of the compounds to avoid possible damage to the TGA instrument because from their DSC runs, the copper complexes were found to sublime (see "Differential Scanning Calorimetry").

3.2.5 Mid-infrared (MIR) spectra

The mid-infrared spectra (4000 - 400 cm^{-1}) were recorded on a Perkin-Elmer Spectrum 2000 FT-IR spectrophotometer. Samples were run in a KBr matrix as a pressed disc.

3.2.6 Far-infrared (FIR) spectra

The far-infrared spectra (500 - 50 cm^{-1}) were determined as Nujol mulls between polyethylene disks using a Perkin-Elmer Spectrum 2000 FT-IR spectrophotometer.

3.2.7 Electronic spectra (UV/vis solution)

Ultraviolet-visible (UV/vis) spectra were recorded on a Varian Cary 500 Scan UV-VIS-Near-infrared spectrophotometer in the absorbance mode using 1 cm quartz cells. The concentration of sample after dissolving (in ethanol, dimethylformamide or methanol) was around 2.0 x 10^{-4} M. The spectra were collected at a spectra band width of 2 nm and at a rate of 200 nm. min^{-1} in the range 700 - 200 nm. The spectra have been smoothened and derivatized by using the Savitsky-Golay method.

3.3 EXPERIMENTAL (SYNTHESIS OF THE LIGAND AND THE COMPLEXES)

All reagents used to obtain the ligands and the corresponding complexes were analytical grade from Sigma-Aldrich Chemical Company Inc., USA. The solvents were dried and distilled before use according to standard procedures.

3.3.1 Synthesis of the Schiff base ligand

The Schiff base ligand, 2-OH-*o*VANPN, was prepared by a reported method (Nishida and Kida, 1986). A 15 ml of methanolic solution of 1,3-diaminopropan-2-ol (0.54 g, 4.66 mmol) was slowly added to a 5 ml ethanolic solution of *o*-vanillin (1.81 g, 11.9 mmol). The reaction mixture was refluxed for 2 hours. The precipitate was cooled; collected by filtration; washed with 20 ml of cold ethanol, followed by recrystallization from ethanol and drying at 70 ^{o}C. The ligand was obtained as yellow crystals with an 83% yield. This yield falls within the 78 - 92% yields found in the literature with similar ligands (Ku *et al*., 2000).

Copper(II), cobalt(II) and cobalt(III) complexes, respectively, were synthesized employing methods by Mazurek and co-workers as well as Zolezzi and co-workers (Mazurek *et al*., 1986, Mazurek *et al*., 1982 and Zolezzi *et al*., 1999).

3.3.2 Syntheses of the copper(II) complexes

3.3.2.1 Method 1

A methanolic solution (15 ml) of 2-OH-*o*VANPN (0.72 g, 2 mmol) was added to a methanolic solution (10 ml) of copper(II) chloride dihydrate ($CuCl_2 \cdot 2H_2O$) (0.341 g, 2 mmole). A methanolic solution (15 ml) of potassium hydroxide (0.32 g, 5.7 mmole) was mixed into the resulting solution. The solution was left to stand at room temperature for approximately 16 hours. The green crystalline product was collected by vacuum filtration; washed with cold methanol, and dried in a dessicator. The crude yield was 0.62 g. 0.55g Crude was recrystallised from boiling ethanol and yielded 0.48 g crystals.

3.3.2.2 Method 2

An ethanolic solution (5 ml) of 2-OH-*o*VANPN (0.72 g, 2 mmol) was added to an ethanolic solution (30 ml) of copper(II) chloride dihydrate ($CuCl_2 \cdot 2H_2O$) (0.34 g, 2 mmole). The mixture was reduced to 20 ml on a hot plate, cooled, swirled, and left undisturbed at room temperature for approximately 16 hours. Green crystals were collected by vacuum filtration, washed with cold ethanol and air-dried to give 0.32 g complex. Recrystallisation (ethanol) yielded 0.28 g complex.

3.3.2.3 Method 3

An ethanolic solution (5 ml) of *o*-vanillin (1.52 g, 10 mmole) was added to a methanolic solution (12 ml) of 1,3-diaminopropan-2-ol (0.45 g, 5 mmole) in methanol. The ligand mixture was warmed to 64 ^oC for an hour before being mixed into an ethanolic solution (100 ml) of $CuCl_2 \cdot 2H_2O$ (1.7 g, 10 mmole). The solution was left at room temperature for approximately 16 hours; the green precipitate was isolated by vacuum filtration under nitrogen, and washed with cold ethanol. The 1.28 g of green solid was isolated after air-drying and was found to react immediately with air so that recrystallisation was not possible under normal conditions.

3.3.2.4 Method 4

2-OH-*o*VANPN (0.10 g; 0.3 mmole) was dissolved in anhydrous dichloromethane (30 ml) and slowly added drop wise over a suspension of $CuCl_2.2H_2O$ (0.12 g; 0.3 mmole) in the same solvent (30 ml). The resulting slurry was stirred for three hours, the excess metal filtered off and the filtrate left overnight. The filtrate yielded dark green crystals, which was recrystallised from boiling dichloromethane to yield 0.23 g.

3.3.3 Syntheses of the cobalt(II) complexes

3.3.3.1 Method 1

A methanolic solution (15 ml) of 2-OH-*o*VANPN (0.72 g, 2 mmol) was added to a methanolic solution (10 ml) of cobalt(II) hexahydrate ($CoCl_2 \cdot 6H_2O$) (0.476 g, 2 mmole). A methanolic solution (15 ml) of potassium hydroxide (0.32 g, 5.7 mmole) was added. The mixture was left to stand at room temperature for approximately 16 hours. White crystals (KCl) were removed by filtration. The solvent was removed under vacuum to yield a green-black solid, which was treated with 10 ml cold ether to crystallize the complex. The solid was vacuum-filtered under nitrogen, washed with cold methanol, and dried in vacuo. The crude yield was 0.43 g and the recrystallised (EtOH) yield was 0.084 g of brown complex from 0.26 g crude.

3.3.3.2 Method 2

An ethanolic solution (5 ml) of 2-OH-*o*VANPN (0.72 g, 2 mmole) was added to an ethanolic solution (30 ml) of cobalt(II) chloride hexahydrate ($CoCl_2 \cdot 6H_2O$) (0.48 g, 2 mmole). The volume was reduced to 5 ml on a steam bath. The resulting oil was treated with 10 ml cold ether to aid in crystallization of the complex. Brown crystals were collected by vacuum filtration under nitrogen, washed with cold ethanol and dried *in vacuo*. Recrystallization (ethanol) yielded 0.28 g of brown complex.

3.3.3.3 Method 3

An ethanolic solution (15 ml) of *o*-vanillin (3.04 g, 20 mmole) was added to a methanolic solution (15 ml) of 1,3-diaminopropan-2-ol (0.9g, 10 mmole). The ligand mixture was

warmed for an hour and then added to an ethanolic solution (230 ml) of cobalt(II) chloride hexahydrate ($CoCl_2 \cdot 6H_2O$) (4.76 g, 20 mmole). The solution was left to stand at room temperature for approximately 16 hours. The green precipitate was collected by vacuum filtration under nitrogen, washed with cold ethanol, and dried in vacuo to yield 1.50g. Recrystallisation (EtOH) yielded 0.4 g of green complex.

3.3.3.4 Method 4

2-OH-*o*VANPN (0.89 g, 2.5 mmole) was dissolved in anhydrous dichloromethane (30 ml) and slowly added drop wise over a suspension (dichloromethane, 30 ml) of $CoCl_2 \cdot 6H_2O$ (0.59 g, 2.5 mmole). The resulting slurry was stirred for three hours and the excess metal filtered off and the filtrate allowed to stand for 24 hours. The filtrate yielded 0.27 g, 0.26 g of which was recrystallized (butan-1-ol) to yield 0.03 g of dark green complex.

3.3.4 Syntheses of the cobalt(III) complexes

3.3.4.1 Method 1

The same procedure as described under 3.3.3.1 was employed, except the $CoCl_2 \cdot 6H_2O$ (0.47 g, 2 mmole in 10 ml MeOH) was treated with 0.11 mL of acetic acid (99.8 % m/m; 1.05 $g.mL^{-1}$) and then the Co(II) in it oxidized to Co(III) with 0.10 mL of H_2O_2 (30 %m/m; 1.10 $g.mL^{-1}$), according to the redox reaction:

$$2Co^{2+} + 2H^{+} + H_2O_2 \rightarrow 2Co^{3+} + 2H_2O$$

The 0.32-g of dark green solid yielded 0.15 g of green recrystallized (MeOH) complex.

3.3.4.2 Method 2

The same procedure as described under 3.3.3.2 was employed, except the $CoCl_2 \cdot 6H_2O$ (0.47 g, 2 mmole in 10 ml MeOH) was treated with 0.11 mL of acetic acid (99.8 % m/m; 1.05 g. mL^{-1}) and then the Co(II) in it oxidized to Co(III) with 0.10 mL of H_2O_2 (30 % m/m; 1.10 g. mL^{-1}), before the ligand solution was added, according to the redox reaction: $2Co^{2+} + 2H^{+} + H_2O_2 \rightarrow 2Co^{3+} + 2H_2O$

The product required no treatment with cold ether. Crude yield was 0.24 g, 0.103 g of which gave 0.037 g of green complex upon recrystallization (butan-1-ol).

3.3.4.3 Method 3

The same procedure as described under 3.3.3.3 was employed, except the $CoCl_2 \cdot 6H_2O$ (0.47 g, 2 mmole in 10 ml MeOH) was treated with 0.11 mL of acetic acid (99.8 % m/m; 1.05 g. mL^{-1}) and then the Co(II) in it oxidized to Co(III) with 0.10 mL of H_2O_2 (30 %m/m; 1.10 g. mL^{-1}) before the warmed ligand solution was added. The crude weighed 0.44 g. Recrystallization (EtOH) was unsuccessful due to low solubility in the solvent.

3.3.4.4 Method 4

The same procedure as described under 3.3.3.4 was employed, except the $CoCl_2 \cdot 6H_2O$ (0.47 g, 2 mmole in 10 ml MeOH) was treated with 0.11 mL of acetic acid (99.8 % m/m; 1.05 g. mL^{-1}) and then the Co(II) in it oxidized to Co(III) with 0.10 mL of H_2O_2 (30 %m/m; 1.10 g. mL^{-1}) before the ligand solution was added. The mass of ligand and $CoCl_2.6H_2O$, respectively, was double that of the Co(II) synthesis. The crude weighed 0.41 g. Recrystallization of 0.34 g of the crude from boiling dichloromethane yielded 0.18 g of brown complex.

3.4 RESULTS

The results obtained from the physical and analytical techniques used to characterize the ligand and the corresponding copper(II), cobalt(II) and cobalt(III) complexes are summarized in the following tables.

3.4.1 Physicochemical data for the Schiff base ligand

Table 3:1 Microanalysis and analytical data for the Schiff base ligand

		% Found % Calculated						
Ligand	Molecular formula	% C	% H	% N	Color	Yield (%)	M.p. (°C)	Molar mass (g. $mole^{-1}$)[a]
2-OH-*o*VANPN	$C_{19}H_{22}N_2O_5$	63.31 63.67	6.29 6.19	7.68 7.82	Yellow	83	119-22	358.40

Footnote a: Based on microanalytical data

3.4.2 Physicochemical data for the complexes

Table 3:2 Microanalysis and analytical data for the Schiff base (and 2-OH-*o*VANPN-based) Cu(II) complexes

		% Found % Calculated						
No.	Molecular formula	% C	% H	% N	% Cu	Yield (%)	M.p. (°C)	Molar mass (g.mole^{-1})[a]
(A1)	$K[Cu(C_{19}H_{20}N_2O_5)(OH)]\cdot 2H_2O$[b]	44.29	4.02	5.73	13.19	53	260[c]	512.06
	(Green)	44.50	4.92	5.47	12.41			
(A2)	$[Cu(C_{11}H_{15}N_2O_3)(Cl)_2]\cdot 2H_2O$	33.74	4.38	6.58	c	36	174[c, e]	394.74
	(Green)	33.47	4.85	7.10	16.10			
(A3)	$[Cu(C_{11}H_{16}N_2O_3)(Cl)_2]$	36.65	3.75	7.84	17.72	71	174[c, e]	358.71
	(Green)	36.83	4.20	7.81	17.71			
(A4)	$\{Cu_3(C_{11}H_{14}N_2O_3)(Cl)_4(H_2O)_6\}$	19.58	3.19	4.53	28.75	29	152[c]	662.79
	(Green)	19.93	3.95	4.23	28.76		174[e]	

Footnote a: Based on microanalytical data
b: % K = 7.20 (Found); 7.62 (Calculated)
c: Decomposition temperature; no melting observed
d: Not analysed for
e: sublimation

Table 3:3 Microanalysis and analytical data for the 2-OH-*o*VANPN-based Co(II) complexes

		% Found % Calculated						
No.	Molecular formula	% C	% H	% N	% Co	Yield (%)	M.p. (°C)	Molar mass (g.mole^{-1})[a]
(B1)	$[Co_2(C_{19}H_{19}N_2O_5)(OH)]$	46.92	4.87	5.37	23.91	28	204[b]	490.24
	(Brown)	46.55	4.11	5.71	24.04			
(B2)	$[Co(C_{17}H_{17}N_2O_5)(Cl)]\cdot 1½H_2O$	45.11	5.21	6.21	13.21	31	116[c]	450.74
	(Green)	45.30	4.47	6.21	13.07		180[b]	
(B3)	$[Co(C_{19}H_{22}N_2O_5)(Cl)_2]\cdot 5½H_2O$	39.11	4.82	4.72	13.90	03	194[b]	587.32
	(Green)	38.85	5.66	4.77	10.03			
(B4)	$[Co(C_{19}H_{22}N_2O_5)(Cl)_2]\cdot 5½H_2O$	38.20	5.64	6.27	9.80	02	194[b]	587.32
	(Green)	38.85	5.66	4.77	10.03			

Footnote a: Based on microanalytical data
b: Sublimation
c: Decomposition temperature; no melting observed

Table 3:4 Microanalysis and analytical data for the 2-OH-*o*VANPN-based Co(III) complexes

		% Found % Calculated						
No.	Molecular formula	% C	% H	% N	% Co	Yield (%)	M.p. (°C) (thermal event)	Molar mass ($g.mole^{-1}$)[a]
(C1)	$[Co(C_{19}H_{19}N_2O_5)]$	55.21	5.53	6.50	b	18	190[c]	414.30
	(Brown)	55.08	4.62	6.76	14.22			
(C2)	$[Co(C_{19}H_{21}N_2O_5)(Cl)_2]\cdot 5H_2O$	38.94	4.61	5.09	10.26	08	200[c]	577.30
	(Brown)	39.53	5.41	4.85	10.21			
(C3)	$[Co(C_{19}H_{20}N_2O_5)(Cl)]\cdot 3H_2O$	45.76	4.92	5.50	11.71	44	174	504.81
	(Green)	45.21	5.19	5.55	11.67			
(C4)	$[Co(C_{19}H_{20}N_2O_5)(Cl)]$	49.88	5.31	5.79	14.17	24	116-8	450.77
	(Green)	50.63	4.47	6.21	13.07			

Footnote a: Based on microanalytical data
b: Not analysed for
c: Sublimation

3.4.3 Mid infrared data for the Schiff base ligand

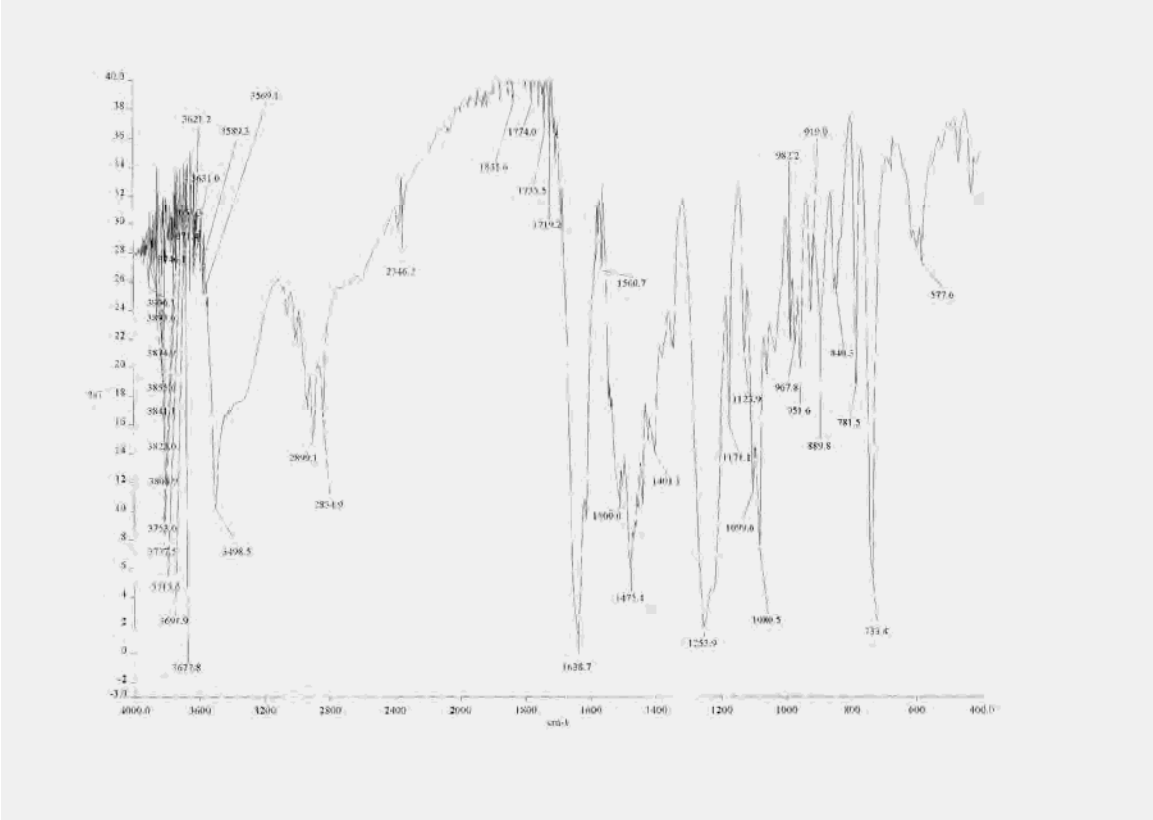

Figure 3.5: The mid infrared spectrum of the Shiff base ligand in this work

Table 3:5 Mid infrared frequencies (cm^{-1}) for the Schiff base ligand and similar ligands

	Compound	νO-H	νC=N	νC-O	Other
Ref	2-OHSALPN	3394	1611	1275	1635s, 1579m, 1497m, 1339w, 1156w, 1104w, 1084w, 1048m, 940w, 844m, 752s
	2, 3-OHSALPN	3360	1640	1235	Not reported
This work	2-OH-*o*VANPN	3498	1639	1254	1638s, 1561m, 1475m, 1401w, 1171w, 1124w, 1080w, 1054m, 952w, 840m(br), 734s

3.4.4 Mid and far infrared data for the complexes

3.4.4.1 Some mid and far infrared spectra and data of the Cu(II) complexes

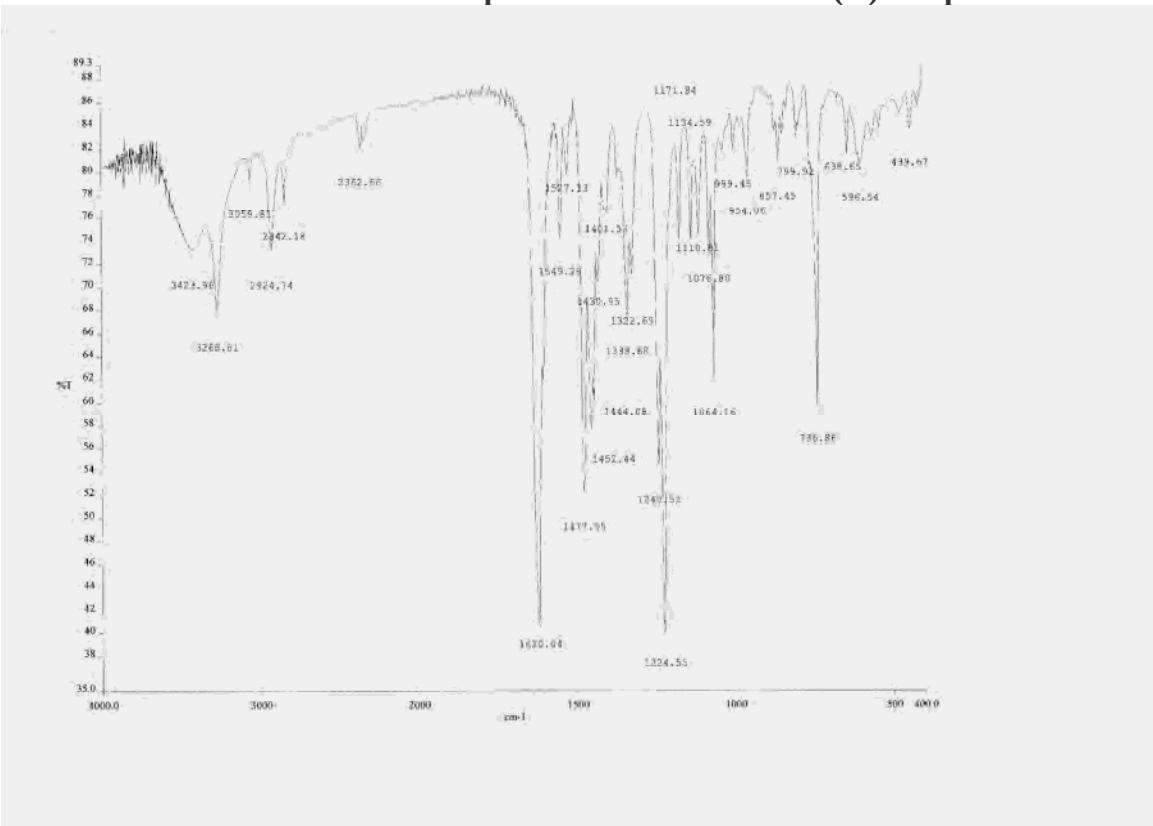

Figure 3.6: The mid infrared spectrum of $K[Cu(C_{19}H_{20}N_2O_5)(OH)]\cdot 2H_2O$ **(A1)**

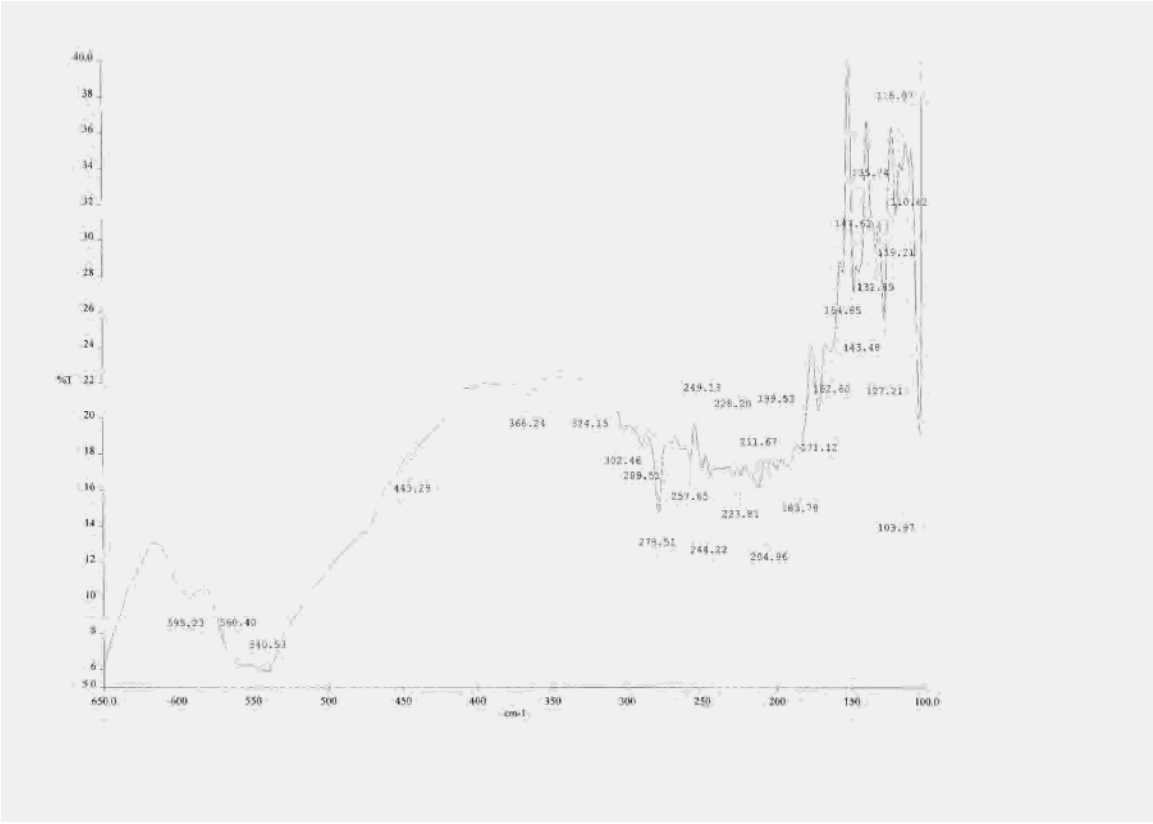

Figure 3.7: The far infrared spectrum of $K[Cu(C_{19}H_{20}N_2O_5)(OH)]\cdot 2H_2O$ **(A1)**

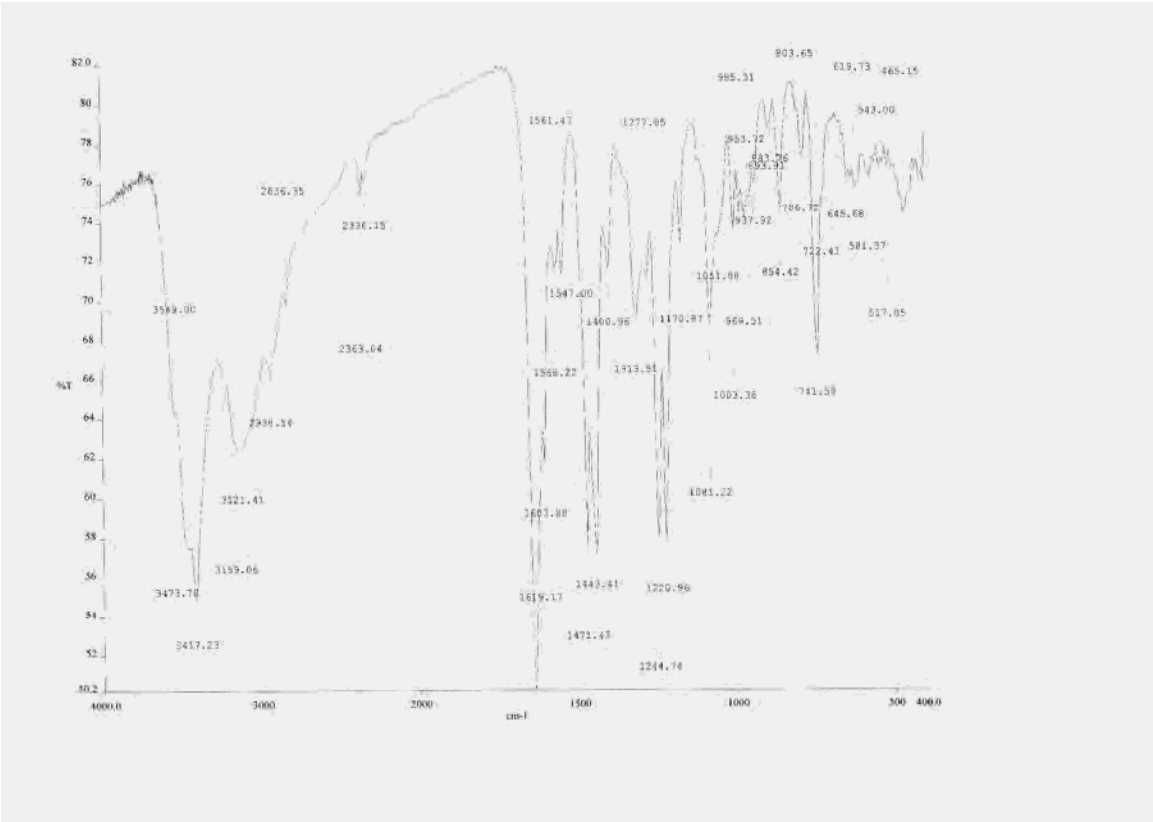

Figure 3.8: The mid infrared spectrum of $[Cu(C_{11}H_{16}N_2O_3)(Cl)_2]$ **(A3)**

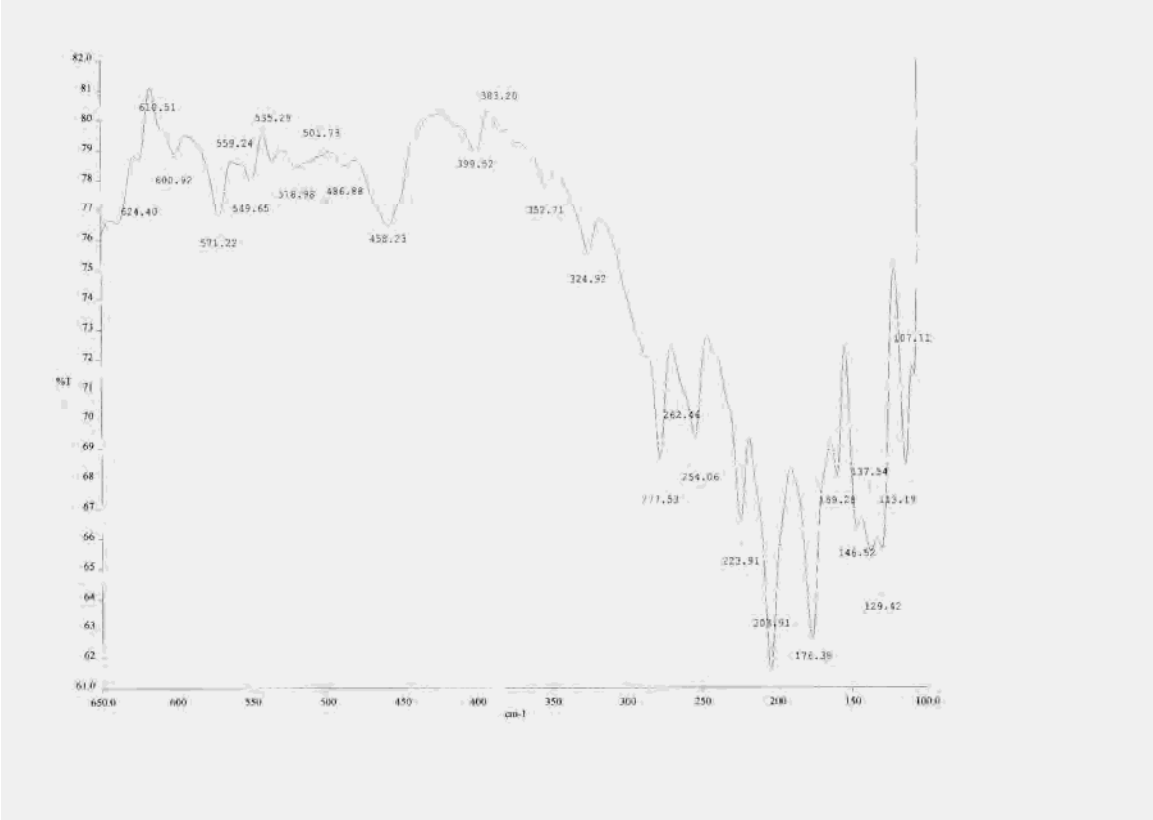

Figure 3.9: The far infrared spectrum of $[Cu(C_{11}H_{16}N_2O_3)(Cl)_2]$ **(A3)**

Table 3:6 Mid and far infrared frequencies (cm^{-1}) for the 2-OH-*o*VANPN-based Cu(II) complexes

		Mid infrared				Far infrared		
	Compound	νO-H 3300-3500	νNH_2 3305-3233	νC=N 1620-1650	νC-O 1240-1260	νM-O 529-553	νM-N 425-504	νM-Cl 358, 116
Ligand	2-OH-*o*VANPN	3498	3290	1638	1254	-	-	-
(A1)	$K[Cu(C_{19}H_{20}N_2O_5)(OH)]\cdot 2H_2O$	3424	-	1620	1240	540	443	-
(A2)	$[Cu(C_{11}H_{15}N_2O_3)(Cl)_2]\cdot 2H_2O$	3415	3268	1640	1244	544	458	358, 114
(A3)	$[Cu(C_{11}H_{16}N_2O_3)(Cl)_2]$	3435	shoulder	1641	1244	535	458	353, 113
(A4)	$\{Cu_3(C_{11}H_{14}N_2O_3)(Cl)_4(H_2O)_6\}$	3381	-	1622	1244	550	448	358, 116

2.4.4.2 Some mid and far infrared spectra and data of the Co(II) complexes

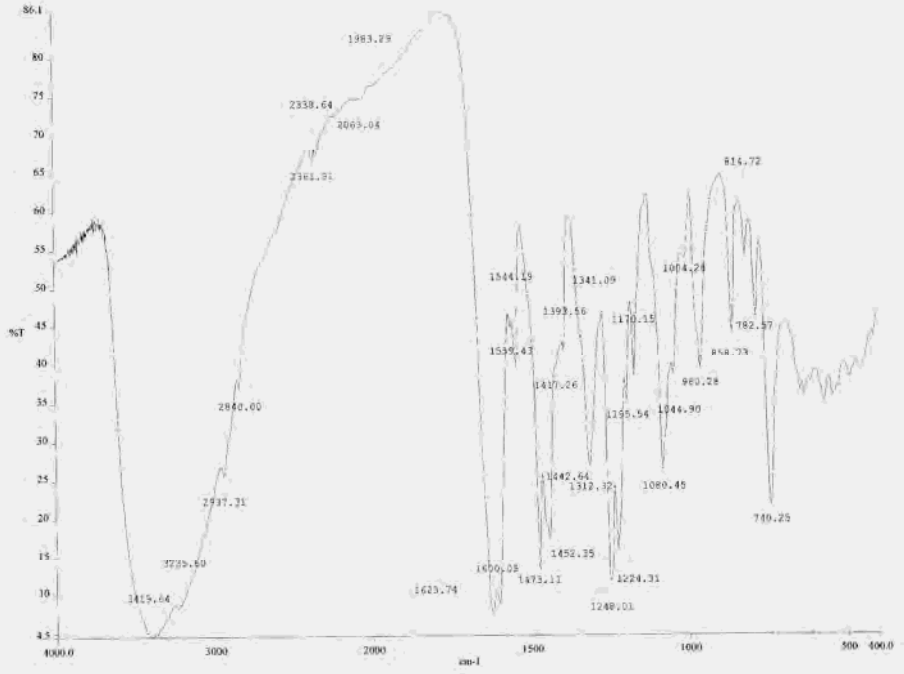

Figure 3.10: The mid infrared spectrum of $[Co(C_{17}H_{17}N_2O_5(Cl))]\cdot 1\frac{1}{2}H_2O$ **(B2)**

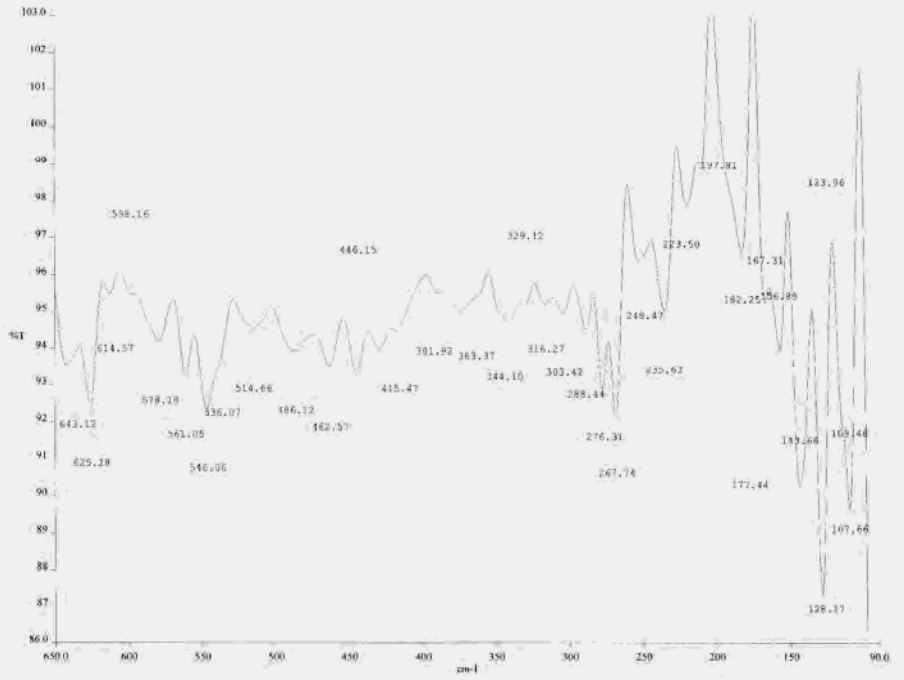

Figure 3.11: The far infrared spectrum of $[Co_2(C_{19}H_{19}N_2O_5)(OH)]$ **(B1)**

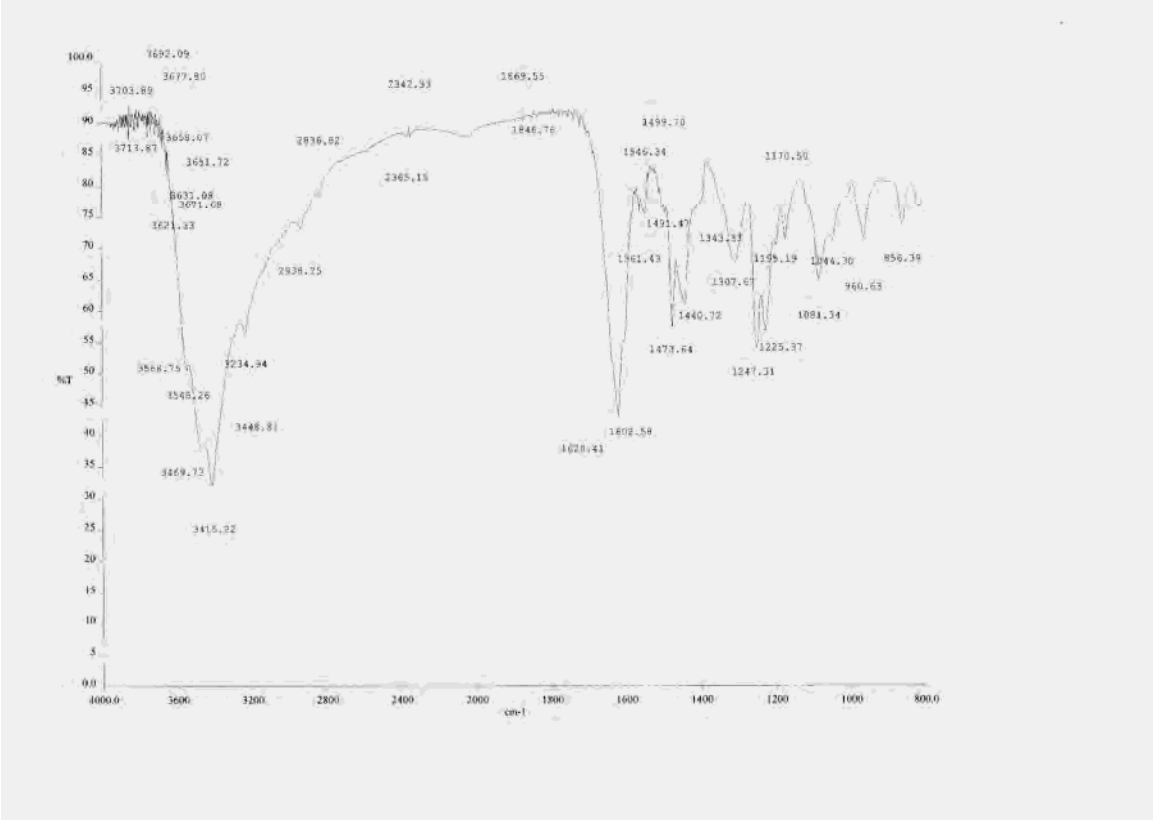

Figure 3.12: The mid infrared spectrum of $[Co(C_{19}H_{22}N_2O_5)(Cl)_2]\cdot 5\frac{1}{2}H_2O$ **(B4)**

Table 3:7 Mid and far infrared frequencies (cm^{-1}) for the 2-OH-*o*VANPN-based Co(II) complexes

		Mid infrared			Far infrared		
	Compound	νO-H 3300-3500	νC=N 1620-1650	νC-O 1240-1260	νM-O 529-553	νM-N 425-504	νM-Cl 358, 116
Ligand	2-OH-*o*VANPN	3498	1637	1254	-	-	-
(B1)	$[Co_2(C_{19}H_{19}N_2O_5)(OH)]$	3420	1627	1243	546	446	-
(B2)	$[Co(C_{17}H_{17}N_2O_5)(Cl)]\cdot 1\frac{1}{2}H_2O$	3420	1624	1248	550	448	359, 114
(B3)	$[Co(C_{19}H_{22}N_2O_5)(Cl)_2]\cdot 5\frac{1}{2}H_2O$	3415	1620	1233	543	450	363, 113
(B4)	$[Co(C_{19}H_{22}N_2O_5)(Cl)_2]\cdot 5\frac{1}{2}H_2O$	3415	1620	1247	543	450	363, 116

2.4.4.3 Some mid and far infrared spectra and data of the Co(III) complexes

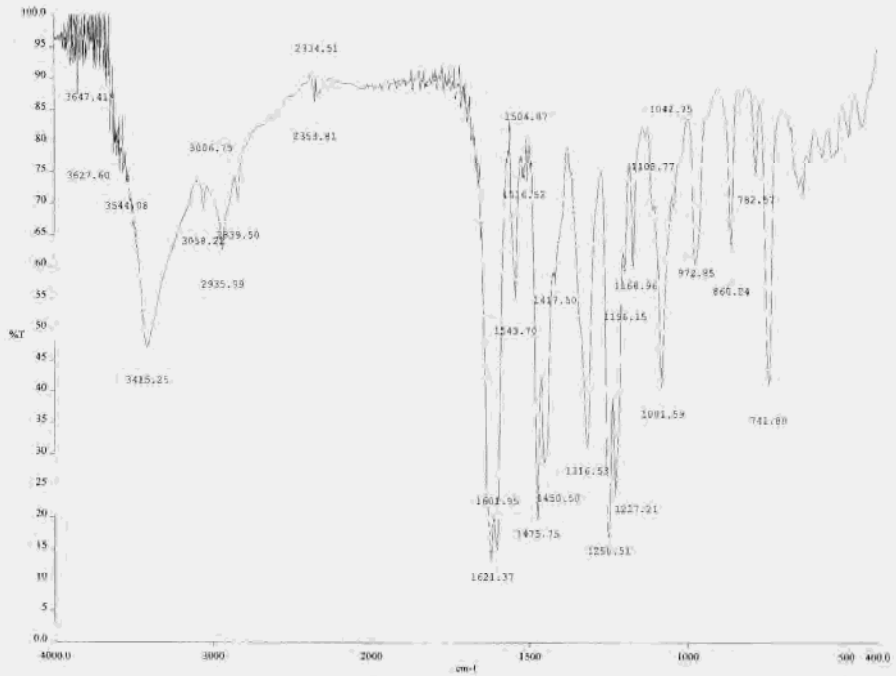

Figure 3.13: The mid infrared spectrum of $[Co(C_{19}H_{19}N_2O_5)]$ **(C1)**

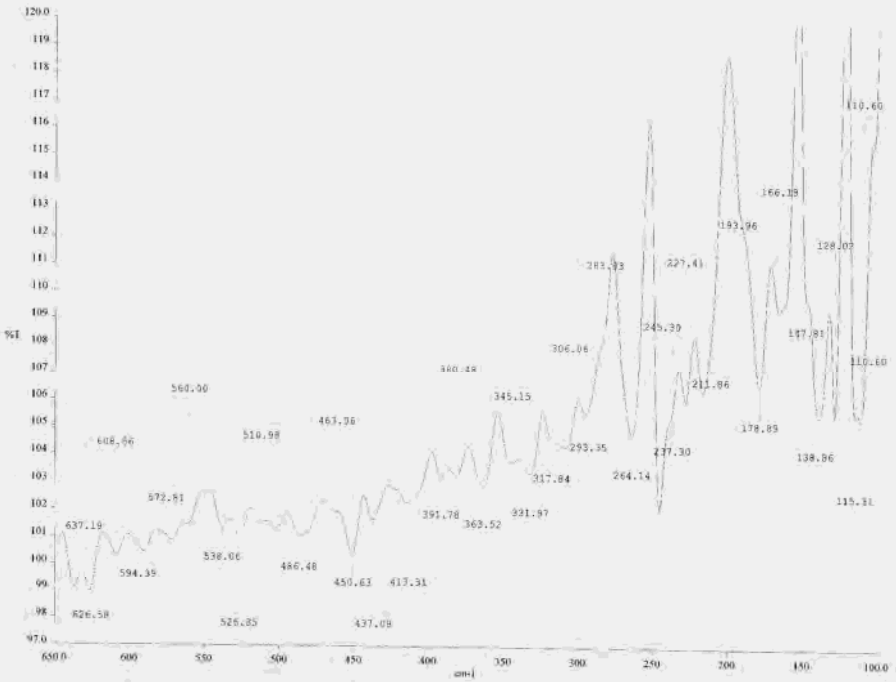

Figure 3.14: The far infrared spectrum of $[Co(C_{19}H_{19}N_2O_5)]$ **(C1)**

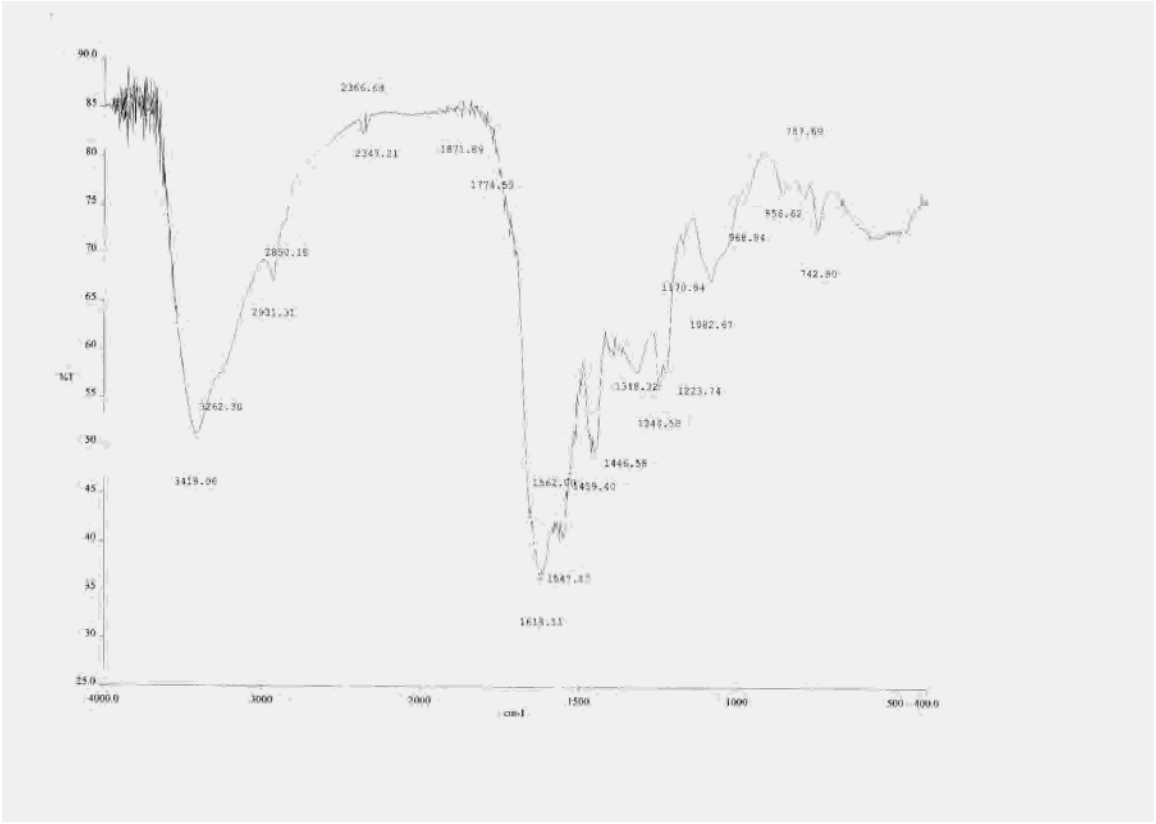

Figure 3.15: The mid infrared spectrum of $[Co(C_{19}H_{21}N_2O_5)(Cl)_2]\cdot 5H_2O$ **(C2)**

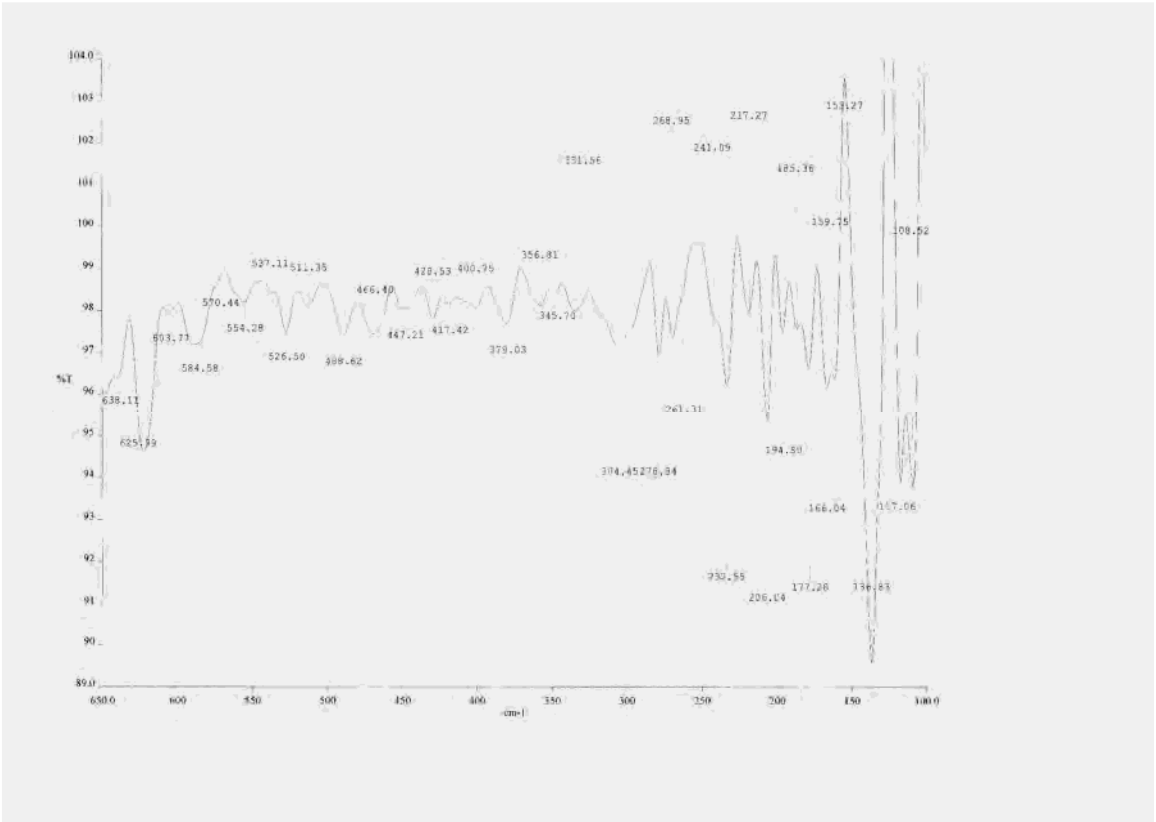

Figure 3.16: The far infrared spectrum of $[Co(C_{19}H_{21}N_2O_5)(Cl)_2]\cdot 5H_2O$, complex **(C2)**

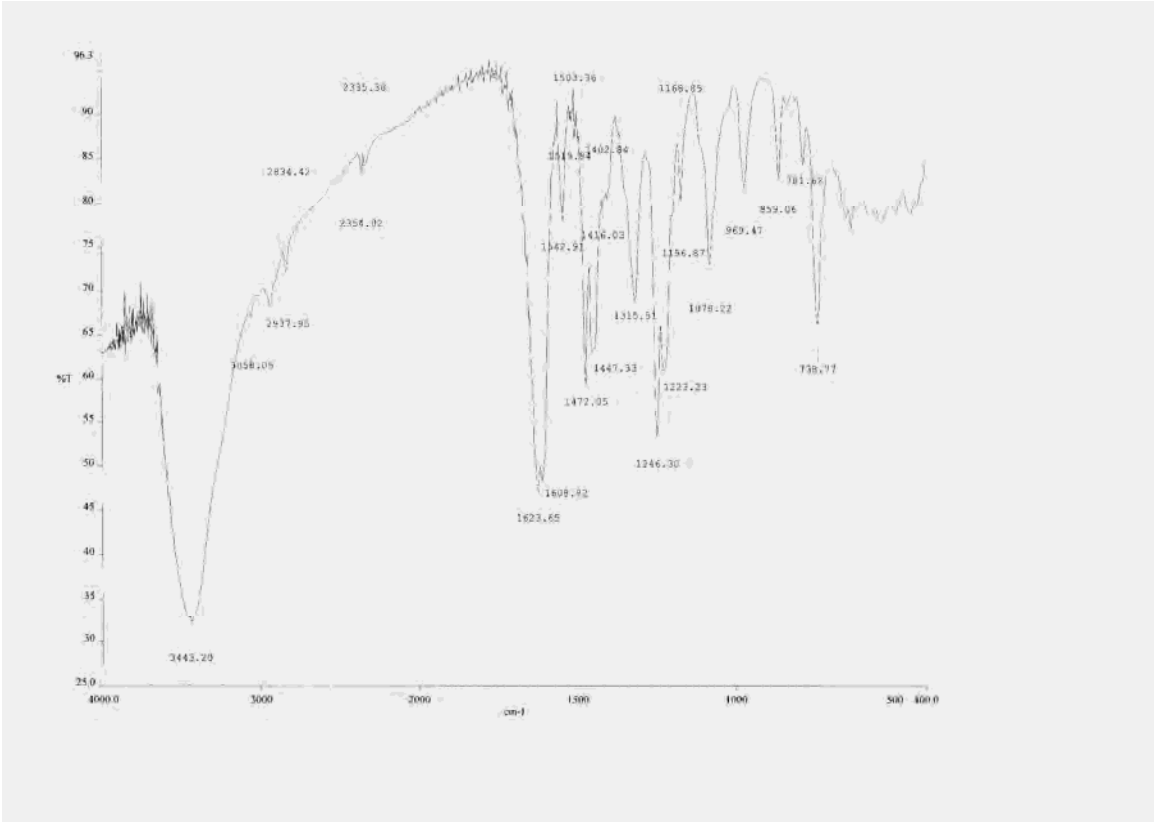

Figure 3.17: The mid infrared spectrum of $[Co(C_{19}H_{20}N_2O_5)(Cl)]$ **(C4)**

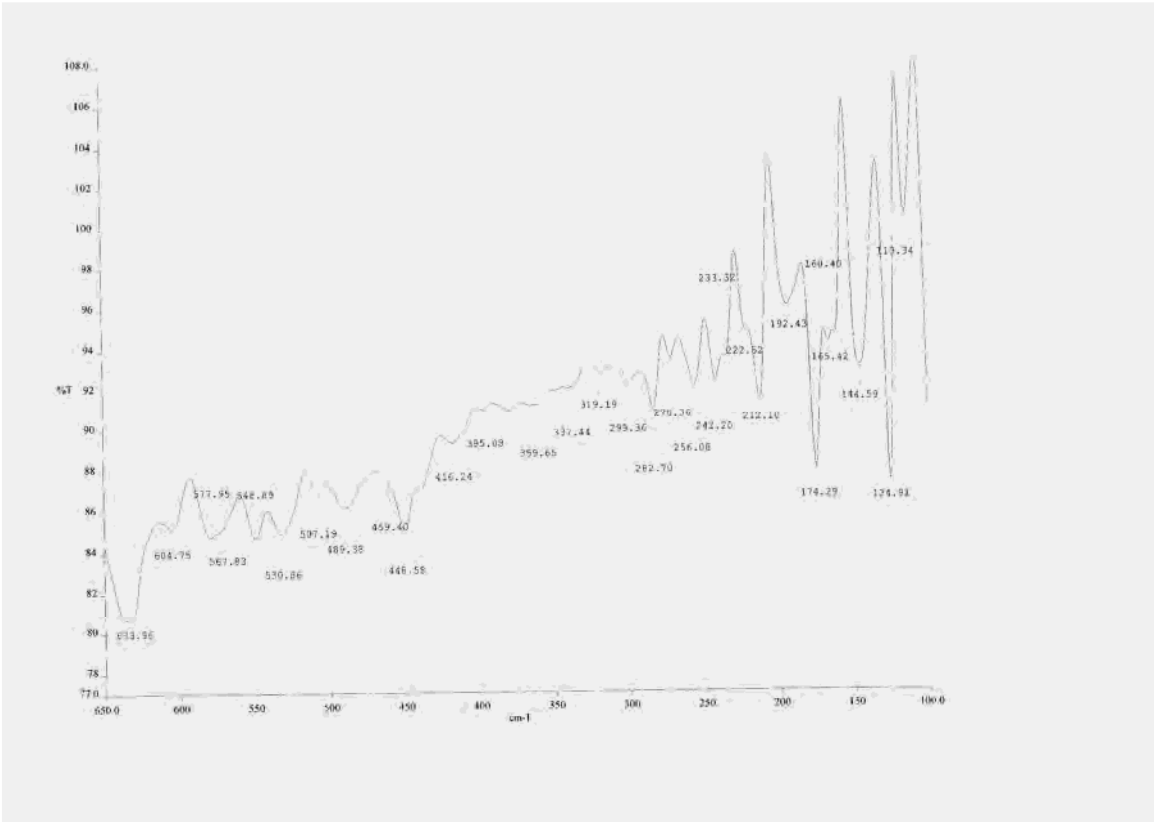

Figure 3.18: The far infrared spectrum of $[Co(C_{19}H_{20}N_2O_5)(Cl)]$ **(C4)**

Table 3:8 Mid and far infrared frequencies (cm^{-1}) for the 2-OH-*o*VANPN-based Co(III) complexes

		Mid infrared			Far infrared		
	Compound	νO-H 3300-3500	νC=N 1620-1650	νC-O 1240-1260	νM-O 529-553	νM-N 425-504	νM-Cl 116, 358
Ligand	2-OH-*o*VANPN	3498	1637	1254	-	-	-
(C1)	$[Co(C_{19}H_{19}N_2O_5)]$	3415	1621	1250	538	451	-
(C2)	$[Co(C_{19}H_{21}N_2O_5)(Cl)_2]\cdot 5H_2O$	3418	1618	1245	537	447	357, 114
(C3)	$[Co(C_{19}H_{20}N_2O_5)(Cl)]\cdot 3H_2O$	3434	1618	1244	548	446	361, 115
(C4)	$[Co(C_{19}H_{20}N_2O_5)(Cl)]$	3434	1623	1246	549	449	360, 113

3.4.5 Electronic spectra (UV/visible region) and data for the Schiff base ligand

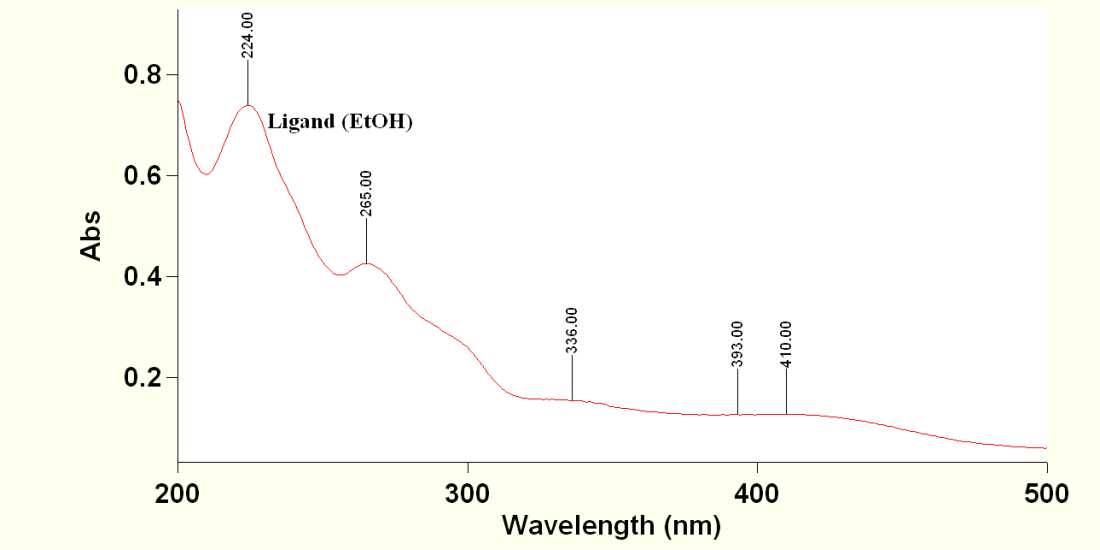

Figure 3.19: The UV/visible spectrum of the ligand (EtOH)

Table 3:9 UV/visible spectral data for the ligand and a similar ligand

	Compound	Solvent	200-240 nm	250-300 nm	305-350 nm	360-600 nm
Ref	2, 3-OHSALPN	Methanol	225	270, 290	330	425
Ligand	2-OH-*o*VANPN	Methanol	225	268, 288	330	438
		Ethanol	224	265, 295	336	410

3.4.6 Electronic spectra (UV/visible region) and data for the complexes

3.4.6.1 Some UV/visible spectra and data of the copper(II) complexes

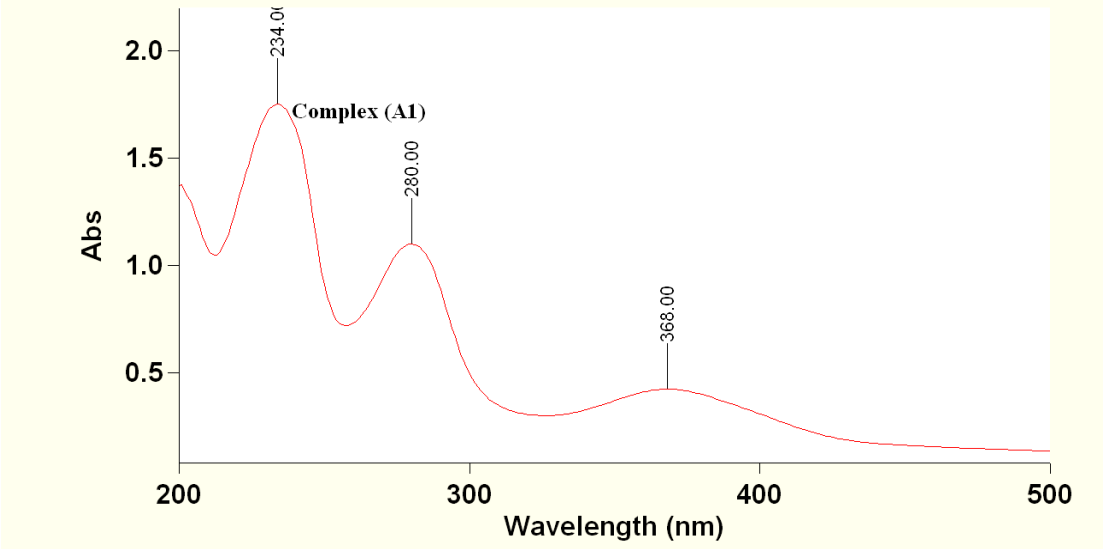

Figure 3.20: The UV/visible spectrum of $K[Cu(C_{19}H_{20}N_2O_5)(OH)]\cdot 2H_2O$ **(A1)** (MeOH)

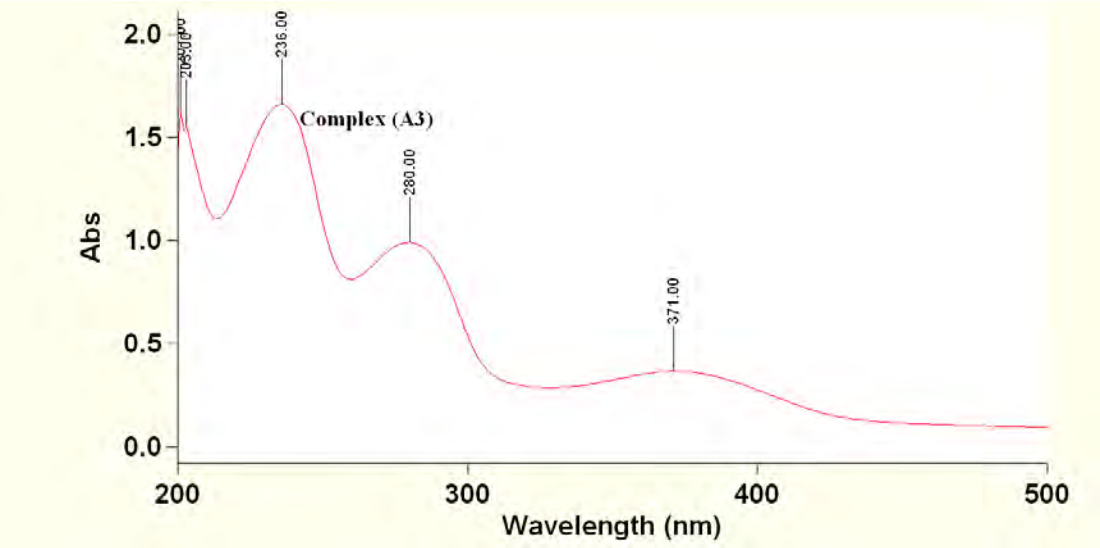

Figure 3.21: The UV/visible spectrum of $[Cu(C_{11}H_{16}N_2O_3)(Cl)_2]$ **(A3)** (MeOH)

Table 3:10 UV/visible spectral data for the 2-OH-*o*VANPN-based Cu(II) complexes

	Compound	Solvent	200-240 nm	250-300 nm	305-350 nm	360-500 nm
Ligand	2-OH-*o*VANPN	Methanol	225	268, 288	330	438
		Ethanol	224	265, 295	336	410
(A1)	$K[Cu(C_{19}H_{20}N_2O_5)(OH)]\cdot 2H_2O$	Methanol	234	280	-	368
(A2)	$[Cu(C_{11}H_{15}N_2O_3)(Cl)_2]\cdot 2H_2O$	Methanol	234	280	-	371
(A3)	$[Cu(C_{11}H_{16}N_2O_3)(Cl)_2]$	Methanol	236	280	-	371
(A4)	$\{Cu_3(C_{11}H_{14}N_2O_3)(Cl)_4(H_2O)_6\}$	Methanol	236	276	-	371

3.4.6.2 Some UV/visible spectra and data of the cobalt(II) complexes

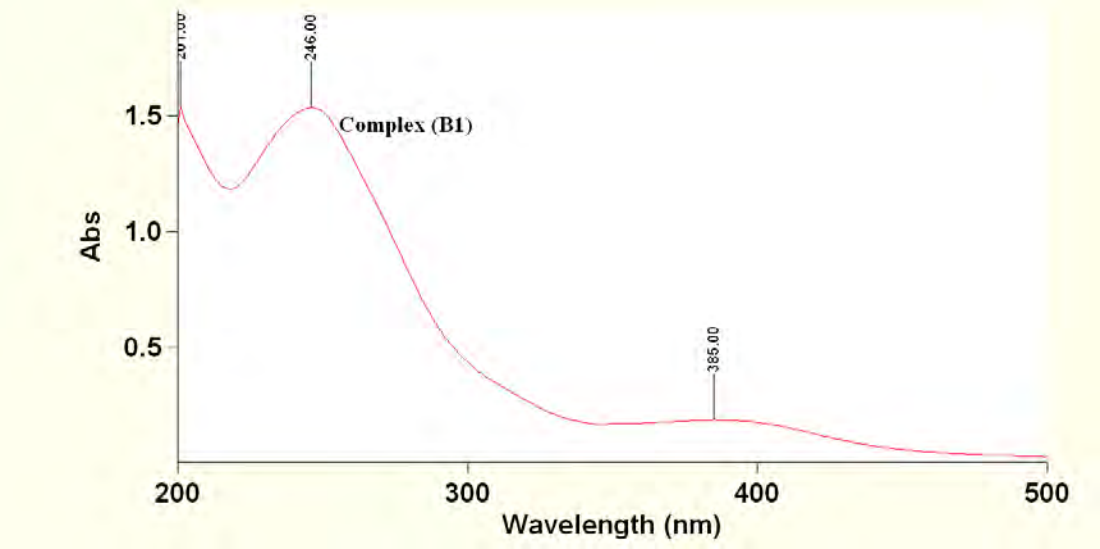

Figure 3.22: The UV/visible spectrum of $[Co_2(C_{19}H_{19}N_2O_5)(OH)]$ **(B1)** (MeOH)

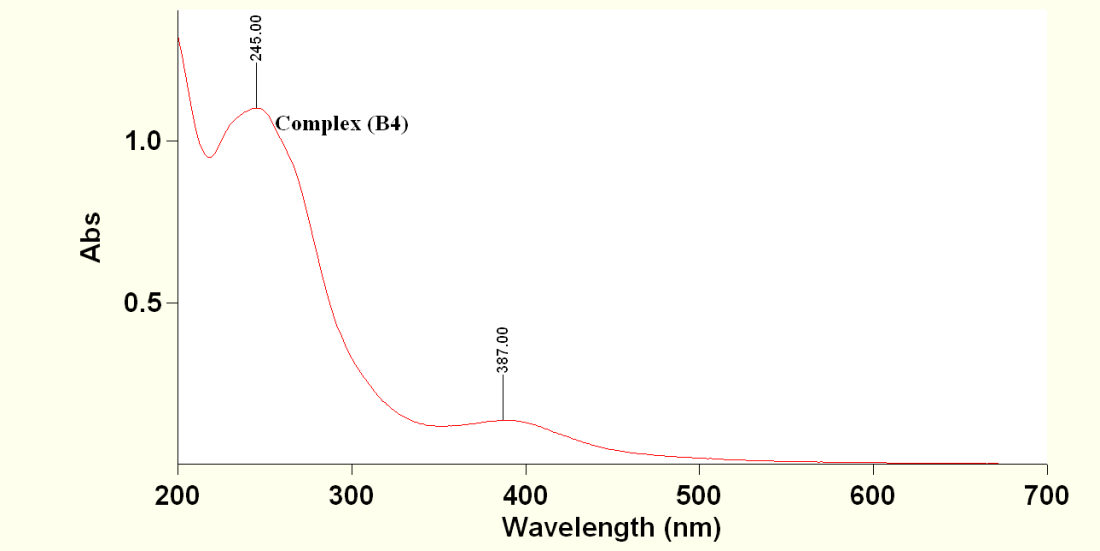

Figure 3.23: The UV/visible spectrum of $[Co(C_{19}H_{22}N_2O_5)(Cl)_2]\cdot5½H_2O$ **(B4)** (EtOH)

Table 3:11 UV/visible spectral data for the 2-OH-*o*VANPN-based Co(II) complexes

	Compound	Solvent	200-240 nm	250-300 nm	305-350 nm	360-500 nm
Ligand	2-OH-*o*VANPN	Methanol	225	268, 288	330	438
		Ethanol	224	265, 295	336	410
(B1)	$[Co_2(C_{19}H_{19}N_2O_5)(OH)]$	Methanol	-	246	-	385
(B2)	$[Co(C_{17}H_{17}N_2O_5)(Cl)]\cdot1½H_2O$	Ethanol	-	239	305	381
(B3)	$[Co(C_{19}H_{22}N_2O_5)(Cl)_2]\cdot5½H_2O$	Ethanol	-	244	-	387
(B4)	$[Co(C_{19}H_{22}N_2O_5)(Cl)_2]\cdot5½H_2O$	Ethanol	-	245	-	387

3.4.6.3 UV/visible spectral data of the cobalt(III) complexes

Table 3:12 UV/visible spectral data for the 2-OH-*o*VANPN-based Co(III) complexes

Compound		Solvent	200-240 nm	250-300 nm	305-350 nm	360-500 nm
Ligand	2-OH-*o*VANPN	Methanol	225	268, 288	330	438
		Ethanol	224	265, 295	336	410
(C1)	$[Co(C_{19}H_{19}N_2O_5)]$	Ethanol	-	259, 279	-	389
(C2)	$[Co(C_{19}H_{21}N_2O_5)(Cl)_2]\cdot 5H_2O$	Ethanol	-	265	318	386
(C3)	$[Co(C_{19}H_{20}N_2O_5)(Cl)]\cdot 3H_2O$	Ethanol	-	256	-	386
(C4)	$[Co(C_{19}H_{20}N_2O_5)(Cl)]$	Ethanol	-	261	-	387

3.4.7 Thermal studies on the Schiff base ligand and the copper(II) complexes

Table 3:13 Differential Scanning Calorimetry (DSC) data for the ligand and the corresponding Cu(II) complexes in air/ nitrogen

		Air		Nitrogen	
Compound		Temperature	Assignment	Temperature	Assignment
Ligand	2-OH-*o*VANPN	125 ºC	Endotherm (sharp)	-	-
		290 ºC	Endotherm (broad)		
(A1)	$K[Cu(C_{19}H_{20}N_2O_5)(OH)]\cdot 2H_2O$	290 ºC	Exotherm (sharp)	275 ºC	Exotherm (sharp)
(A2)	$[Cu(C_{11}H_{15}N_2O_3)(Cl)_2]\cdot 2H_2O$	185 ºC	Exotherm (broad)	320 ºC	Exotherm (broad)
		235 ºC	Exotherm (broad)	540 ºC	Endotherm (sharp)
		320 ºC	Exotherm (broad)	545 ºC	Endotherm (sharp)
		540 ºC	Endotherm (sharp)		
(A3)	$[Cu(C_{11}H_{16}N_2O_3)(Cl)_2]$	190 ºC	Exotherm (broad)	180 ºC	Exotherm (broad)
		415 ºC	Exotherm (broad)	415 ºC	Exotherm (broad)
		540 ºC	Endotherm (sharp)	540 ºC	Endotherm (sharp)
		545 ºC	Endotherm (sharp)	545 ºC	Endotherm (sharp)
(A4)	$\{Cu_3(C_{11}H_{14}N_2O_3)(Cl)_4(H_2O)_6\}$	90 ºC	Endotherm (broad)	90 ºC	Endotherm (broad)
		375-425 ºC	Exotherm (broad)	375-425 ºC	Exotherm (broad)
		540 ºC[a]	Endotherm (sharp)	540 ºC[a]	Endotherm (sharp)
		545 ºC[a]	Endotherm (sharp)	545 ºC[a]	Endotherm (sharp)

Footnote a: This peak was again observed upon re-run of the sample

3.5 DISCUSSION

3.5.1 Structure and physicochemical properties of the Schiff base ligand

The ligand in this work, 2-OH-*o*VANPN (H_3L) (Figure 3.24), was obtained as a condensation product of *o*-vanillin and diaminopropan-2-ol and gave a bright yellow solid. The colour intensity can be attributed to the positions of auxochromic (the hydroxy and methoxy) groups on the phenyl attached to the imine (C=N) group. The presence of the hydroxyl and methoxy in the conjugated system resulted in the enhancement of the delocalization of the π-electrons in the ligand molecule. It should be noted that various

reports show that the hydroxyl group in the *ortho*-position is the cause of the high colour intensity. While ligands obtained from *o*-vanillin are intensely coloured, those derived from vanillin are cream-like, less intense, because the OH is *para*-substituted.

2-OH-*o*VANPN (Figure 3.24), has 5 potential donor sites, N_2O_3.

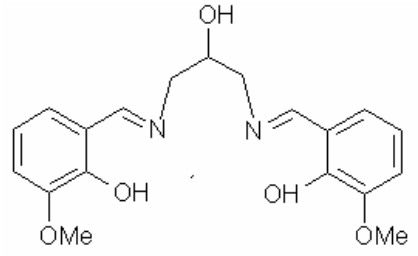

Figure 3.24: The ligand in the present work, 2-OH-*o*VANPN (LH_3)

The elemental analyses (Table 3:1) are in good agreement with the chemical formula proposed for the Schiff base ligand. The structure of Schiff bases is related to the possibilities for tautomeric transformation, formation of hydrogen bonds and conformational effects (Garnovskii *et al*., 1993). These properties, as depicted by the IR (Figure 3.5) and UV-Vis (Figure 3.20) results for 2-OH-*o*VANPN in this work, are responsible for the factors influencing the structure of metal complexes derived from this ligand. The UV-Vis (MeOH) results have been used to explain tautomeric transformation in this ligand and IR to identify the important functional groups.

3.5.1.1 Mid-infrared: The OH- and phenolic C-O stretching vibration

The earliest known and most studied IR band is the one arising from the O-H valence vibration (Bellamy, 1975). When hydrogen bonding occurs, an increase in bond-length occurs which causes the O-H absorption band to shift to a lower frequency (Bellamy, 1975). Three types of hydroxyl group bonding are known: intermolecular, intramolecular and chelation. The absorption range of the OH valence-stretching vibration of an unbounded hydroxyl group is usually 3700 - 3500 cm^{-1} (Bellamy, 1975).

The ligand in the present work gave a broad IR band (Figure 3.5) in this range. The free ligand in the present work also gave a band in the range 2500 – 2800 cm^{-1}, which

corresponds to a phenolic OH group. Substituents that enhances resonance stabilization (mesomeric effect), as is the case with the methoxy group in position 3 of the aromatic ring (Figure 3.5), decreases the bond order and results in lower frequency for the phenolic C-O stretching vibration (Kemp, 1975). The phenolic C-O stretching frequency of the ligand in this work appeared at 1275 cm^{-1}.

3.5.1.2 Mid-infrared: The C=N stretching vibration

Much investigation has been done into the position of the C=N (imine) stretching frequency for a variety of compounds, and it has been found that the physical state of the compound, the position of the substituent group, the nature of the substituent group, hydrogen bonding and conjugation with either the C=N-carbon or the C=N-nitrogen, or both, affect the position of this band (Faniran *et al*., 1974).

The ligand in this work gave the C=N band (Figure 3.5) at 1637 cm^{-1}. This value falls within the range 1620 – 1640 cm^{-1} reported for salicylaldimine complexes (Mazurek *et al*., 1986; Naik *et al*., 2006 and Wang and Chang, 1994) and 1650 – 1638 cm^{-1} reported for compounds of the type Ar-CH=N-R (Fabian and Legrand, 1956). The presence of the methoxy group in position 3 of the aromatic ring (Figure 3.24) has an electron donating effect on the aromatic ring thereby causing shortening of the length of the C=N (imine); thus, resulting in the observed frequency.

3.5.1.3 Far infrared: Metal-ligand stretching frequencies (ν_{M-O}, ν_{M-N}, ν_{M-Cl})

The far infrared wavenumber region includes both ligand vibrations and vibrations arising from coordination of the metal to the ligand. The latter vibrations are influenced by the nature of the ligand.

The ligand, 2-OH-*o*VANPN, in the present study has an additional donor site, the alkyllic OH. In addition, the use of copper(II) chloride and cobalt(II) chloride salts introduces the possibility of halide coordination. Both facilitates coordination numbers exceeding four for the resulting metal complexes, which in turn results in far infrared spectra with

potentially higher complexity than those for distorted tetrahedral *N*-arylsalicylaldimine metal(II) complexes.

3.5.2 Structure of the metal complexes

There are three possible types of complexes resulting from the reaction of Schiff bases with transition-metal compounds. The most common of these is the inner-chelate complex in which the Schiff base is bonded to the metal through the oxygen atoms of its deprotonated hydroxy groups and the nitrogen atoms of its C=N groups (Bowden and Ferguson, 1974). That is, those in which the ligand binds as a dianionic N_2O_2 donor system. Schiff bases have also been known to coordinate via nitrogen atoms only (Bowden and Ferguson, 1974). This is the system in which the ligand acts as a neutral N_2 donor binding via imine groups. This occurs when transition metal halides are used. The third possibility involves the hydrogenation of the C=N group, and formation of an inner-chelate complex between the secondary amine ligands and the metal in a higher oxidation state (Bowden and Ferguson, 1974).

Upon complexation, 2-OH-*o*VANPN (Figure 3.24) in the present work, may bond via two imine nitrogens, two phenol oxygens and the oxygen from the alkylic OH. Ligands of this LH_3-type can be deprotonated at the phenolic oxygens to form a conventional Schiff base ligand, LH^{2-} (Butcher, 1986). Further deprotonation at the alkanolic oxygen results in a binucleating ligand, L^{3-} (Butcher, 1986). Intramolecular hydrogen bonds in Schiff bases may form six- or five-membered ring cycles. The hydrogen bonds participating in six-membered rings are stronger than those in five-membered rings due to the formation of quasi-aromatic type in the former case (Garnovskii *et al.*, 1993).

For the four synthesis methods employed, the copper(II) complexes are denoted as **(A1)**, **(A2)**, **(A3)** and **(A4)**; the cobalt(II) complexes as **(B1)**, **(B2)**, **(B3)** and **(B4)**, and the cobalt(III) complexes as **(C1)**, **(C2)**, **(C3)** and **(C4)**. The complexes are grouped according to the type or oxidation state of the metal used in preparing them. In all, this work has three categories of complexes based on copper(II), cobalt(II) and cobalt(III). The four synthetic methods, 1 to 4, were applied to each of copper(II), cobalt(II) and

cobalt(III), and efforts were made to successfully characterize the 12 complexes as can be seen from the data (Tables 3:2 - 3:12).

The elemental analyses (Tables 3:2 – 3:4) are in good agreement with the chemical formulae proposed for all of the complexes, except for the % Co found for complex **(B3)** and the % N found for complex **(B4)**.

While most of the complexes (Tables 3:2 – 3:4) are green, **(B1)**, **(C1)** and **(C2)** are brown in colour. The colour of the M^{2+} complexes is linked to the extent of coordination to the metal:- Green complexes correspond to a coordination number greater than four and brown complexes are four-coordinated (Zolezzi *et al*., 1991). None of the complexes were soluble in water and all of them were soluble or slightly soluble in non-polar solvents (methanol, dimethylformamide, ethanol, etc.).

Analyses of the Schiff base and the corresponding complexes are based on previous IR and UV-Vis assignments of similar Schiff bases and complexes. Many cases have been reported of ligand IR bands shifting to lower or higher frequencies when a chelate is formed (Garnovskii *et al*., 1993; Dianzhong, 1993; Seminara, *et al*., 1999 and Tumer *et al*., 1999). This is confirmed when inspecting Tables 3:5 – 3:8. Mid-IR assignments are based on characteristic group frequencies, such as stretching frequencies of OH, C=N (imine), and C-O, for salicylaldimines. A shift of the C=N strectching band in the mid infrared spectrum of a particular complex compared to the position observed for this band in the mid infrared spectrum of the corresponding Schiff base ligand suggests the presence of N-coordination to the metal center (Chattopadhyay and Sinha, 1996 and Vogel, 1975). Far-IR spectroscopic data was used to assign metal-ligand stretching frequencies such as ν_{M-O}, ν_{M-N} and ν_{M-Cl}. Vibrations arising from coordination of the metal to the ligand are influenced by the nature of the ligand. The metal-ligand frequencies are known to occur below 600 cm^{-1} and both M-O and M-N are associated with the imine and hydroxyl group, respectively of *N*-arylsalicylaldimine complexes.

3.5.2.1 The Copper(II) complexes

The copper(II) complexes with LH^{2-}-type ligands, to which the ligand (Figure 3.5) in the present work belongs to, are monomeric with LH^{2-} acting as a tetradentate ligand, with two Cu-N bonds and two shorter Cu-O bonds to the phenolic oxygens thereof (Butcher, 1986). The alkanolic OH group possibly remains protonated by not coordinating to the metal atom (Butcher, 1986). Except for the trinuclear Cu(II) complex, all other complexes in Table 3:2 fits the above description. The ligand, 2-OH-*o*VANPN (Figure 3.24), can deprotonate at the phenolic oxygens and then further deprotonate at the alkanolic oxygen (Butcher, 1986) such that, in conjunction with anionic ligands (OH^-, Cl^-, etc.) and alkali-metal ions, it can lead to the formation of polynuclear complexes (Bertoncello *et al*., 1991) like the trinuclear Cu(II) complex formulated in Table 3:2.

3.5.2.1.1 *Structure and characterization of complex (A1)*

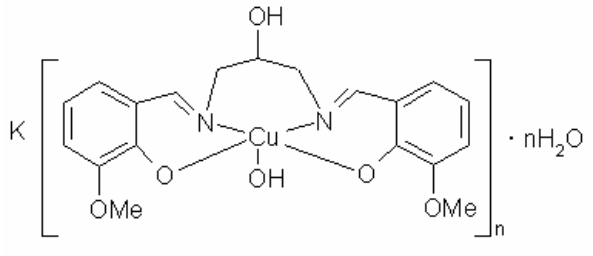

Figure 3.25: The structure of complex **(A1)** (n = 2)

From Figure 3.6, the carbonyl stretch (νC-O) is observed at 1240 cm^{-1}, a shift of -15 cm^{-1} which indicates coordination. The imine stretch (νC=N) is observed at 1620 cm^{-1}, a shift of -17 cm^{-1}, also indicating coordination, whilst νCu-OH is observed at 540 cm^{-1} in Figure 3.7. The hydroxo species (νCu-OH) is normally distinguished from the aquo group since the former lacks the bending mode δOH_2 near 1600 cm^{-1} (Nakamoto, 1963). The solvated compound does not permit an unambiguous identification at 1600 cm^{-1}. The δM-O-H bend lies below 1200 cm^{-1}, a region rich in the fundamentals associated with the substituted benzene ring (Várs inyi and Szöke, 1969) and can not be easily identified. Possible candidates for this bend are 1134 cm^{-1}, the medium strong bend, and 1110 cm^{-1}, the medium strong bend (Figure 3.6). νOH is observed at 3498 cm^{-1} in the ligand spectrum (Figure 3.5) and is absent in the spectrum (Figure 3.6) for complex **(A1)**. This

O-H stretch, which is associated with the aliphatic alcohol, is expected to be absent if it is in the anionic form, or is expected to be lowered if it is coordinated (Nakamoto, 1963). With the solvated compound it is not possible to identify the structure unambiguously. The structure given in Figure 3.25 is tentative based on the reported distorted tetrahedral geometries of [Cu(2-OHSALPN)] and [Cu(*o*VANPN)] (Nishida, 1991), and the square pyramidal structure of the dinuclear compound Cu_2(2OH-SALPN)Br.6H_2O (Naik *et al.*, 2006). The expected weak band (650 nm) is not noticeable in the UV spectrum (Figure 3.20) of compound **(A1)** beyond 500 nm. The absence of this band is due to possible dissociation of the OH or M-O bonds in solution.

3.5.2.1.2 *Structure and characterization of complex (A2) and (A3)*

Except for the degree of hydration, complexes **(A2)** and **(A3)** are identical. Products **(A2)**

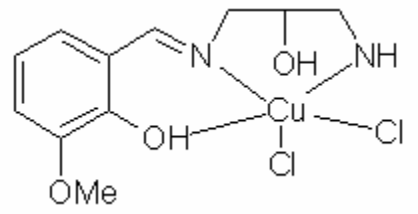

Figure 3.26: The structure of complex **(A2)** and **(A3)**

and **(A3)** (Figure 3.26) indicates that in the absence of a basic medium, the condensation of both amine and aldehyde sites is not favoured when the complexation proceeds using the Schiff base precursors (Method 3, section 3.3.4.3), and suggests that in the synthesis using the preformed Schiff base (Method 2, section 3.3.4.2), $CuCl_2$ is a strong enough Lewis acid in that the one imine site is susceptible to hydrolysis. This also possibly explains why the compound decomposes with sublimation (Table 3:2) of the aldehyde.

The presence of the methoxy group ortho to the phenolic group destabilizes the keto-enol tautomerisation associated with salicylaldimine due to structure (ii) in Figure 3.27. The reduced effectiveness of the keto-enol stabilization by the 2-OH substituent makes the imine more susceptible to hydrolysis. This accounts for the different behaviour on complexation to that observed for 2-OHSALPN. From Figure 3.8, it is deduced that the

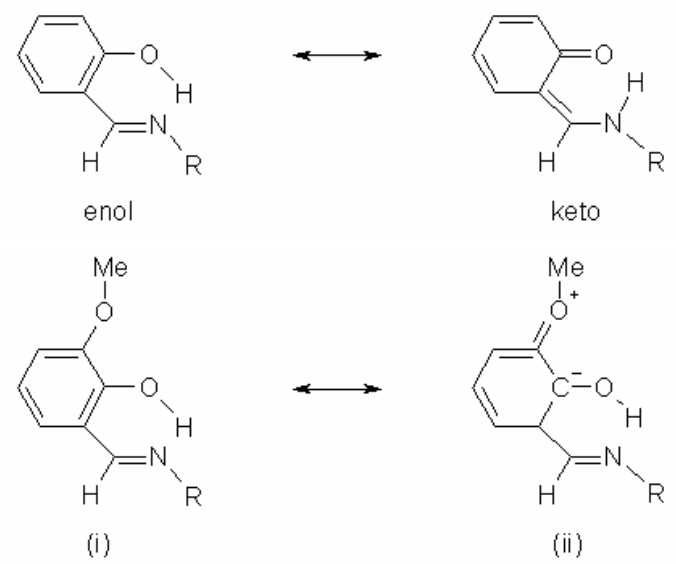

Figure 3.27: Comparison of keto-enol stabilisation for 2-OH-oVANPN versus 2-OHSALPN

imine is not involved in coordination because νC=N (1640 cm^{-1}, which is not labelled in Figure 3.8) is unshifted. The coordination of the phenolic and aliphatic OH is suggested by the -10 cm^{-1} shift in νC-O. The presence of the amine nitrogen can only be recognized by comparison Figure 3.8 **(A3)** with Figure 3.5 (the free ligand), since there is potential for masking of the amine fundamentals by the rich vibrational spectrum associated with the rest of the molecule. The νNH_2 stretch observed in copper(II) halide complexes with ethylenediamine is observed between 3305 and 3233 cm^{-1} (Bennett *et al.*, 1990). This could be slightly masked by the strongly hydrogen bonded νO-H in the complex as is the case in Figure 3.8 for **(A3)**, but is seen at 3244 cm^{-1} for **(A2)**. The NH_2 wag is expected as a band of medium strong intensity between 1300 and 1270 cm^{-1} (Bennett *et al.*, 1990) and is only tentatively assigned at 1285 cm^{-1} **(A2)** and 1277 cm^{-1} **(A3)** (Figure 3.8) as it is easily confused with the CH_2 twist of the aliphatic chelate ring (Bennett *et al.*, 1990). The medium to weak NH_2 twist (expected at about 660 cm^{-1}, Bennett *et al.*, 1990) can not be distinguished from bands associated with a 1, 2, 3 vicinyl trisubstituted benzene of similar intensity (Draeger, 1985 and Varsányi and Szöke, 1969).

Coordination of the metal to the oxygen and the amine nitrogen has been identified in the far infrared spectrum data (Table 3:6) of complex **(A3)** in agreement with the literature (Mazurek *et al.*, 1986; Daniel *et al.*, 2008; Holm *et al.*, 1966 and Bennett *et al.*, 1990).

The presence of terminal Cu-Cl coordination is suggested by the appearance of a band at 353 cm^{-1} (Figure 3.9) in the far infrared assigned to νCu-Cl with the δCl-Cu-Cl (a bend) assigned at 113 cm^{-1} (Figure 3.9).

3.5.2.1.3 *Structure and characterization of complex (A4)*

From the microanalysis (Table 3:2), product **(A4)** appears to be a polynuclear polymer of composition $\{Cu_3(C_{11}H_{14}N_2O_3)Cl_4(H_2O)\}$.

The infrared spectrum is similar to products **(A2)** and **(A3)**, indicating a ligand possessing both an imine and an amine nitrogen. One significant difference is that the imine nitrogen is coordinated to a metal centre as νC=N is observed at 1244 cm^{-1} (Table 3:6), which corresponds to a shift of -11 cm^{-1}. This is expected with dinuclear binding anticipated to occur between the imine nitrogen, the phenolic oxo, the bridged alkoxo atom and the imine nitrogen, similar to that seen in Figure 3.3.

The nature of the binding of the third copper ion, and the additional chloride is not easily determined as a surprisingly complex far infrared spectrum was observed for complex **(A4)**. Attempts to elucidate this polymeric structure were not further pursued.

3.5.2.1.4 *Brief summary of UV/vis spectra of the copper(II) complexes*

Figure 3.20 and 3.21 indicates that complexes **(A1)** and **(A3)** result in absorption maxima at slightly different wavelengths, whilst Table 3:10 shows that complexes **(A2)** and **(A3)** gave maxima at same wavelengths. The latter observation is anticipated as the structures of these two complexes are the same.

3.5.2.2 The Cobalt(II) complexes

Complex **(B1)** (Table 3:3) in the present work is binuclear. Binucleating ligands such as the ligand (Figure 3.24) in the present work are able to hold, on demand, pairs of metal atoms in close physical proximity (Butcher, 1986). The ligand LH_3 can deprotonate at the phenolic oxygens and then further deprotonate at the alkanolic oxygen to form a binucleating ligand, L^{3-} (Butcher, 1986). 2-OHSALPN and the ligand in the present work,

2-OH-*o*VANPN, in conjunction with anionic ligands, and alkali-metal ions can lead to formation of mono-, bi-, or polynuclear complexes (Bertoncello *et al*., 1991). All other Co(II) complexes, **(B2)** to **(B4)** (Table 3:3), are mononuclear with chloride ions coordinating to the metal centre. The molecular formula of complex **(B2)** (Table 3:3) indicates the replacement of each methoxy group of the ligand with a hydroxyl group. This replacement is addressed later on when discussing this complex. The general trend for the cobalt(II) complexes (Table 3:7) is that the O-H stretching frequency is shifted to lower frequencies and that this band appears much narrower compared to that of the ligand. Medium and broad νO-H were found (Table 3:7) in the range 3431 - 3415 cm^{-1}.

The infrared data (Table 3:7) from all cobalt(II) IR spectra are consistent with the presence of the imine (C=N) group as νC=N for each falls within the expected range of 1650 - 1620 cm^{-1} (Mazurek *et al*., 1986; Naik *et al*., 2006 and Wang and Chang, 1994). This suggests the presence of N-coordination to the metal center (Chattopadhyay and Sinha, 1996 and Vogel, 1975). All (Table 3:7), except compound **(B3)**, shows lowering of the νC=N suggesting significant back bonding from the cobalt ion into the antibonding orbital of the imine. All of the cobalt(II) complexes (Table 3:7) gave far infrared frequencies that fall within the reported range for νM-N.

3.5.2.2.1 *Structure and characterization of complex (B1)*

Product **(B1)** is a binuclear complex, the analogue of the Schiff base copper complex with 1,5-diaminopentan-3-ol and salicylaldehyde (Mazurek *et al*., 1982). Zolezzi and co-workers found that four-coordinated M^{2+} complexes are brown in colour (Zolezzi *et al*., 1991). According to this observation, the brown colour of complex **(B1)** (Table 3:3) may be linked to its four-coordinated cobalt centres (Figure 3.28).

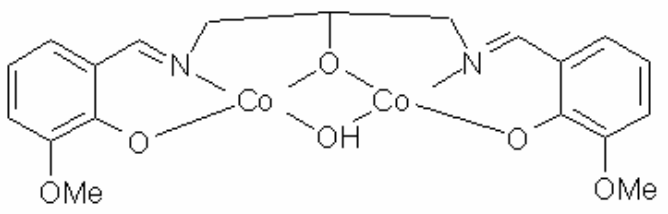

Figure 3.28: The structure of complex **(B1)**

The structure of the product **(B1)** is evidenced in the infrared spectrum data (Table 3:7). The νO-H of the endogenic bridged hydroxo moiety is observed at 3419 cm^{-1}. The endogenic bridged hydroxo group also displays a M-O-H bend below 950 cm^{-1} (Nakamoto, 1978). This may be masked by a medium intensity out-of-plane bend associated with the vicinyl trisubstituted aromatic ring (Draeger, 1985 and Varsányi and Szöke, 1969), but is tentatively identified as a relatively weak band at 905 cm^{-1}.

Coordination to the imine nitrogen is identified by the -10 cm^{-1} shift by the νC=N, observed at 1627 cm^{-1}. Coordination to the phenolic and the endogenic bridge alkoxy groups are seen by a 12 cm^{-1} shift to lower frequency by νC-O. The metal-ligand far infrared vibrations (Figure 3.11) have tentatively been assigned (Table 3:7) in agreement with the literature (Mazurek *et al*., 1986; Daniel *et al*., 2008; Holm *et al*., 1966).

3.5.2.2.2 *Structure and characterization of complex (B2)*

Complex **(B2)** is monomeric. The extent of coordination observed for the Co(II) (Figure 3.29) resulted from the synthesis method employed.

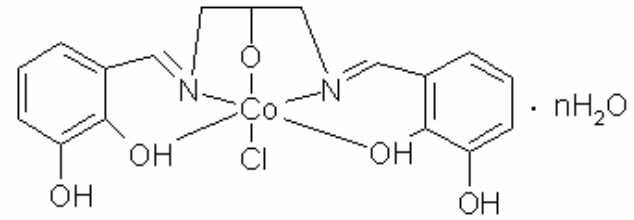

Figure 3.29: The structure of complex **(B2)** (n = 1½)

As with syntheses of the copper(II) complexes, the synthesis here produced an unexpected product, *viz* the replacement of the methoxy moieties by hydroxyls (Figure 3.29). The loss of the methyl groups is best observed here by comparing the infrared spectrum of **(B2)**, Figure 3.10, with that of the free ligand, Figure 3.5. The νC-H are observed (Draeger, 1985) at 2900 cm^{-1} for the ligand in Figure 3.5, but is absent in the complex **(B2)** (Figure 3.10). The δCH_3 expected at 1450 cm^{-1} in the ligand (Draeger, 1985) may be masked by the strong to medium intensity ring stretch of the vicinyl trisubstituted benzene component of the ligand (Varsányi and Szöke, 1969).

From Table 3:7, the phenolic OH group remains protonated and is coordinated to the metal atom. The coordination of the phenolic OH is suggested by the -7 cm^{-1} shift in νC-O. Coordination to the imine nitrogen is observed by a -14cm^{-1} shift of νC=N. The far infrared data in Table 3:7 supports these assignments as indicated by νM-O and νM-N. Coordination of the chloride is evident from the terminal νCo-Cl at 358 cm^{-1}.

3.5.2.2.3 *Structure and characterization of complex (B3) and (B4)*

Complexes **(B3)** and **(B4)** (Table 3:3) have the same structures although different syntheses were used.

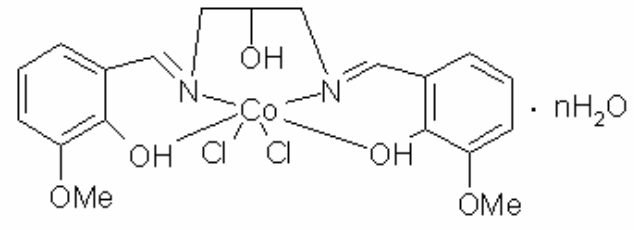

Figure 3.30: The structure of complex **(B3)** and **(B4)** (n = 5½)

The presence of waters of crystallization prevents determination of the exact nature of the aliphatic alcohol for complexes **(B3)** and **(B4)** (Figure 3.30). νOH is observed at 3498 cm^{-1} in the ligand (Figure 3.5) and is masked in the complex (Figure 3.12).

Coordination at the imine nitrogen is identified by the -17cm^{-1} shift by the νC=N, observed at 1620 cm^{-1} in Figure 3.12). The phenolic OH group remains protonated, and is coordinated to the metal atom. The coordination of the phenolic OH is suggested by the νC-O shifting from 1254 cm^{-1} (Figure 3.5) to 1247 cm^{-1}(Figure 3.12). Coordination of the metal to the oxygen and the amine nitrogen have been identified and tentatively assigned in the far infrared spectrum (Table 3:7) in agreement with the literature (Mazurek *et al*., 1986; Daniel *et al*., 2008; Holm *et al*., 1966 and Bennett *et al*., 1990). The presence of terminal Co-Cl coordination is suggested by the appearance of a band at 353 cm^{-1} (Table 3:7) for **(B3)** and 358 cm^{-1} (Table 3:7) for **(B4)** in the far infrared assigned to νCo-Cl with the δCl-Cu-Cl (a bend) assigned at 113 cm^{-1} (Table 3:7) and 116 cm^{-1} (Table 3:7) in the same sequence (Bennett *et al*., 1990 and Nakamoto, 1963).

3.5.2.2.4 *Brief summary of the UV/vis spectra of the cobalt(II) complexes*

From Figures 3.22 and 3.23 it is evident that, as expected, complexes **(B3)** and **(B4)** gave similar spectra, whereas the summary in Table 3:11 shows that complex **(B1)** and **(B2)** gave absorption bands at slightly different wavelengths.

3.5.2.3 The Cobalt(III) complexes

All of the cobalt(III) complexes (Table 3:4) are mononuclear. A shift to lower (Table 3:8) wavenumber of the νC=N (imine) band compared to the ligand is observed with each of the cobalt(III) complexes, suggesting significant back bonding from the cobalt into the antibonding orbital of the C=N (imine). νM-N and νM-O have tentatively been assigned (Table 3:8) in agreement with the literature (Mazurek *et al*., 1986; Daniel *et al*., 2008; Holm *et al*., 1966). These are inner-chelate complexes in which the Schiff base is bonded to the metal through the oxygen atoms of its deprotonated hydroxy groups and the nitrogen atoms of its C=N groups (Bowden and Ferguson, 1974).

Co^{3+} is likely to be octahedral because of the large degree of crystal field stabilization energy (222 kJ. mol^{-1}) compared to octahedral Co^{2+} (111 kJ. mol^{-1}) and octahedral Cu^{2+} (151 kJ. mol^{-1}). Co^{3+} is also more likely to be low spin (i.e. diamagnetic) with the imine ligand, especially as $Co(en)_3^{3+}$ is low spin (Lee, 1991), and an imine is higher in the spectrochemical series than an amine. The d-d UV transitions will thus be:-

$^1A_{1g} \rightarrow {}^1T_{1g}$; $^1A_{1g} \rightarrow {}^2T_{2g}$ (Visible)

$^1A_{1g} \rightarrow {}^1E_g$; $^1A_{1g} \rightarrow {}^1A_{2g}(G)$; $^1A_{1g} \rightarrow {}^1A_{2g}(F)$ (Vaccuum UV below 200 nm)

3.5.2.3.1 *Structure and characterization of complex (C1)*

Complex **(C1)** (Table 3:4) indicates deprotonation of the alkylic OH group (Butcher, 1986) in its proposed structure (Figure 3.31). Coordination to the phenol and endogenic bridge alkoxy groups is seen by the νC-O shifting from 1254 cm^{-1} (Figure 3.5) for the ligand to 1250 cm^{-1} (Figure 3.13) for complex **(C1)**. Coordination to the imine is identified by the νC=N shifting from 1639 cm^{-1} (Figure 3.5) for the ligand to 1621 cm^{-1} (Figure 3.14) for complex **(C1)**. The metal-ligand vibrations (Figure 3.14) for complex **(C1)** have tentatively been assigned (Table 3:8) in agreement with the literature (Mazurek

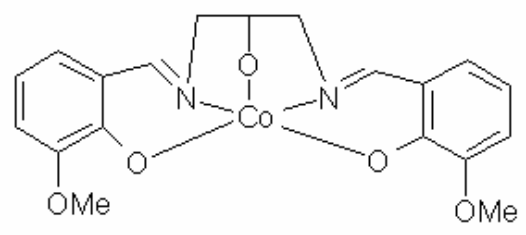

Figure 3.31: The structure of complex **(C1)**

et al., 1986; Daniel *et al*., 2008; Holm *et al*., 1966). Compound **(C1)** gave bands at about 264 and 128 nm (Figure 3.14), which are characteristic of νCo-N as octahedral geometry. This suggests that in solution, a solvent molecule coordinates to the other axial site.

3.5.2.3.2 *Structure and characterization of complex (C2)*

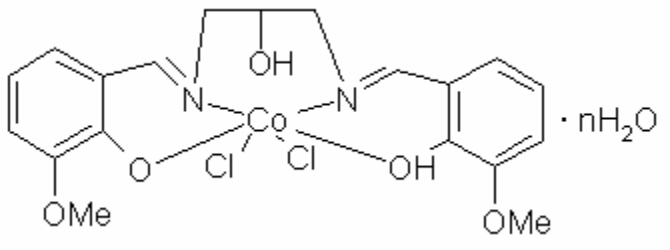

Figure 3.32: The structure of complex **(C2)** (n = 5)

The proposed structure (Figure 3.32) of compound **(C2)** indicates that the alkylic OH group remains protonated and that chloride ions coordinate to the metal centre. Coordination to the imine nitrogen is observed by a -12 cm^{-1} shift of νC=N when comparing the ligand IR frequency (1640 cm^{-1} in Figure 3.5) with that of complex **(C2)** (1618 cm^{-1} in Figure 3.15). The phenol coordination is suggested by a -11cm^{-1} shift of νC-O from the ligand's 1254 cm^{-1} (Figure 3.5) to 1245 cm^{-1} (Figure 3.15) for this complex. The far infrared spectrum (Table 3.7) supports these assignments as indicated by νM-O and νM-N. Coordination of the chloride is evident from the terminal νCo-Cl at 358 cm^{-1}. Compound **(C2)** gave far IR frequencies (Figure 3.6) at 357 and 117 cm^{-1}, which is similar to that reported (Bennett *et al*., 1990) for νM-Cl. In addition, this complex gave bands at 232 and around 220 cm^{-1}, which are characteristic for νCo-Cl (octahedral). Formation of an inner chelate complex in which the metal is coordinated to

two chloride ions in an octahedral geometrical arrangement, agrees well with the proposed structure (Figure 3.32).

3.5.2.3.3 *Structure and characterization of complexes (C3) and (C4)*

Compounds **(C3)** and **(C4)** are both pointing towards the same structure (Figure 3.33) based on their microanalysis data (Table 3:4), differing only in their degree of hydration.

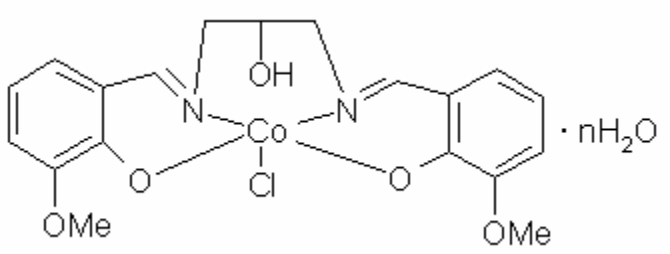

Figure 3.33: The structure of complex **(C3)** (n = 3) and **(C4)**

Coordination of the phenolic OH is suggested by an -8 cm^{-1} shift of νC-O from 1254 cm^{-1} (Figure 3.5) for the ligand to 1246 cm^{-1} (Figure 3.17) for complex **(C4)**. Coordination to the imine nitrogen is observed by a shift of νC=N from 1638- to 1624 cm^{-1} from the same figures. The far infrared spectrum (Figure 3.18) supports these assignments as indicated by observed bands at 549- and 449 cm^{-1} falling within the reported (Mazurek *et al*., 1986; Daniel *et al*., 2008; Holm *et al*., 1966) range for νM-O and νM-N, respectively. Coordination of the chloride is evident from the terminal νCo-Cl at 360- and 113 cm^{-1} in the same spectrum. Compounds **(C3)** and **(C4)** also gave far infrared frequencies (Table 3:8) similar to that reported (Bennett *et al*., 1990) for νM-Cl (Table 3:8). In addition, these complexes gave bands characteristic of νCo-Cl (octahedral) at around 233 and 222 cm^{-1} (Figure 3.18). Formation of inner chelate complexes in which the metal is coordinated to one or more chloride ions in an octahedral geometrical arrangement, agrees well with the proposed structures of these Co(III) complexes.

3.5.2.3.4 *Brief summary of the UV/visible spectra of the cobalt(III) complexes*

As expected, complexes (C3) and (C4) gave absorption maxima at similar wavelengths (Table 3:12) whereas complexes (C1) and (C2) gave band maxima at differing. wavelengths.

3.5.2.4 Thermal studies on the Schiff base ligand and its corresponding complexes; DSC studies on the Cu(II) complexes

The ligand:- The ligand, 2-OH-*o*VANPN, melts in the range 119-22 ^{o}C (Table 3:1). Table 3:13 lists the melting endotherm 123 ^{o}C and possibly an oxidative decomposition endotherm at 290 ^{o}C.

The Cu(II) complexes:- All of the Cu(II) complexes in the present work decompose without melting as judged by the absence of a sharp endotherm earlier on in their thermograms (see Table 3:13). Complex **(A1)** sublimes at 260 ^{o}C (Table 3:2) and then decomposes at 290 ^{o}C (Table 3:13). The green sublimate was observed at 260 ^{o}C with the cold finger (copper block) method. The cold finger method showed that compounds **(A2)**, **(A3)** and **(A4)** undergo sublimation at 174 ^{o}C (Table 3:2); then undergo decomposition, reduction or some phase transition (Sanmartín *et al*., 2000) between 320 and 425 ^{o}C (Table 3:13), and finally undergoes oxidative decomposition at 540 ^{o}C (Table 3:13). The cold finger (copper block) method revealed a white "sublimate" at 190 ^{o}C and a yellow "sublimate" above this temperature for **(A2)** and **(A3)**. The yellow compound implies loss of the ligand during decomposition and the white compound is due to loss of either the aldehyde or the diamine. The endotherm at 85 ^{o}C (Table 3:13) for **(A4)** is assigned to loss of water due to the irreversibility and broad nature of this peak and the fact that around this temperature, condensed water was observed on the cold finger (copper block method) and in the melting point tube (melting point apparatus).

Compound **(A2)** is stable, under nitrogen flux, up to 300 ^{o}C (Table 3:13) when the organic constituents of the complexes start decomposing, finally leaving the metal oxides (Daniel, *et al*., 2008) at temperatures exceeding 540 ^{o}C.

The Co(II) complexes:- From Table 3:3 it is observed that all of the Co(II) complexes in the present work sublimes before (or without) melting. Complex **(B1)** undergoes sublimation at 204 ^{o}C. This has been confirmed by the presence of a brown sublimate on the cold finger of the copper block at around this temperature. Compound **(B2)** undergoes some kind of decomposition at around 116 ^{o}C and then sublimes at 180 ^{o}C. Both **(B3)** and **(B4)** sublime at 194 ^{o}C. All sublimations have been confirmed by the copper block method. DSC analyses of the complexes in this group were not carried out because DSC runs had to be terminated after analyses of the copper(II) complexes because of possible damage to this instrument by the possible hygroscopic sublimates.

The Co(III) complexes:- Complex **(C1)** sublimes at 190 ^{o}C and **(C2)** at 200 ^{o}C (Table 3:4). Sublimation temperatures have been confirmed by the copper block cold finger method. Compounds **(C3)** and **(C4)** melted at 174- and 116 ^{o}C, respectively (Table 3:4). DSC analyses of the above cobalt(III) complexes, just as was the case with the cobalt(II) group of complexes in the present work, were not carried out because DSC runs had to be terminated after analyses of the copper(II) complexes because of the possibility of damage to this instrument by the possible hygroscopic sublimates.

3.6 CONCLUSIONS

According to Table 3:1, the synthesis of the ligand in the current investigation resulted in the expected (Nishida and Kida, 1986) product.

The copper(II) complexes that resulted from methods 2 to 4 were similar (Table 3:2) in that the ratio between aldehyde and diamine was 1:1 in their structures, but they differed in coordination to the metal center. A similar observation is made for the cobalt(II) complexes in Table 3:3, but a 2:1 ratio between aldehyde and diamine was found. Method 1, which involved addition of KOH to the reaction mixture, resulted in a different product to the others in each of the set of copper(II) and cobalt(II) complexes,

respectively. All the cobalt(III) complexes in Table 3:4 gave the same ratio between the cobalt(III) ion and the ligand, differing only in coordination to the metal ion.

All structures were substantiated by the various instrumental techniques mentioned in section 3.2 and all the results discussed in section 3.5. An estimate of the geometrical arrangement of the synthesized complexes was attempted based on far infrared data (Tables 3:6 to 3:8), but solid-state spectroscopic studies and or X-ray studies would be required to conclude the geometries of these complexes.

The thermal studies that formed part of the present work revealed sublimation of most of the complexes synthesized – moisture accumulation in the DSC furnace possibly resulted from hygroscopic products of the copper(II) complexes.

3.7 REFERENCES

1. Adams, D.M. *J. Chem. Soc*. **1964**. 1771-6.
2. Alexander, P.W. and Sleet, R.J. *Aust. J. Chem*. **1970**. 23. 1183-90.
3. Ali, M.A. and Livingstone, S.E. *Coord. Chem. Rev*. **1974**. 13. 101-132.
4. Battistoni, C.; Mattogno, G,; Monaci, A. and Tarli, F. *J. Inorg. Nucl. Chem*. **1971**. 33. 3815-3832.
5. Bellamy, L.J. *The infra-red spectra of complex molecules*. 3rd edition. **1975**. Chapman and Hall. London.
6. Bennett, A.M.A.; Foulds, G.A.; Thornton, D.A. and Watkins, G.M. *Spectrochimica Acta*. **1990**. 46A. 13-22.
7. Bertoncello, K.; Fallon, G.D.; Murray, K.S. and Tiekink, E.R.T. *Inorganic Chemistry*. **1991**. 30. 3562-8.
8. Bowden, F.L. and Ferguson, D. *J. Chem. Soc. Dalton Trans*. **1974**. 460-2.
9. Butcher, R.J.; Diven, G.; Erickson, G.; Jasinski, J.; Mockler, G.M.; Pozdniakov, R.Y. and Sinn, E. *Inorganica Chimica Acta*. **1995**. 239. 107-16.

10. Calligaris, M. and Randaccio, L. *Comprehensive coordination chemistry*. Vol. 2. **1987**. Wilkinson, G. (Ed.), Pergamon Press, Oxford.
11. Carlin, R.L. *Stereochemistry of Cobalt(II) in transition metal chemistry: A series of advances*. **1965**. Volume 1. Edward Arnald (Publisher) Ltd. London. Marcel Dekker Inc. New York.
12. Chattopadhyay, P. and Sinha, C. *Indian Journal of Chemistry Section A: Inorganic, Physical, Theoretical and Analytical*. **1996**. 35. 523-6.
13. Costamagna, J.; Vargas, J.; Latorre, R.; Alvarado, A. and Mena, G. *Coord. Chem. Rev*. **1992**. 119. 67-88.
14. Cotton, F.A. and Soderberg, R.H. *J. Am. Chem. Soc*. **1962**. 84. 872-9.
15. Cotton, F.A. and Wilkinson, G. *Advance Inorganic Chemistry*. 4th edition. **1980**. Wiley Interscience. New York.
16. Daniel, V.D.; Murukan, B.; Sindhukumari, B. and Mohanan, K. *Spectrochimica Acta Part A: Molecular and Biomolecular Spectroscopy*. **2008**. 70. 403-10.
17. Dianzhong, F.W. *Trans. Met. Chem*. **1993**. 18. 101-3.
18. Draeger, J.A. *Spectrochim. Acta*. **1985**. 41A. 607-27.
19. Fabian, J. and Legrand, M. *Bull. Soc. Chim. France*. **1956**. 1461-3.
20. Faniran, J.A.; Patel, K.S. and Bailar, J.C. JR. *Inorg. Nuc. Chem*. **1974**. 36. 1547-51.
21. Ferguson, J. *J. Chem. Phys.* **1964**. 40. 3406-10.
22. Ferraro, J.R. *Low-Frequency Vibrations of Inorganic and Coordination Compounds*. **1971**. Plenum Press. New York.
23. Garnovskii, A.D.; Nivorozhkin, A.L.and Minkin, V.I. *Coord. Chem. Rev*. **1993**. 126. 1-69.
24. Goodgame, M. and Cotton, F.A. *J. Phys. Chem*. **1961**. 65. 791-2.
25. Goodgame, D.M.L. and Goodgame, M. *Inorg. Chem*. **1965**. 4. 139-43.
26. Harris, D.C. and Bertolucci, M.D. *Symmetry and Spectroscopy*. **1978**. Oxford University Press. New York.
27. Hartfield, W.E. and Whyman, R. *Trans. Met. Chem.* **1969**. 47. 5-9.
28. Holm, R.H.; Everett, G.W, JR. and Chakravorty, A. *Progress in Inorganic Chemistry*. **1966**. 7. 83-203.

29. Hulett, L.G. and Thornton, D.A. *Spectrochimica Acta*. **1971**. 27A. 2089-9.
30. Jorgenson, C.K. *Inorganic complexes*. **1963**. Academic. London.
31. Kemp, W. "*Organic Spectroscopy*". **1975**. Macmillan. London.
32. Kitajima, N.; Whang, K.; Moro-oka, Y.; Uchida, A. and Sasada, Y. ***J. Chem. Soc. Chem. Comm***. **1986**. 20. 1504-5.
33. Ku, S-M.; Wu, C-Y. and Lai, C.K. ***J. Chem. Soc. Dalton Trans***. **2000**. 3491-2.
34. Kuzniarska-Biernacka, I.; Bartecki, A. and Kurzak, K. *Polyhedron*. **2003**. 22. 997-1007.
35. Lee, J.D. *Concise Inorganic Chemistry*. 4th edition. **1991**. Chapman and Hall. London.
36. Lever, A.B.P. ***Inorganic Electronic Spectroscopy.*** 2nd edition. **1978**. Elsevier. New York.
37. Mazurek, W; Berry, K.J.; Murray, K.S.; O'Connor, M.J.; Rodgers, J.R.; Snow, M.R. and Wedd, A.G. *Inorganic Chemistry*. **1982**. 21. 3071-80.
38. Mazurek, W; Bond, A. M.; O'Connor, M.J. and Wedd, A.G. ***Inorg. Chem***. **1986**. 25. 906-15.
39. Mukherjee, A.; Rudra, I.; Naik, S.G.; Ramasesha, S.; Nethaji, M. and Chakravarty, A.R. *Inorganic Chemistry*. **2003**. 42. 5660-8.
40. Naik, S.G.; Mukherjee, A.; Rughunathan, R.; Nethaji, M.; Ramasesha, S. and Chakravarty, A.R. *Polyhedron*. **2006**. 25. 2135-41.
41. Nakamoto, K. *Infrared Spectra of Inorganic and Coordination Compounds*. **1963**. Wiley. New York.
42. Nakamoto, K. *Infrared and raman spectra of inorganic and coordination compounds*. 3rd edition. **1978**. Wiley Interscience. New York.
43. Nicholls, D. In: *Comprehensive Inorganic Chemistry*. Volume 3. **1973**. Bailar, J.C.; Emeleus, H.J.; Nyholm, Sir R. and Trotman-Dickenson, A.F (Eds.). Pergamon Press. Oxford. 1039-94.
44. Nishida, Y and Kida, S. ***J. Chem. Soc. Dalton Trans***. **1986**. Issue 1. 2633-3.
45. Nishida, Y.; Unoura, K.; Watanabe, I. and Yokomizo, T. *Inorganica Chimica Acta*. **1991**. 181. 141-3.

46. Hall, P.S. Master of Science Thesis. **1983**. University of Cape Town. South Africa.
47. Popovic, Z.; Pavlovic, G.; Roje, V.; Doslic, N.; Matkovic-Calovic, D. and Leban, I. *Struct. Chem*. **2004**. 15. 587-98.
48. Ramesh, R. and Maheswaran, S. *J. Inorg. Biochem*. **2003**. 96. 457-62.
49. Sanmartín, J.; Bermejo, M.R.; Garía-Deibe, A.M.; Maneiro, M.; Lage, C. and Costa-Filho, A.J. *Polyhedron*. **2000**. 19. 185-92.
50. Seminara, A.; Giuffrida, S.; Musumei, A. and Fragala, I. *Inorg. Chim. Acta*. **1984**. 201-5.
51. Shephard, G.S. and Thornton, D.A. *Helv. Chim. Acta*. **1971**. 54. 2212-21.
52. Swarzenbach, G.; Anderreg, G.; Schneider, W. and Senn, H. *Helv. Chim. Acta*. **1955**. 38. 4147-52.
53. Tumer, M.; Celik, C.; Koksal, H. and Serin, S. *Trans. Met. Chem*. **1999**. 24. 525-32.
54. Varsányi, G. and Szöke, S. *Vibrational spectra of benzene derivatives*. **1969**. Academic Press. New York.
55. Vogel, A.I. *Elemental Practical Inorganic Chemistry. Part 3. Quantitative Inorganic Analysis*. **1975**. Longman. London.
56. Wang, G. and Chang, J.C. *Synthesis and reactivity in Inorganic and Metal-Organic Chemistry*. **1994**. 24. 623-30.
57. Yildiz, M.; Kilic, Z. and Hokelec, T. *J. Mol. Struct*. **1998**. 441. 10-0.
58. Zhou, Y.; Ye, X.; Xin, F. and Xin, X. *Trans. Met. Chem.* **1999**. 24. 118-20.
59. Zolezzi, S.; Decinci, A. and Spodine, E. *Polyhedron*. **1999**. 18. 897-904.

4. BIOLOGICAL TESTING OF THE LIGAND AND THE METAL COMPLEXES

Chemists go through a lot of trouble synthesizing, characterizing, and publishing results of compounds without any biological testing whatsoever. The useful biological activities of such compounds can remain unknown for years. If biologically active compounds from the literature have similarity(s) to a newly synthesized compound, then a bioactivity-directed screening of that compound may be done. For example, Schiff bases which contain the >C=N group are known to have slight antitumor activities (Hodnett *et al*., 1970); thus, ideally newly synthesized compounds containing this group should undergo screening for broad spectrum pharmacological activity before performing specific antitumor tests (Anderson *et al*., 1991). In search of specific (e.g. antibacterial, antitumor and antihistamine) pharmacological activity, researchers often make use of bioassays and they often result in detection of other useful biological activities that are not under investigation (Solis *et al*., 1993).

As already mentioned in chapters 1 and 2, the focus is turned to metal complexes for possible pharmacological action as many discoveries have already been made. To mention but a few:-

Ag(I) and Au(I) complexes:- Anti-fungal and anti-cancer activity of $[Ag_2(NH_3)_2(salH_2)]$ ($salH_2$ = salicylic acid) showed that this silver complex greatly inhibited cell reproduction in *Candida albicans* (that is, minimum inhibitory concentration for *C. albicans* was found to be 5.0 μM) and produced a dose-dependent cytotoxic response against the three human derived cancer cell lines, Cal-27 (toxicity = 27 ± 2 μM), Hep-G2 (toxicity = 20 ± 1 μM) and A-98 (toxicity = 18 ± 2 μM) (Coyle et al., 2004). The ligand and metal complexes in the present work are sufficiently similar to make these worth testing for antifungal and anti-cancer activity. Complexes of Ag(I) are reported to have bactericidal activity (Guo and Sadler, 2000). Complexes of Au(I) are used in treatment of arthritis (Guo and Sadler, 2000).

Cisplatin:- The search for antitumour activity among metal compounds has been greatly stimulated by the success of *cis*-diamminedichloroplatinum (Cisplatin) (Guo and Sadler, 2000). Cisplatin, cis-$[PtCl_2(NH_3)_2]$, is currently one of the most successful cancer chemotherapeutics (Guo and Sadler, 2000). The search for antitumor activity amongst metal compounds has been greatly stimulated by the success of this compound (Guo and Sadler, 2000).

Bi(III) complexes:- Complexes of Bi(III) are reported to have bactericidal activity (Guo and Sadler, 2000).

Co(II) complexes:- At the Chemotherapy National Service Center, Co(II) derivatives of Schiff bases of salicylaldehyde showed activity against one form of Walker Sarcoma of the rat (Hodnett *et al*., 1970). Cobalt complexes investigated by Vol'pin and Novodarova had demonstrated high fungicide activity toward rice blast disease (Vol'pin and Novodarova, 1992). $[Co(acacen_2en)(NH_3)_2]Cl$ complexes and their analogs showed anticancer, in particular antimetastatic activity (Osinsky *et al*., 2000). Vol'pin and Novodarova investigated the possibility of using cobalt chelates as catalytic generators of active oxygen radicals aimed at various cell targets, especially DNA and RNA (Vol'pin and Novodarova, 1992), especially in the light of destroying cancerous cells. The complex $[Co(acacen)L_2]^+$, where L = ammonia or methylimidazole, has been shown to inhibit the replication of the herpes virus.

Co(III) complexes:- Co(III) complexes with tetradentate ligands have displayed selective anticancer activity (Osinsky *et al*., 2000). Alkylcobalt(III) complexes generate alkyl radicals, which are known to damage biological targets (e.g. cancer cells) and especially to cleave nucleic acids (Guo and Sadler, 2000). Osinsky and co-workers have shown that cobalt(III) complexes with tetradentate Schiff bases have been shown to display selective anticancer activity, in particular antimetastatic activity (Osinsky *et al*., 2000).

Copper complexes:- Copper complexes of salicylaldehyde derivatives, such as is studied in the present work, (Guo and Sadler, 2000) are active against a variety of tumor cell lines. It is possible that a Cu(II) amino acid phenanthroline complex will soon enter clinical trials (Sykes, 2000). Strong anticancer activity against Ehrlich ascites carcinoma (EAC) was observed with complexes derived from the Schiff base, hydroxysalicylaldehyde, and its amine analogues (Golcu *et al*., 2005). A Cu(I) complex with the Schiff base derived from 2,4-dihydroxybenzaldehyde and L-arginine gave 32.2%, 51.7% and 53.3% inhibition rates, respectively, to EAC (Chunhua *et al*., 1993). The first copper complex showing efficient DNA cleavage activity was bis(1,10-phenanthroline)copper(I) (Reddy, *et al*., 2004). Photocleavage experiments were conducted at different complex concentrations with phenanthroline-based and salicylaldimine-based Cu(II) complexes. The results showed red light-induced photocleavage activity, which are of importance in the development of the chemistry of copper-based reagents for photodynamic therapy (PDT) (Reddy, *et al*., 2004). Cu(II) complexes of bidentate Schiff base ligands showed antibacterial and antifungal activity.

4.1 A REVIEW OF SOME METHODS, MICROORGANISMS AND ANTIMICROBIAL STANDARDS USED FOR BIOLOGICAL TESTING OF COMPOUNDS

Many methods are available for testing the biological activity of newly synthesized or natural compounds (Fisch *et al*., 2003). Antioxidant or free radical scavenging assays, antimicrobial (e.g. antifungal, antibacterial, etc.) tests, brine shrimp lethality assay and cytotoxicity tests are among the many tests available for biological testing. In all (or most) of these tests, a control test, which omits the test sample or employs a compound with known biological activity, is used as comparison.

4.1.1 Review of brine shrimp lethality assay

The brine shrimp bioassay is a rapid (that is, results are obtained within 24 hours following introduction of shrimp), inexpensive (that is, no analytical instrumentation is necessary and the eggs of brine shrimp, Artemia salina leach, are readily available at low cost in pet shops as a food for tropical fish), and simple (no aseptic techniques required)

test which can detect a broad spectrum of pharmacological activities in compounds at low cost; hence, it is not a test specific for antitumor or any particular physiological action (Meyer et al., 1982).

4.1.2 Review of antioxidant or free radical scavenging testing (Bleaching experiments)

4.1.2.1 The role of antioxidants and free radicals in cancer

Free radicals are chemical species or fragments of molecules that possess an unpaired electron and are continuously produced in cells during normal metabolism. Free radicals can cause extensive damage to macromolecular components (DNA, carbohydrates, lipids and protein) if allowed to react uncontrollably; hence, eukaryotic cells have developed defence mechanisms to protect against these free radicals (Ottino and Duncan, 1997), mostly by making use of antioxidants to quench (or deactivate or scavenge) these free radicals. Tumor cells are believed to have defective enzymatic antioxidant activity and may be deficient in antioxidant vitamins and minerals (Ottino and Duncan, 1997). This explains why it is important for cancer patients or healthy, potential cancer patients to be treated with fresh fruit and vegetables. This treatment is called chemoprevention. Chemoprevention involves the systematic use of specific natural or synthetic chemical blocking or reversing agents to the carcinogenic process before the development of invasive cancer, and these chemopreventers are found in all classes of food and non-nutritive (that is, vitamins, spices, polyphenols, etc.) components of food (Ottino and Duncan, 1997). It has been shown that the antitumor activities of vitamin E, for example, may lie in its ability to quench highly reactive radicals by directly affecting the activity of the cyclooxygenase enzyme, which in turn affects the level of the free radicals and lipid peroxidation within cells (Ottino and Duncan, 1997). The metal binding ability of curcumin, a spice used in making curry dishes, similarly reduces metal-induced lipid peroxidation and protein oxidation (Daniel *et al*., 2004 and Dairam *et al*., 2007).

It is therefore necessary for researchers to discover or synthesize alternative, more effective antioxidants; hence, the approach in the present work to test the synthesized (and characterized) ligand and metal complexes for antioxidant activity.

4.1.2.2 The 2,2-diphenyl-1-picrylhydrazyl radical (DPPH·) in antioxidant tests

Whether a discovered or newly synthesized sample has antioxidant or radical scavenging properties towards free radicals, can quickly be established using bleaching experiments on thin-layer chromatography (TLC) plates (Cavin *et al*., 1998). The 2,2-diphenyl-1-picrylhydrazyl radical (DPPH·) is usually employed in such experiments because it is stable, but the β-carotene radical can also be used (Cavin *et al*., 1998). It can be seen from the DPPH structure (Figure 4.1) that the DPPH radical would be able to accept an electron or hydrogen radical to result in a stable, diamagnetic molecule. As the electron becomes paired off (that is, the free radical is quenched), the absorption vanishes, and

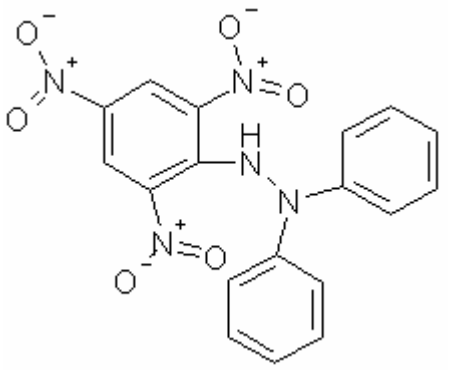

Figure 4.1: 2,2 –Diphenyl-1-picrylhydrazyl (DPPH) (Blois *et al*., 1958)

the resulting loss of color is stoichiometric with respect to the number of electrons (or free radicals) consumed (or quenched). The radical oxidizes (and is decolorized by) polyhydroxy aromatic compounds and aromatic amines, such as the Schiff base compounds being investigated in this work, as follows (Blois *et al*., 1958):-

$$\underset{\text{(purple colour)}}{DPPH\cdot} + AH \rightarrow \underset{\text{(yellow colour)}}{DPPH\text{-}H} + A\cdot$$

4.1.2.3 A typical qualitative antioxidant (radical scavenging) test

For qualitative antioxidant testing, a solution of the test compound as well as that of a known antioxidant (such as vitamin C) is spotted on a silica gel thin layer chromatography (TLC) plate (Hay *et al*., 2004). The plate is developed with a suitable solvent (or used as is), dried and then sprayed with DPPH (0.2% solution in MeOH) (Hay *et al*., 2004). The plates are then examined 30 minutes after spraying for a yellow spot against a purple background, which would be an indication of antioxidant activity (Hay *et al*., 2004).

4.1.2.4 A brief overview of quantitative antioxidant (radical scavenging) testing

DPPH is employed because the radical is stable and it has a strong absorption band at 517 nm in EtOH and 520 nm in MeOH as long as the pH is kept between 5.0 and 6.5 and it is protected from air (stored under nitrogen atmosphere) and light (covered with aluminum foil) (Parejo *et al*., 2000). DPPH is also intensely coloured in 5 x 10^{-4} M alcoholic solutions, obeying the Beer-Lambert law (Blois *et al*., 1958) and is therefore used in quantitative DPPH testing, which involves determining the effect of the test sample on the DPPH radical in a cell-free system using UV Spectrophotometry (Parejo *et al*., 2000). The DPPH· does not oxidize glucose, which forms part of almost all biological material, and is therefore a good choice for assaying biological materials (Blois *et al*., 1958).

4.1.3 Review of antimicrobial testing

4.1.3.1 A review of some methods employed for antimicrobial testing

To follow the course of growth of a microorganism in the presence (or absence) of a newly discovered or newly synthesised compound as a potential anti-microbial agent, necessitates quantitative measurements (Stanier, *et al*., 1987).

Spectrophotometric method of measuring microbial cell mass:- The method of choice for measuring the cell mass is an optical one: the determination of the amount of light scattered by a suspension of microbial cells (Stanier *et al*., 1987). This spectrophotometric (or photometric) technique is based on the fact that small particles

scatter light proportionally, within limits, to their concentration; hence, the amount of light absorbed as a consequence of scattering increases as the microbial mass increases (Stanier *et al*., 1987). This is an indirect method (Stanier *et al*., 1987).

Obtaining dry weight of cell material as a measure of microbial cell mass:- The only direct way to measure cell mass is to determine the dry weight of cell material in a fixed volume of culture by removing the cells from the medium, drying them, and weighing them (Stanier *et al*., 1987). Ordinary analytical balances do not give accurate weight measurements at less than 1 mg, yet such a dry weight of cells may represent as many as 5 billion bacterial cells! This method is not often used as such determinations are time-consuming and relatively insensitive (Stanier et al., 1987).

Disk-plate (disk diffusion) method:- The disk-plate technique (also called the disk difussion method or antibiogram method) (Andrews, 2001; Cimanga *et al*., 2002; Furones, 2001; Gülgür *et al*., 2003; Pelczar *et al*., 1993 and Shivankar *et al*., 2003) is commonly used by researchers to study antimicrobial activity of antibiotics, plant extracts, and other chemical compounds. Shivankar and co-workers used the disk-plate method to study the antibacterial activity of 8-hydroxyquinoline and $CoCl_2.6H_2O$ against *E. coli* and *S. aureus,* and observed activity at 200 and 100 ppm, respectively, of the test compounds. Briefly, this method involves uniform spreading (using a glass spreader) of 0.1 mL of bacterial inoculum on the surface of nutrient agar; placing sample-solution-dipped filter paper disc and the sample-solvent-dipped disk, used as blank, on the resulting surface, and incubating the resulting plate at 37 $^{\circ}$C for 24 hours. During the incubation, the sample diffuses radially from the filter paper into the agar whilst the microorganism is reproducing to form a uniform lawn across the surface of the agar. The microbial growth inhibition zone or radial diffusion zone is measured in millimeters (mm) and the results of the test samples compared with that of a positive control such as tetracycline or ampicillin (Andrews, 2001; Cimanga *et al*., 2002; Furones, 2001; Gülgür *et al*., 2003; Pelczar *et al*., 1993 and Shivankar *et al*., 2003).

Tube-dilution method:- The tube-dilution method is commonly followed for antibacterial and antimycotic (that is, against species such as *Candida albicans*) testing (Menozzi *et al*., 2004). The tube-dilution method (Pelczar *et al*., 1993; Stanier *et al*., 1987 and Shivankar *et al*., 2003) uses a series of tubes or bottles containing sterile culture medium and various concentrations of each test sample or antibiotic. Some tubes, which serve as blanks, are inoculated with each test sample's solvent. All tubes are inoculated with the microorganism to be tested and then incubated. The solutions in the tubes are then subjected to spectrophotometric (or photometric) absorbance measurements at around 600 nm, which is the wavelength at which the cells give optimal absorbance readings. The absorbance values are compared with that of a positive control such as tetracycline. Shivankar and co-workers used the tube-dilution technique to study the antifungal and antimycotic activity of their metal complexes against *Aspergillus niger* and *Candida* albicans, respectively, and obtained positive results at concentrations at and above 100 ppm of the complexes and of $CoCl_2.6H_2O$ (Shivankar *et al*., 2003).

The disk-plate and the tube-dilution method were both used in studying the antimicrobial (that is, antibacterial, antifungal and antimycotic) activity of the ligand and its complexes in the present work. As was the case in the present work, antifungal testing of filamentous fungi generally suffers from incomparability or insensitivity of results when using the afore-mentioned methods; hence, the agar-infusion method is sometimes used or the dried mass of cell material is determined as a measure of microbial growth.

Agar-infusion method of antifungal testing:- The experiment is carried out on 9cm diameter Petri dishes containing 2% water agar and maintained at 25ºC during the growth phase (Mota *et al*., 2003). A disc of culture containing a particular microbial species is placed in the centre of each dish (Mota *et al*., 2003). The diameter of the colonies is measured when one of the cultures had reached the edge of the plates (Mota *et al*., 2003). Biologically derived materials, obtained as commercial and raw materials were tested for their ability to support fungal growth using a modified ASTM (American Society for Testing and Materials) standard as well as a new method where 10 µl of a spore suspension is

placed in a spot on the test sample (Bergenholtz and Nielsen, 2006). The new method gave additional information about fungal growth on biologically derived materials, revealing a clear difference between survival and growth with incubation at 30°C (Bergenholtz and Nielsen, 2006).

A modified version of the agar infusion test was used for antifungal testing, against *Aspergillus niger*, in the present work.

4.1.3.2 A review of microorganisms for antimicrobial testing

Microbial resistance to current drugs necessitates further development in the search for bactericidal, fungicidal and antiviral drugs amongst metal compounds. The Food and Drug Administration (FDA), which has been responsible for a scientific and regulatory program for protecting the general public from harmful patent medicines, often selects the organisms for bactericidal testing of newly discovered or synthesized compounds (Smith *et al*., 1997). In particular *Escherichia coli*, *Pseudomonas aeruginosa* and *Staphylococcus aureus* are selected by the FDA because of their prevalence and life-threatening potential (Smith *et al*., 1997). The next few paragraphs are brief descriptions of the above-mentioned organisms.

4.1.3.2.1 *Escherichia coli*

Escherichia coli (*E. coli*) are Gram-negative rod-shaped bacteria (Figure 4.2) (*Note*: During the Gram stain procedure, Gram-positive bacteria stain blue-purple and the Gram-negative bacteria appear orange or red) (Alcamo, 1994). *Escherichia coli*, a well-known resident of the mammal's intestine, is an opportunistic (that is, this organism does not cause disease in normal humans, but this microorganism is dangerous in compromised humans) pathogen, and is commonly the cause of urinary tract infections in such individuals. *E .coli* is also responsible for milk contamination and meat spoilage. *E. coli* is used industrially in the synthetic production of the amino acid, lysine (Alcamo, 1994).

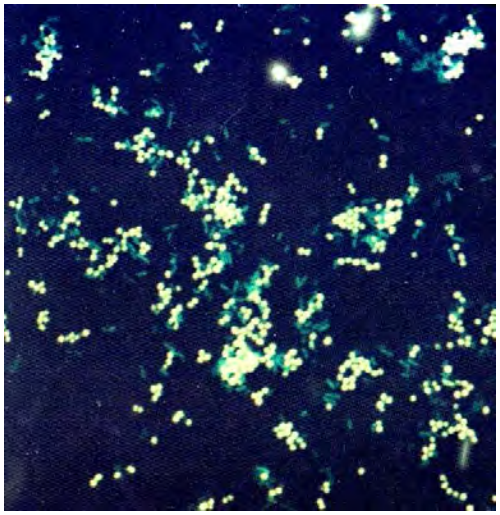

Figure 4.2: A Gram stain of a mixed smear of the Gram-negative rod *Escherichia coli* (shown green here) and the Gram-positive coccus *Staphylococcus aureus* (shown white here) (Alcamo, 1994)

4.1.3.2.2 *Pseudomonas aeruginosa*

Pseudomonas aeruginosa (Figure 4.3) are Gram-negative rod-shaped bacteria (Alcamo, 1994).

Figure 4.3: A Scanning Electron Micrograph of *Pseudomonas aeruginosa* (Alcamo, 1994)

Pseudomonas aeruginosa is an important cause of nosocomial disease, which means that *Ps. aeruginosa*, like *E. coli*, is an opportunistic pathogen, particularly in patients who have suffered burns. In the latter case, the organism grows quickly and produces a sickly sweet odour as well as a green fluorescent pigment that cause the infected, burnt tissue to glow under ultraviolet light. *Ps. aeruginosa*, which was also responsible for skin disease

and earache in cases where healthy individuals swam in contaminated water, is an opportunistic pathogen for eye infections (Alcamo, 1994).

4.1.3.2.3 *Staphylococcus aureus*

Staphylococcus aureus (*S. aureus*) forms a Gram-positive (Figure 4.2) grapelike cluster (Figure 4.4) of bacterial cells (Alcamo, 1994). It is a widespread cause of skin disease if it penetrates the skin barrier or mucous membranes and is therefore also an opportunistic pathogen. It has also been responsible for toxic shock syndrome in woman due to mostly vaginal infections. *S. aureus* have been identified as the cause of chicken spoilage and egg rot (Alcamo, 1994). Life-threatening fungal infections are increasing worldwide. It is

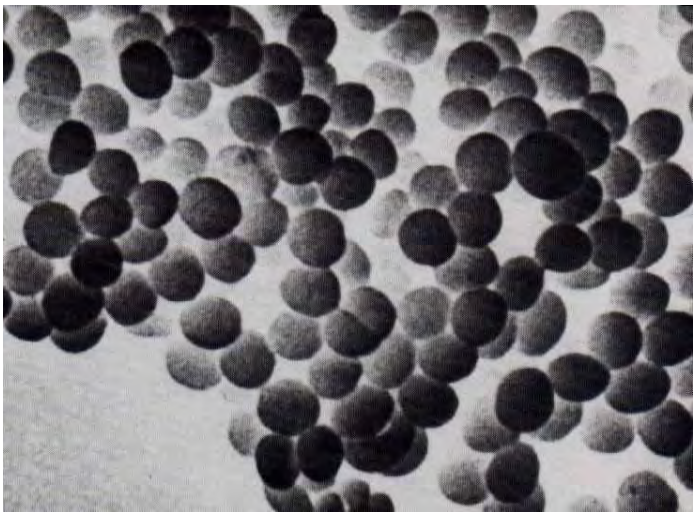

Figure 4.4: A Scanning Electron Micrograph of *Staphylococcus aureus* showing the typical grapelike cluster of cocci (x 15,000) (Alcamo, 1994)

clear that effective fungal therapy is critical, especially in Africa where most patients with fungal (or fungal-like) infections have AIDS, which complicates antifungal-drug treatment due to the problem of antifungal drug resistance developing in such patients (Goldman *et al*., 2004). *Aspergillus niger*, which is a fungus, as well as *Candida albicans*, which is a fungus-like yeast, are normally tested for in selected products at pharmaceutical companies such as Aspen-Pharmacare (Pty) Ltd., South Africa. The next few paragraphs are brief descriptions of and the impact of the above-mentioned organisms in human life.

4.1.3.2.4 *Aspergillus niger*

Aspergillus niger (*A. niger*) (Figure 4.5) is used industrially for the production of citric acid, which in turn is used in the production of inks, dyes, soft drinks, coagulants and foods (Alcamo, 1994). *Aspergillus*, a genus of found abundantly in the environment, can cause invasive (opportunistic) fungal infections in nearly every organ in the

Figure 4.5: A scanning electron micrograph of the moldlike phase of *Aspergillus niger* (x 600) (Alcamo, 1994)

immunocompromised (e.g. after prolonged antibiotic or steroid treatment or suffering from debilitating disease such as AIDS) human host - the pulmonary system is most commonly affected (Mohr *et al*., 2008). When the organism is ultimately identified in tissues, the disease may be too advanced for successful treatment (Mohr *et al*., 2008). Therefore, new agents for prevention and treatment of disease caused by this microorganism are needed to reduce patient deaths due to invasive aspergillosis.

4.1.3.2.5 *Candida albicans*

The predominant cause of fungal infections in hospitalized patients is the pathogenic, fungus-like yeast, namely *Candida albicans* (Figure 4.6) (Goldman *et al*., 2004). The organism is yeast that forms filaments when cultivated in the laboratory (Alcamo, 1994);

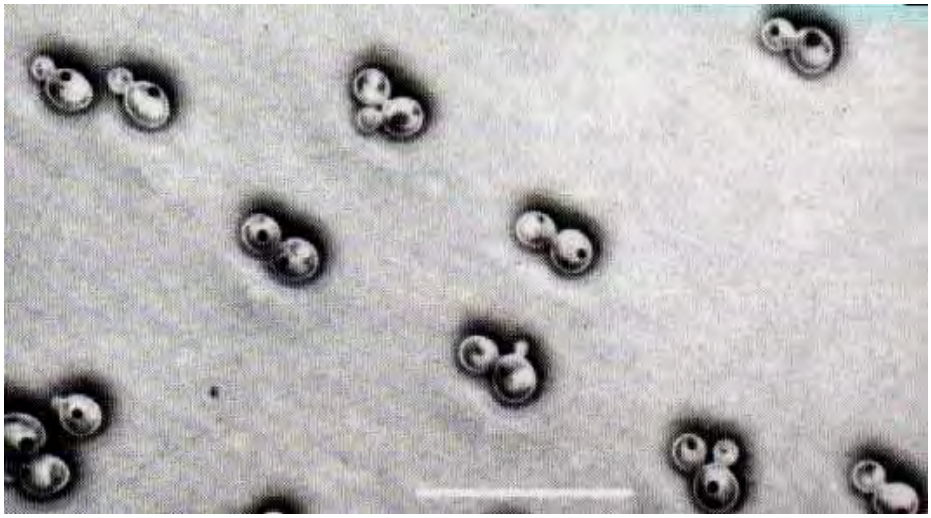

Figure 4.6: Phase-contrast micrograph of the oval yeast form of *Candida albicans* (Alcamo, 1994)

hence, it is fungus-like. *Candida albicans* is often present in the mouth, vagina and intestinal tract of healthy persons, where it lives without causing disease (Alcamo, 1994). As the body defenses are compromised or when changes occur in the microbial population, *Candida albicans* causes oral, vaginal, and systemic infections (Alcamo, 1994 and Goldman *et al*., 2004).

4.1.3.3 A review of an antibacterial standard and antifungal standards related to the present work

Efficacy of antimicrobial standards is expressed in terms of minimal inhibitory concentrations (MICs). Minimal inhibitory concentrations are defined as the lowest concentration of an antimicrobial agent that will inhibit the visible growth of a microorganism after overnight incubation (Andrews, 2001). These are reported in the literature either in terms of mg/L or μM.

4.1.3.3.1 *Ampicillin*

Ampicillin, the antibacterial used in the present work, is bactericidal for both Gram-positive and Gram-negative organisms, but ineffective against most staphylococcal infections (Dollery, 1991). It is reported (Andrews, 2001; Dollery 1991; Parfitt, 1999 and Pelczar *et al*., 1993) to be active against 50% of isolates of *Escherichia coli* and some strains of *Staphylococcus*, but not usually against Pseudomonas. Ampicillin's target

minimum inhibitory concentrations (MICs) against *Escherichia coli*, *Pseudomonas aeruginosa* and *Staphylococcus aureus* are reported to be 4, >128 and 0.06 mg/L, respectively, depending on the particular species of each bacterial strain involved (Andrews, 2001). The drug has no other clinical pharmacological activity apart from its antibacterial effect (Dollery, 1991).

4.1.3.3.2 *Benomyl*

Benomyl is used as a fungicide for the control of certain diseases of roses, flowers, ornamentals, turf, fruit and vegetables. It is also effective against mites and is used as pre and post-harvest sprays or dips for the control of storage rots of fruit and vegetables (Benomyl. http://www.speclab.com/ Accessed 2005).

4.1.3.3.3 *Fluconazole*

Fluconazole, the antifungal used predominantly in the present work, is commonly used to treat *Candida albicans* infection; however, resistant strains often result from long-term use or prophylactic treatment used by AIDS patients (Goldman *et al*., 2004 and Parfitt, 1999).

4.1.4 A review of anticancer tests against human tumor cell lines

The change of emphasis at the National Cancer Institute (NCI) from leukaemia to solid tumor bioassays in the early 80s, and from in vivo to in vitro screens, has compelled cancer researchers to re-evaluate bench-top assays and opt for testing potential anti-cancer compounds against human tumor cells in culture (Anderson *et al*., 1991). Cytotoxicity tests uses human tumor cell lines (e.g., A-549 lung carcinoma, MCF-7 breast carcinoma and HT-29 colon adenocarcinoma), and if the ED_{50} (or LD_{50}) values for pure compounds are found to be greater than 4 μg/mL, the compounds are considered inactive by the National Cancer Institute (NCI) (Anderson *et al*., 1991). The ED_{50} (or LD_{50}) value, also called the median-effective dose, for a pure compound is the minimum concentration required to result in a toxic reaction or to cause biological response (Horn, 1956).

4.2 EXPERIMENTAL

4.2.1. DPPH radical scavenging assay

Materials:- Silica gel F_{254} thin layer chromatography (TLC) plates; diphenylpicrylhydrazyl (DPPH); MeOH; capillary tubes and glass vacuum spray gun.

Qualitative TLC:- 10 μL of the ligand (1.5 mg. mL^{-1}, methanol) and 10 μL of a solution (1.5 mg. mL^{-1}, methanol) of each of the complexes tested, respectively, were spotted on a silica gel F_{254} thin layer chromatography (TLC) plate. 10 μL of a solution (in MeOH) of vitamin C, which is a known antioxidant, and 10 μL of a solution (in MeOH) of *o*-vanillin (*o*-methoxysalicylaldehyde) were also spotted on the same plate. The plate was dried and then sprayed with DPPH (0.2% solution in MeOH). The plates were examined 30 minutes after spraying. The reference, Vitamin C, was expected to give a positive test result; that is, a yellow spot on a purple background (Hay *et al*., 2004). The results for samples tested were tabulated as either positive (that is, a yellow spot on a purple background) or negative (that is, no yellow spot) for antioxidant activity.

4.2.2 Antimicrobial testing

Methodology:- The Schiff base and its corresponding Cu(II), Co(II) and Co(III) complexes employed the disk-plate, tube-dilution and agar infusion method of antimicrobial testing. *Escherichia coli*, *Pseudomonas aeruginosa*, *Staphylococcus aureus*, *Candida albicans* and *Aspergillus niger* served as test microorganisms in these tests. The concentration range for sample solutions was 10 – 1.5 mg. mL^{-1}, with solvents including methanol (MeOH), acetonitrile (CH_3CN), dichloromethane (CH_2Cl_2) and dimethylformamide (DMF).

Materials:- The three bacterial strains (*Escherichia coli*, *Pseudomonas aeruginosa*, *Staphylococcus aureus*), as well as the fungus species (*Aspergillus niger*), were supplied by the Microbiology department, Rhodes University, South Africa. The yeast strain

(*Candida albicans*) was supplied by Aspen Pharmacare (Pty) Ltd., South Africa. Nutrient agar, nutrient broth and malt extract agar were supplied by Biolab (Biolab Catalogue number HG000C1.500). Sartorius membrane filters (13 mm diameter), Whatman filter papers (13 mm diameter) and sterile 0.45 μm membrane filter units (Teflon nylon filters) were purchased directly from Sigma-Aldrich, Steinheim, Germany. Other standard materials used were syringes (5 mL or less) to fit membrane filter units; small stainless steel forcepts; autoclave-safe tubes or bottles (5 mL capacity) with lids; bacterial loop; glass spreader; stab wire; sterile petri dishes; sterile latex gloves; face mask; Eppendorf auto pipette; tips (0.100 and 1.000 mL) for auto pipette; an autoclave; a 37 ^{o}C-constant-environment-room; a 28 ^{o}C-constant-environment-room; a PowerWave^{TM} XS Microplate spectrophotometer.

4.2.2.1 Disk-plate (antibiogram) method of antimicrobial testing

4.2.2.1.1 *Disk-plate method (MeOH, CH_3CN or CH_2Cl_2 as solvent for metal complexes)*

Sample preparation and sterilization:- A solution (1.5 mg. mL^{-1}) (Gülgür *et al.*, 2003) in MeOH, CH_3CN or CH_2Cl_2 of the test compound was filtered through a sterile 0.45 μm membrane filter, which strained out all organisms, into a previously sterilized sample container (Smith and Navilliat, 1997). The broad spectrum antibiotic injection "Ampicillin-Fresenius injection 250 mg" was prepared as follows:- Distilled water was used to quantitatively transfer the contents of the injection preparation vial (250 mg of ampicillin) into a 200-mL volumetric flask to give a concentration of 1.25 mg. mL^{-1} or 1.25 μg. L^{-1}. The resulting ampicillin solution was filter sterilized and used as a positive control in the disc method of antibacterial testing. The antifungal agent used as control (intended to be used as a positive control, but which was later found not to be active against the particular strain of *Apergillus niger* employed in these tests) was "Fluzol ^{TM}IV infusion", which contained 2 mg fluconazole per 1 mL ready-made, sterile solution. Benomyl (5 mg. mL^{-1} in sterile water) was later used as positive control in the agar infusion method of antifungal testing.

Preparation of nutrient broth:- A solution of the nutrient powder was prepared in an autoclave-safe Erlenmeyer flask according to the recipe of the supplier and the quantities required for antibacterial testing of the ligand and metal complexes for each antibacterial test in the present work. The opening of the flask was then covered with aluminium foil and the solution autoclaved for 15 minutes at 121 ^{o}C. 3- mL Aliquots of the cooled (room temperature) broth were poured into sterile tubes (fitted with lids) and the tubes incubated for 24 hours at 37 ^{o}C. In order to ensure that the nutrient broth was sterile for use in antimicrobial testing, the tubes were inspected for growth (turbidity of the solution normally implies growth of micro-organisms).

Nutrient agar plates:- A solution of the nutrient powder was prepared in an autoclave-safe Erlenmeyer flask according to the recipe of the supplier and the volume required to prepare enough petri dishes for antibacterial testing of the control, the ligand and all the metal complexes. The opening of the flask was then covered with aluminium foil and the solution autoclaved for 15 minutes at 121 ^{o}C. The solution was left to cool until the flask was just comfortable to handle by hand and 15-20 mL of this hot solution aseptically poured into each of the required number of sterile petri dishes and each covered with its lid. Once the agar was set, the plates were inverted, placed in plastic bags and incubated at 37 ^{o}C for 24 hours. To ensure that sterile growth medium was used for antimicrobial testing, the closed plates were then visually inspected for possible growth of micro-organisms.

Malt extract agar plates:- A solution of the malt extract agar powder was prepared in an autoclave-safe Erlenmeyer flask according to the recipe of the supplier and the volume required to prepare enough petri dishes for antifungal testing of the ligand and all the metal complexes. The rest of the procedure was as for agar plates above, except the plates were incubated at 28 ^{o}C instead of 37 ^{o}C.

Obtaining a disk-plate (antibiogram):- The bacterial strains (***Pseudomonas aeruginosa***, ***Escherichia coli*** and ***Staphylococcus aureus***, respectively) and the fungus species (***Aspergillus niger***) were grown as pure cultures on non-selective media (nutrient

agar for each of the bacterial strains and malt extract agar for the fungus species). For each bacterial strain, 0.1 mL of a pure culture suspended in nutrient broth was evenly spread over the surface of the nutrient agar using a sterile glass spreader. For ***Aspergillus niger***, a loopful of the fungal spores from a pure culture of this species was suspended in approximately 2 mL of a mixture of a few drops of tween and sterile distilled water. This spore suspension was transferred aseptically into 4 mL nutrient broth to form a suspension and 0.1 mL of this suspension was aseptically and evenly spread over a malt extract agar surface using a sterile glass spreader. Approximately 30 minutes were allowed for adsorption or diffusion of the microbial inoculums into the agar before inversion, placing in plastic bags, and incubation of the plates. Conditions for incubation are shown in Table 4:1.

Table 4:1 Conditions for incubation of anti-microbial test plates

Microorganism	Incubation conditions
Pseudomonas aeruginosa	34 °C in air for 36 h
Escherichia coli	37 °C in air for 36 h
Staphylococcus aureus	37 °C in air for 36 h
Aspergillus niger	28 °C in air for 36 h

All the above actions required minimal manipulation of the sample (Furones *et al*., 2001) and only basic equipment (e.g., sterile tubes, sterile petri dishes, sterile glass spreaders, sterile growth media, etc.), which should be available to any microbiological laboratory.

For each test sample, a sterile paper disk (Whatman, 13 mm diameter) was soaked in a sterile solution (see sample preparation and sterilisation) of the sample, drip-dried and carefully placed on a lawn of microbial growth (Gülgür *et al*., 2003). On the same plate was placed four more test disks, of which

- one was soaked in the solvent used for dissolving the sample, and drip-dried;
- one was soaked in a solution of metal salt (that is, $CoCl_2.6H_2O$ if the sample was a cobalt complex or $CuCl_2.2H_2O$ if the sample was a copper complex), and drip-dried;
- one was soaked in a solution (in sterile distilled water) of ampicillin for antibacterial testing (Fluconazole or Benomyl was used for antifungal testing).

The soaked disk was drip-dried and placed in the center of each test plate (Figure 4.7);

- one was soaked in a solution of the ligand, and drip-dried.

The total of 5 test disks on each antimibrobial test plate was arranged as follows and the position of each indicated (and labelled) with a permanent marker pen on the plate bottom before placing the discs on the microbial lawn.

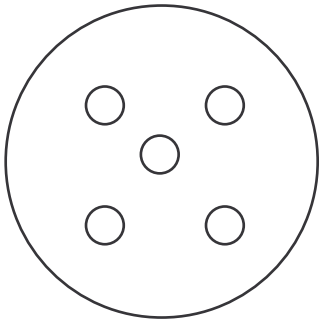

Figure 4.7: Arrangement of test disks for antimicrobial testing on the microbial lawn grown on the surface of growth agar

Triplicate plates of each test sample for antibacterial and antifungal testing, respectively, was prepared. All the plates were inverted, sealed in plastic bags, and incubated at the respective temperatures for 24 hours after which they were removed and the surface of the nutrient agar examined. A clear zone, which is called a halo or inhibition zone or radial diffusion zone, around a test-solution-dipped disc would indicate bactericidal activity against the bacterial species grown on the particular nutrient agar plate or fungicidal activity against *Aspergillus niger* on the malt extract agar (Gülgür *et al*., 2003). If no halo is found around a test disc, it could indicate either no bactericidal (or fungicidal) activity against the microbial species grown underneath the disc or resistance of the microbial species to the test material (Gülgür *et al*., 2003). The ampicillin-dipped disc was expected to definitely give an inhibition zone (halo) against *Staphylococcus aureus* and *Escherichia coli* because ampicillin is reported to be active against these (Andrews, 2001; Dollery , 1991; Parfitt, 1999 and Pelczar *et al*., 1993). Fluconazole was not necessarily expected to give an inhibition zone against *Aspergillus niger* because fluconazole is reported to be inactive against resistant strains of *Aspergillus niger* (Parfitt, 1999).

Calculation of antimicrobial index:- For each set of three replicates, the halos (growth inhibition or radial diffusion zones) were measured across diameters, which included filter paper diameters. The mean for each set of replicates was calculated (Gülgür *et al*., 2003). The mean sample value so obtained was corrected by subtracting from it the sample blank (solvent) diameter. The antimicrobial index was obtained by dividing the corrected mean sample value by the corresponding control diameter, which was also corrected for the control blank (solvent) diameter. If a test sample has an antimicrobial index value equal to 1, this would imply that the test sample has the same antimicrobial activity as the antimicrobial (antibacterial or antifungal) control used; a value less than 1 would imply less activity than the control, and a value more than 1, more microbial activity than the control. Calculating the "antimicrobial index" simultaneously enables direct comparison of sample activities with that of the antimicrobial control used as well as the direct comparison of antimicrobial activity amongst test samples (Vlaches *et al*., 1996). Reporting diameters only, a practice often found in literature, does not give a direct account of solvent effects and the antimicrobial activities of test samples compared to that of established antimicrobial agents. Pure solvents, especially organic solvents, may have antimicrobial activity and this is corrected for during the calculation of the antimicrobial index of the dissolved sample.

4.2.2.1.2 *Disk-plate method (dimethylformamide, DMF, as solvent for metal complexes)*

The process used here, was the same as that described under 4.2.2.1.1, except:-

- dimethylformamide (DMF) was used as the solvent for the ligand and the metal complexes;
- the samples were also tested for antimycotic (that is, against *Candida albicans*, which is a yeast-like fungus) activity;
- *Aspergillus niger* was omitted from the testing;
- the sample concentrations were 10 mg. mL^{-1} and 5 mg. mL^{-1} for antibacterial and antimycotic testing, respectively, instead of the 1.5 mg. mL^{-1} used in 4.2.2.1.1;
- the filter paper (Sartorius – membrane filter, 13 mm diameter) used for dipping into each sample solution was thicker and much more absorbent than the one

(Whatman filter paper disks, 13 mm diameter) used before; thus, more sample solution could be soaked up and thus, more sample could diffuse into the agar containing the bacteria;

- the bacterial and *Candida albicans* suspensions, which were known to have around 10^5 colony forming units (cfu) per mL, that were each spread over the surface of nutrient agar, were not allowed to first grow a bacterial lawn. Sample-dipped filter paper discs were placed immediately on each bacterial spread. For antimycotic testing, dry filter paper disks were first placed on the *Candida albicans* spread and exactly 50 µL of sample solution pipetted onto the center of each such disk;
- the *Candida albicans* plates were incubated for 48 hours, which was longer than the 24 hours required for bacterial plates, and
- fluconazole was expected to give a halo against *Candida albicans* because it is reported to be active against *Candida* species, except following long-term prophylaxis with fluconazole (Parfitt, 1999).

4.2.2.2 Tube dilution method of antibacterial testing (DMF as solvent for metal complexes)

Sample solution preparation and sterilization:- For this antimicrobial test, samples were chosen for testing based on the results from the disk-plate method of antimicrobial testing with DMF as solvent for the ligand and the metal complexes. A solution (5.0 mg. mL^{-1}) (Gülgür *et al*., 2003) in DMF (distilled water for $CoCl_2.6H_2O$ and $CuCl_2.2H_2O$, respectively) of the test compound was filtered through a sterile 0.45 µm Sartorius membrane filter, which strained out all organisms, and into previously sterilised sample bottles (Smith and Navilliat, 1997). The broad spectrum antibiotic injection "Ampicillin-Fresenius injection 250 mg" was prepared as follows:- 4 mL of sterile distilled water was pipetted into the injection preparation vial (250 mg of ampicillin) and the ampicillin dissolved to give a stock solution of 62.5 mg. mL^{-1} ampicillin.

Preparation of bacterial cultures for use in tube dilution method:- A loop full of a pure culture of *Pseudomonas aeruginosa*, *Escherischia coli* and *Staphylococcus aureus*,

respectively, was each suspended in nutrient broth. Except for the *Pseudomonas aeruginosa* suspension, the tube-dilution method of microbial growth determination, serial dilutions of the resulting suspensions were prepared and the tubes incubated at 37 ^{o}C for 24 hours, after which the growth (as colony forming units or CFU) per mL of each dilution in the series of tubes were determined. For each bacterial species, the tube that gave 10^5 colony-forming units (cfu) per millilitre (that is, 10^5 cfu/ mL) was used in the tube-dilution method of antibacterial testing (Behra-Miellet *et al*., 2003 and Yam *et al*., 1997).

Preparation and incubation of blank, control and test samples:- A solution of the nutrient powder was prepared according to the recipe of the supplier and the quantities required for antibacterial testing of the ligand and metal complexes in the present work. For each test sample, a 3-mL-aliquot of the cooled (room temperature) broth was accurately pipetted into a clean, dry McCarthy bottle, the cap loosely fitted, and the bottle autoclaved for 15 minutes at 121 ^{o}C. Each blank, control and test solution/ suspension was prepared in triplicate. The bottles were then incubated for 24 hours at 37 ^{o}C, after which they were inspected for growth (turbidity of the solution usually implies growth of microorganisms and therefore non-sterility of the broth). The latter procedure ensured that only sterile nutrient broth was used in the rest of the testing procedure. Tables 4:2 to 4:4 show the additions made to each 3 mL of sterile nutrient broth for antibacterial testing against *Pseudomonas aeroginosa*, *Escherischia coli* and *Stahylococcus Aureus*, respectively {*Note*: Except for the blank solutions, which contained no micro-organism, 20 µL of each 10^5cfu/mL-concentration of bacterial suspension was pipetted into each test solution to give an inoculation concentration of approximately 10^5 colony forming units (cfu) of the respective bacterial species per test solution}. The concentration of ampicillin in each ampicillin control tube was 2.0 mg. mL^{-1} ampicillin (100 µL of 62.5 mg. mL^{-1} ampicillin stock solution was added to 3 mL nutrient broth and 20 µL bacterial suspension).

After the necessary additions had been completed, the bottles were incubated (37 ^{o}C, 16 hours) on a rotary shaker, which was set at a speed of 100 rpm.

Absorbance readings using a PowerWave^{TM} XS Microplate Spectrophotometer:- The bottles were removed from the constant temperature room. Each bottle was thoroughly swirled before 200 µL of suspension (or solution if there was no microbial growth) was transferred from it to a particular well (that is, each well was previously assigned to a particular sample/ blank/ control solution) on a 96-well microplate. The corresponding microplate was positioned inside a PowerWave^{TM} XS Microplate Spectrophotometer and the absorbance read at 600 nm and 800 nm, respectively (The instrument had been set to shake the micro plate for 10 seconds just prior to taking the absorbance readings for the plate; thus, having ensured a homogeneous suspension of bacterial cells in those wells that contained bacterial suspensions). The readings were taken at room temperature.

Table 4:2 Antibacterial testing against *Ps. aeruginosa*

Type	Sample	Addition 1	Addition 2
Blank	water-blank	100 µL H_2O	20 µL broth[a]
	DMF-blank	100 µL DMF	20 µL broth[a]
	Sample-blank	100 µL sample[b]	20 µL broth[a]
Control	Control-water	100 µL H_2O	20 µL *Ps. aerug.*[a]
	Control-DMF	100 µL DMF	20 µL *Ps. aerug.*[a]
Sample	Ampicillin	100 µL ampicillin[c]	20 µL *Ps. aerug.*[a]
	$CuCl_2.2H_2O$	100 µL $CuCl_2$[c]	20 µL *Ps. aerug.*[a]
	$CoCl_2.6H_2O$	100 µL $CoCl_2$[c]	20 µL *Ps. aerug.*[a]
	2-OH-*o*VANPN	100 µL 2-OH-*o*VANPN[d]	20 µL *Ps. aerug.*[a]
	Complex **(A1)**	100 µL complex **(A1)**[d]	20 µL *Ps. aerug.*[a]
	Complex **(A3)**	100 µL complex **(A3)**[d]	20 µL *Ps. aerug.*[a]
	Complex **(A4)**	100 µL complex **(A4)**[d]	20 µL *Ps. aerug.*[a]
	Complex **(B1)**	100 µL complex **(B1)**[d]	20 µL *Ps. aerug.*[a]
	Complex **(B2)**	100 µL complex **(B2)**[d]	20 µL *Ps. aerug.*[a]
	Complex **(B3)**	100 µL complex **(B3)**[d]	20 µL *Ps. aerug.*[a]
	Complex **(B4)**	100 µL complex **(B4)**[d]	20 µL *Ps. aerug.*[a]
	Complex **(C2)**	100 µL complex **(C2)**[d]	20 µL *Ps. aerug.*[a]
	Complex **(C3)**	100 µL complex **(C3)**[d]	20 µL *Ps. aerug.*[a]

a: nutrient broth

b: sterile sample solutions, "ampicillin-blk", "CuCl-blk", "CoCl-blk", etc.

c: distilled water = solvent

d: Dimethylformamide (DMF) = solvent

Table 4:3 Antibacterial testing against *E. coli*

Type	Sample	Addition 1	Addition 2
Blank	water-blank	100 µL [a]H_2O	20 µL broth[a]
	DMF-blank	100 µL DMF	20 µL broth[a]
	Sample-blank	100 µL sample[b]	20 µL broth[a]
Control	Control-water.	100 µL H_2O	20 µL *E. coli*. [a]
	Control-DMF	100 µL DMF	20 µL *E. coli*. [a]
Sample	Ampicillin	100 µL ampicillin[c]	20 µL *E. coli*. [a]
	$CuCl_2.2H_2O$	100 µL $CuCl^c{}_2$[c]	20 µL *E.coli*. [a]
	$CoCl_2.6H_2O$	100 µL $CoCl^c{}_2$[c]	20 µL *E. coli*. [a]
	2-OH-*o*VANPN	100 µL 2-OH-*o*VANPN [d]	20 µL *E. coli*. [a]
	Complex **(A3)**	100 µL complex **(A3)** [d]	20 µL *E. coli*. [a]
	Complex **(A4)**	100 µL complex **(A4)** [d]	20 µL *E. coli*. [a]
	Complex **(B2)**	100 µL complex **(B2)** [d]	20 µL *E. coli*. [a]
	Complex **(B3)**	100 µL complex **(B3)** [d]	20 µL *E. coli*. [a]
	Complex **(C3)**	100 µL complex **(C3)** [d]	20 µL *E. coli*. [a]

See Table 4:2 for footnotes

Table 4:4: Antibacterial testing against *S. aureus*

Type	Sample	Addition 1	Addition 2
Blank	water-blank	100 µL [a]H_2O	20 µL [b]broth[a]
	DMF-blank	100 µL DMF	20 µL broth[a]
	Sample-blank	100 µL sample[b]	20 µL broth[a]
Control	Control-water	100 µL H_2O	20 µL *S. aureus* [a]
	Control-DMF	100 µL DMF	20 µL *S. aureus* [a]
Sample	Ampicillin	100 µL ampicillin[c]	20 µL *S. aureus* [a]
	Complex **(A3)**	100 µL complex **(A3)** [d]	20 µL *S. aureus* [a]
	Complex **(A4)**	100 µL complex **(A4)** [d]	20 µL *S. aureus* [a]
	Complex **(C2)**	100 µL complex **(C2)** [d]	20 µL *S. aureus* [a]
	Complex **(C3)**	100 µL complex **(C3)** [d]	20 µL *S. aureus* [a]

See Table 4:2 for footnotes

Calculation of %Inhibition of microbial growth:- The growth of the bacterial species in the control tube, which contained neither antibacterial agent nor sample, was assumed 100% (Shivankar *et al*., 2003). The inhibition (%) was calculated as follows:-

$$\%Inhibition = \frac{A_{control\,(corrected)} - A_{sample\,(corrected)}}{A_{control\,(corrected)}} x100\%$$

$$A_{control(corrected)} = (A_{control-water} - A_{nb+water-blk}) \text{ or}$$

$$A_{control(corrected)} = (A_{control-DMF} - A_{nb+DMF-blk});$$

$$A_{sample(corrected)} = (A_{sample} - A_{Sample-blk})$$

The results were compared against those of the control (ampicillin), which was screened simultaneously.

4.2.3 Tube-dilution method of antimycotic testing (DMF as solvent for metal complexes)

Sample preparation and sterilization:- Sample preparation was the same as for the tube dilution method of antibacterial testing. The antifungal agent used for preparing the control was "Fluzol ^{TM}IV infusion", which contained 2 mg fluconazole per 1 mL ready-made solution.

Preparation of yeast culture for use in tube dilution method:- A loop full of a pure culture of *Candida albicans* was suspended in nutrient broth. Using the tube-dilution method of microbial growth determination, serial dilutions of the resulting suspensions were prepared and the dilutions/ tubes incubated at 37 ^{o}C for 24 hours, after which the growth (colony forming units or CFU) per mL of each dilution in the series were determined. For each bacterial species, the dilution that gave 10^5 colony-forming units (cfu) per millilitre (that is, 10^5 cfu/mL) was used in this tube-dilution method of antimycotic testing (Behra-Miellet *et al*., 2003 and Yam *et al*., 1997).

Preparation of blank, control and test samples:- The preparation of blank, control and test samples was the same as for the tube dilution method of antibacterial testing, except that the *Candida albicans* suspension was added to each control and sample solution instead of a bacterial suspension and the antifungal agent used for preparing the control was "Fluzol ^{TM}IV infusion". The resulting bottles were incubated for 36 hours on a rotary shaker, which was set at 200 rpm, in a constant environment room (37 ^{o}C). The rest of the

procedure was the same as for tube-dilution method of antibacterial testing and the blank, control and sample tested were the same as for *Pseudomonas aeruginosa* with the only exceptions:- (i) fluconazole was used instead of ampicillin and (ii) *Candida albicans* suspension (10^5cfu/ mL) was added to each control and sample tube instead of a bacterial suspension.

4.2.4 Tube-dilution method of antifungal testing with DMF as solvent for the ligand and metal complexes

Initially the method of Shivankar and co-workers (Shivankar *et al*., 2003) was employed, but for reasons mentioned in the last paragraph in this section, it was replaced with the agar infusion technique of antifungal testing.

Sample preparation and sterilization:- Sample preparation was the same as for the tube dilution method of antibacterial testing. The antifungal agent used for preparing the control was "Fluzol ^{TM}IV infusion", which contained 2 mg fluconazole per 1 mL ready-made solution.

Preparation of fungal spore suspension:- *Aspergillus niger* was grown on malt extract agar and the spores suspended in about 5 mL of sterilised distilled water. The suspension of spores was transferred to a sterile tube. Except for the blank solutions, which contained no microorganism, 20 μL of this suspension was pipetted into each test solution. Much difficulty was experienced in trying to keep the spore suspension homogeneous before each 20-μL transfer.

Preparation of blank, control and test samples:- The preparation of blank, control and test samples was the same as for the tube dilution method of antibacterial testing, except that the *Aspergillus niger* spore suspension was added to each control and sample solution instead of a bacterial suspension, and the antifungal agent used for preparing the control was "Fluzol ^{TM}IV infusion". The resulting bottles were incubated for 24 hours on a rotary shaker, which was set at 200 rpm, in a constant environment room (28 ^{o}C).

During this time the spores had germinated and grown depending on the antifungal activity of the sample in each bottle. Shivankar and co-workers (Shivankar *et al.*, 2003) suggested reading the resulting suspensions at 530 nm, but the fungal growth did one of the following upon or after being vigorously swirled and or shaken:-

- broke up into large particles that could not be sucked into the autopipette tip;
- could not break up into a homogeneous suspension;
- could not maintain a homogeneous suspension for the time required to pipette and read the homogeneous suspension at 530 nm.

Obtaining dry weight of cell material as a measure of microbial cell mass:- All of the above observations would have resulted in inaccurate absorbance readings. Therefore, instead of taking the absorbance readings of the fungal suspensions, the dry weight of cell material as a measure of microbial cell mass was determined as follows:

- the contents of each bottle prepared during the test, was filtered (Büchner funnel) through a Whatman filter paper (Grade 1), which had been previously dried (at 110 ^{o}C) and weighed;
- each filter paper was carefully removed from the Büchner funnel, dried at 50 ^{o}C for 24 hours, and the dried weight recorded;
- the difference in weight of the filter paper was recorded as the mass of fungus that germinated and grew from the spores. The test was done in triplicate;
- the means were calculated, and
- the average mass of *Aspergillus niger* for each control or sample was corrected for the corresponding average mass of the blank (solvent).

A corrected average mass of fungus for any sample less than that of the corrected average mass for the control would indicate more antifungal activity (and therefore less fungal growth) than the control and vice versa.

The tube-dilution method of antifungal testing of the ligand and metal complexes (DMF as the sample solvent) resulted in inaccurate mass readings. Also, the antifungal agent, Fluzol ^{TM}IV infusion (2 mg fluconazole per 1 mL) was intended to be used as a positive

control in this antifungal test, but was found to be inactive against *Apergillus niger*. Benomyl solution (5 mg benomyl per mL) was used in the agar-infusion method (below) of antifungal testing in an attempt to get better results than this (tube-dilution) method.

4.2.5 Agar-infusion method of antifungal testing

Sample preparation and sterilization:- Sample preparation was the same as for the tube dilution method of antibacterial testing. The antifungal agents used for preparing the positive controls were "Fluzol ^{TM}IV infusion", which contained 2 mg fluconazole per 1 mL ready-made solution, and benomyl solution, which contained 5 mg benomyl per mL solution (in sterile water).

Preparation of sample-infused-agar plates:- 800 mL of malt extract agar solution was prepared according to the supplier's instruction. A 50-mL aliquot of the resulting, cooled solution was transferred to each of fourteen 100-mL Erlenmeyer flasks; the flasks covered with aluminium foil, and autoclaved at 121 ^{o}C for 15 minutes. The sterilised malt extract agar was left to cool down such that the flasks were just comfortable to be handled with the bare hand. To each of these 50-mL aliquots of sterile agar was added either 0.5 mL of one of the antifungal agents (that is, fluconazole or benomyl) or 0.5 mL of sample solution. Each resulting solution was swirled thoroughly to produce a homogeneous distribution of sample (or antifungal) in the hot, malt extract agar. A total of 8 sample flasks, 2 positive control flasks and 1 solvent (DMF) blank flask resulted from the above additions. Three replicate plates, which amounts to approximately three 15-mL-aliquots were aseptically poured per 50 mL aliquot of sample-/ blank-/ antifungal-agar mixture. The agar in the petri dishes was first allowed to cool to room temperature; each petri dish was turned upside-down, and the following permanent markings, together with the name of the test solution (that is, sample, antifungal agent or DMF), made on each plate bottom:-

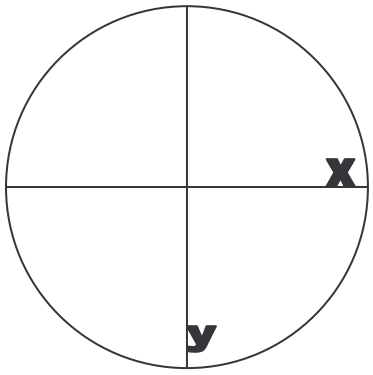

Figure 4.8: Markings on Petri dish/ plate for use in agar-infusion method of antifungal testing

Inoculation of sample-infused agar plates:- A lawn of *Aspergillus niger* was grown on the surface of malt extract agar. A 5-mm-diameter sterile glass tube was used to cut circles of *Aspergillus niger* growth into this lawn of fungal growth. Using a sterile stab wire, each circle of *Aspergillus niger* growth was carefully removed and placed, with the fungal growth facing upwards, at the center of the y-axis and x-axis intercept of each of the plates prepared as described above. The x and y measurement (in mm) of each inoculum was recorded as that for "day 0". The x and y measurement for each plate's inoculum was averaged and this one value, called the radial size (in mm), recorded for each plate's inoculum.

The plates were sealed in plastic bags and incubated overnight in an upright position in a constant temperature room (28 ^{0}C) and thereafter in an upside-down position under the same conditions and inspected (see next paragraph) daily for 5 days.

Calculation of average radial growth/ day and plotting of the corresponding graph:- After each 24-hour-period, the plates were removed and each inoculum's x measurement

(mm) and y measurement (mm) taken with a ruler and then averaged. This average was then subtracted from the original (day 0) radial size of that inoculum to give radial growth/ day. The average radial growth for each of three replicates of sample/ blank/ positive control/ growth control was recorded daily. At the end of the fifth day, the data was used to plot "Average radial growth (in mm)" versus "day number" for each sample, blank, and control tested.

4.3 RESULTS AND DISCUSSION

4.3.1 DPPH radical scavenging assay (Qualitative TLC)

Table 4:5 Results of the DPPH antioxidant activity test

Sample	Positive	Negative
o-Vanillin	√	
Vitamin C	√	
2-OH-*o*VANPN	√	
Complex **(A1)**		√
Complex **(A3)**		√[a]
Complex **(A4)**		√[a]
Complex **(B1)**		√
Complex **(B2)**	√	
Complex **(B3)**	√	
Complex **(B4)**	√	
Complex **(C2)**		√[a]
Complex **(C3)**		√[a]

[a]A halo of yellow around an orange spot was observed for this sample on the TLC plate.

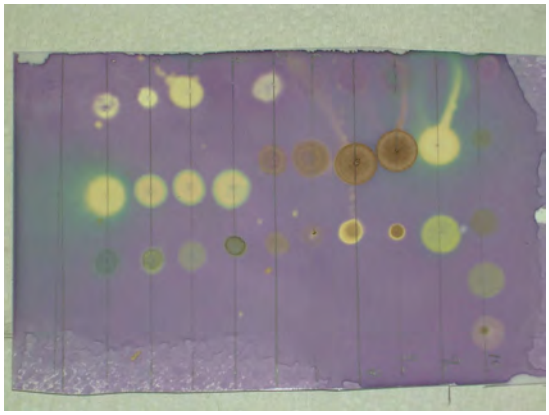

Figure 4.9 Thin Layer Chromatography (TLC) plate (Developed and sprayed) showing some sample spots resulting from the DPPH antioxidant activity test

It can be seen from Table 4:5 and Figure 4.9 that, towards the DPPH radical,

- *o*-vanillin, which is a precursor of 2-OH-*o*VANPN, showed antioxidant (scavenging) activity. This activity is due to the free aldehyde and free hydroxyl group.
- the Schiff base ligand showed antioxidant activity. The ligand has both a free imine and a free hydroxyl group, which are both linked to antioxidant activity, and is in accordance with the following finding: During a study of cyclic voltammograms of several Ni(L_x) {L = *N*,*N*′-polymethylenebis(3,5-di-tert-butylsalicylaldiminato); x = 1 – 4} complexes, the first oxidation peak potentials of all the Ni(II) complexes corresponded to the oxidation of the metal center to the Ni(III) species and the second oxidation was assigned as the ligand based oxidation, which generated a coordinated phenoxy radical species (Özalp-Yaman *et al*., 2005).
- the Cu(II) complex, **(A1)**, showed no antioxidant activity. The results are in accordance with those of Kitajima and co-workers, who found that mononuclear complexes of Cu(II) with 1,3-bis(salicylideneamino)propan-2-ol (2-OHSALPN), which only differs the ligand in the present work by a methoxy group on the aromatic ring, showed no catalytic activity for ethanol oxidation to acetaldehyde under normal reaction conditions (Kitajima *et al*., 1986). Those copper(II) complexes, **(A3)** and **(A4)**, that displayed an orange halo imply that the ligand or its hydrolysed precursor (*o*-vanillin), which has antioxidant activity, may have

dissociated from the complex in the silica gel and then showed activity in the uncomplexed state.

- The cobalt(II) complex, **(B1)**, had no antioxidant activity, probably because of the fact that it is dinuclear and therefore does not have suitable co-ordination geometry to facilitate activity in the DPPH antioxidant test. The other Co(II) complexes, **(B2)**, **(B3)** and **(B4)**, demonstrated antioxidant activity. This finding is in contrast to those of Kitajima and co-workers, who found that mononuclear complexes of Co(II) with 1,3-bis(salicylideneamino)propan-2-ol (2-OHSALPN) showed no catalytic activity for ethanol oxidation to acetaldehyde (Kitajima *et al.*, 1986). The three complexes differ from the mononuclear ones of Kitajima *et al*. in that they have in common the phenolic OH group that remains protonated whilst being coordinated to the metal atom and also in the coordination of chlorides to the cobalt atom. Another possible reason for the differences in biological activity of complexes **(B3)** and **(B4)** (Figure 4.10) compared to the complexes synthesized by Kitajima and co-workers may lie in the presence of a methoxy substituent on each benzene ring of each complex, whilst the alkyllic OH is coordinated in complex **(B2)**.

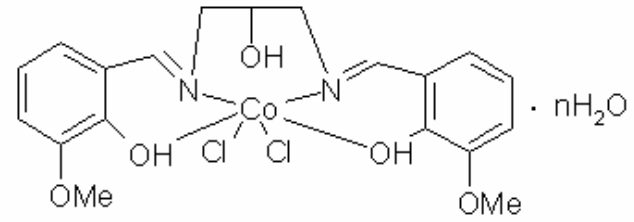

Figure 4.10: The structure of complex **(B3)** and **(B4)** (n = 5½)

- The cobalt(III) complexes, just like some of the Cu(II) complexes that were also tested, resulted in the yellow halo around the sample spot, which implies that the ligand had dissociated from the complex on the silica gel, possibly with some hydrolysis.

In the current work, the interest in antioxidant activity testing was not to determine the extent of antioxidant activity, but simply to establish whether the ligand and/ complexes had antioxidant activity. From the above findings, 2-OH-*o*VANPN, the free ligand and

three Co(II) complexes could act as radical scavengers as the possible mode of action in potential cancer chemotherapy because, as mentioned in section 4.1.2.1, cancer (tumour) cells are believed to have defective enzymatic antioxidant activity (Ottino and Duncan, 1997). The qualitative TLC results clearly indicated that complexes **(B2)**, **(B3)** and **(B4)** in this work would be worth sending to the NCI for cancer cell line testing, and that complexes **(A3)**, **(A4)**, **(C2)** and **(C3)** could possibly show activity through possible hydrolysis products.

4.3.2 Antimicrobial testing

Escherichia coli, *Pseudomonas aeruginosa* and *Staphylococcus aureus* were used as test organisms for antibacterial testing and *Candida albicans*, a fungus-like yeast, was used as test organism for antimycotic testing of the ligand and metal complexes in the present work. *Escherichia coli* and *Pseudomonas aeruginosa* are Gram-negative bacteria, whilst *Staphylococcus aureus* is a Gram-positive bacterial species. The disk-plate method (also called the agar diffusion or antibiogram method) and the tube-dilution method were used to study antibacterial and antimycotic activity.

Aspergillus niger, a fungus species, was used as test organism for antifungal testing of the ligand and the metal complexes. The disk-plate (agar diffusion) method, the tube-dilution method, weighing-of-dried-cell-mass and the agar-infusion method, were used in this antifungal activity study. Only the agar-infusion- and disk-plate method proved useful in the antifungal activity study.

Nature of the cell wall, the ligand, coordination sites, geometry of the complex, hydrophilicity, lipophilicity, presence of co-ligand, pharmacokinetic factors, etc. also play decisive roles in determining antimicrobial activity of the Schiff base and its metal complexes (Daniel *et al*., 2008). The mode of action of the complexes also indulge in the formation of hydrogen bonded interaction through the coordinated anion, hydroxyl group, etc. with the active centers of the microbial cell constituents resulting in interference with the normal cell processes (Daniel *et al*., 2008).

4.3.2.1 Disk-plate method of antimicrobial testing

4.3.2.1.1 *Disk-plate method (MeOH, CH_3CN or CH_2Cl_2 as solvents for metal complexes)*

Advantages of reporting "Antimicrobial index" over "Diameters (mm):- Reporting diameters only does not give a direct account of solvent effects and the antimicrobial activities of test samples compared to that of established antimicrobial agents. Pure solvents, especially organic solvents, may have antimicrobial activity and this is corrected for during the calculation of the antimicrobial index of the dissolved sample. A shortcoming in numerous reported values of antimicrobial activity is that uncorrected values are given, which may falsely indicate activity (positive results) for the test samples. Calculating the "antimicrobial index" simultaneously allows the direct comparison of sample activities with that of the antimicrobial control used as well allowing the direct comparison of antimicrobial activity amongst test samples (Vlaches *et al*., 1996).

Table 4:6 Antimicrobial index of the ligand and the metal complexes against the control (ampicillin or fluconazole)

Sample	Metal	Solvent	Synthesis method	Antimicrobial Index			
				E.coli	Ps. aerug.	*S. aureus*	*A. niger*[a]
2-OH-*o*VANPN	-	MeOH	-	0	0	0	0
Complex **(A1)**	Cu(II)	MeOH	1	0	0	0	0
Complex **(A3)**	Cu(II)	MeOH	3	0	0	0	0
Complex **(A4)**	Cu(II)	MeOH	4	0	0	1.5	1
Complex **(B1)**	Co(II)	MeOH	1	0	0	0	2
Complex **(B2)**	Co(II)	CH_3CN	2	0.5	0	0	0
Complex **(B3)**	Co(II)	CH_3CN	3	0	0	0	0
Complex **(C2)**	Co(III)	MeOH	2	0	0	0	1
Complex **(C3)**	Co(III)	CH_2Cl_2	3	1	0	0	0
$CuCl_2.2H_2O$	Cu(II)	Water	-	1	0	1	1
$CoCl_2.6H_2O$	Co(II)	Water	-	1	0	0	0

a: For the activity index calculation, the denominator was set to one because the control, fluconazole, was found to be inactive)

The ligand:- 2-OH-*o*VANPN showed no activity towards any of the microbial species tested.

The metal complexes (General):- Some metal complexes in Table 4:6 showed antimicrobial activity against a particular microorganism(s), whilst the ligand was not active. These results would suggest that the chelation would facilitate the ability of a complex to cross the respective microorganism's cell membrane, which is explained by Tweedy's chelation theory (Tweedy, 1964). Chelation considerably reduces the polarity of the metal ion because of partial sharing of its positive charge with donor groups and possible electron delocalization over the whole chelate ring. Such a chelation could enhance the lipophillic character of the central metal atom, which consequently favors its permeation through the lipid layer of the cell membrane of the microorganism. If the geometry and charge distribution around the chelate are compatible with those of the pores present in the microbial cell membrane, penetration by the chelate may take place, which in turn may ultimately result in toxic effects on the cell membrane or cellular constituents (Daniel *et al*., 2008).

The copper(II) complexes:- Complex **(A4)**, which was synthesised by reacting the metal salt with the ligand constituents (that is, *o*-vanillin and 1,3-diaminopropan-2-ol), gave activity higher and equal to the respective controls for ***Staphylococcus aureus*** and ***Aspergillus niger***. The copper salt, $CuCl_2.2H_2O$, was active against both ***Escherichia coli*** and ***Staphylococcus aureus,*** and only slightly active against ***Aspergillus niger***.

The cobalt(II) and cobalt(III) complexes:- Complex **(B1)**, which was synthesised in the presence of KOH, showed antifungal activity towards ***Aspergillus niger***, whilst complex **(B2)**, synthesised in the absence of KOH, showed slight activity towards ***Staphylococcus aureus***. The cobalt(II) salt was active against ***Escherichia coli***. Complex **(C3)** was active against ***Escherichia coli***.

Possible explanations for "poor" antimicrobial activies:- Schiff base ligands are known to have antibacterial activity because of the presence of imine groups as well as free hydroxyl groups (Tümer *et al*., 2007). Schiff base complexes are also noted for their significant antibacterial and antifungal activities (Nallasamy *et al*., 2001). Based on these findings, the results in Table 4:6 was found to be very poor (that is, the halos were very

small around the paper discs). One reason for the "poor" positive results could be the fact that the filter paper (Whatman No. 1, 13 mm) used was only slightly absorbent, which resulted in low volumes of sample solution being absorbed by it, and therefore almost immeasurable effect on the microorganism onto which the sample-soaked filter paper was placed. A second reason could be that the concentration of microorganism may have been too high for the particular amount of sample to which it was exposed to, for any antimicrobial effect to be observed. A third reason could be that the sample concentrations were too low to show a measurable effect on the test microorganisms. Spreading the 100 µL of micro-organism suspension over the entire agar surface and then placing the sample-soaked discs on the microorganism-spread agar surface, without allowing the organism to form a lawn of growth first, could have overcome the problem of too much micro-organism per sample-soaked disc. Another advantage of *not* first growing a lawn is that one can also measure the ability of a sample to prevent reproduction/ growth of a particular micro-organism (i.e., bacteriostatic/ fungistatic ability), whereas growing the lawn of micro-organism first, tests mainly bactericidal/ fungicidal (i.e., killing) effect of the test sample.

Strategies to overcome "poor" antimicrobial activities:- As mentioned in section 4.2.2.1.2, the disk-plate method was repeated in an attempt to overcome the problems listed above so that the positive results could be more measurable. The filter paper (Sartorius – membrane filter, 13 mm diameter) used for dipping into each sample solution was thicker and much more absorbent than the one (Whatman filter paper disks, 13 mm diameter) that was used before. Sample-dipped filter paper disks were placed immediately on each bacterial spread instead of growing the bacterial lawn first. For antimycotic testing, dry filter paper disks were first placed on the *Candida albicans* spread and exactly 50 µL of sample solution pipetted onto the center of each such disk. The sample concentrations were 10 $mg.mL^{-1}$ and 5 $mg.mL^{-1}$ for antibacterial and antimycotic testing, respectively, instead of the 1.5 $mg. mL^{-1}$ that was used before.

4.3.2.1.2 *Disk-plate method {dimethyl formamide (DMF) as solvent for metal complexes}*

Table 4:7 Antimicrobial index against the control (ampicillin or fluconazole)

Sample	Metal	Solvent	Synthesis method	Antimicrobial Index			
				E. coli	Ps. aerug.	*S. aureus*	*C. albicans*
2-OH-*o*VANPN	-	DMF	-	6.5	0	0	1.7
Complex **(A1)**	Cu(II)	DMF	1	0	0	0	0.1
Complex **(A3)**	Cu(II)	DMF	3	17.5	7.5	0	0.2
Complex **(A4)**	Cu(II)	DMF	4	0	0	6.5	0.1
Complex **(B1)**	Co(II)	DMF	1	0	0	0	0.4
Complex **(B2)**	Co(II)	DMF	2	1.5	0	0	0.2
Complex **(B3)**	Co(II)	DMF	3	0	0	0	1.1
Complex **(C2)**	Co(III)	DMF	2	0	0	1	0
Complex **(C3)**	Co(III)	DMF	3	0	0	2.5	0.1
$CuCl_2.2H_2O$	Cu(II)	Water	-	2.5	0	1	0
$CoCl_2.6H_2O$	Co(II)	Water	-	4.5	0	0	0.3

Effect of sample concentration:- For this antibacterial and antimycotic disk-plate method, 10 mg. mL^{-1} and 5 mg. mL^{-1} samples were used, respectively, compared to the lower (1.5 mg. mL^{-1}) sample concentrations used for the disk-plate method outlined in section 4.2.2.1.1. It is a well known fact that concentration plays a vital role in increasing the degree of microbial inhibition (Tümer *et al*., 2007) as judged by comparing the results in Tables 4:6 with those in Table 4:7.

The results indicate that most of the samples tested have antimycotic activity and only some of the samples tested have bactericidal activity, but the possibility of bacteristatic activity (that is, slowing down the growth rate of the microbial species) of all test samples may not be excluded from such results.

The ligand:- The ligand, 2-OH-*o*VANPN, showed exceptionally high bactericidal activity towards the Gram-negative *Escherichia coli* and higher antimycotic activity towards the yeast, *Candida albicans*, than the antifungal agent (control) and metal complexes. The remarkable activity of the Schiff base ligand may arise from the hydroxyl groups, which may play an important role in the antibacterial activity, as well as the

presence of two imine groups, which imparts in elucidating the mechanism of transformation reaction in biological systems (Tümer *et al*., 2007).

The copper(II) complexes:- Complex **(A3)**, which was synthesised in the absence of KOH, demonstrated very high antibacterial activity towards *Escherichia coli* and *Pseudomonas aeruginosa* compared to the Schiff base ligand and compared to the positive control, ampicillin. The results for this test are inconsistent with those in Table 4:6, which show no antimicrobial activity for this complex, but the reasons for this inconsistence have already been addressed. Complex **(A4)**, which was synthesized by reacting the metal salt with the ligand constituents (that is, *o*-vanillin and 1,3-diaminopropan-2-ol), gave much higher activity towards *Staphylococcus aureus* than the control (ampicillin) - the Schiff base ligand displayed no activity towards *Staphylococcus aureus*. These results would suggest that the chelation would facilitate the ability of a complex to cross the respective microorganism's cell membrane, which is explained as before by Tweedy's chelation theory (Tweedy, 1964). Chelation considerably reduces the polarity of the metal ion because of partial sharing of its positive charge with donor groups and possible electron delocalization over the whole chelate ring. Such a chelation could enhance the lipophillic character of the central metal atom, which consequently favors its permeation through the lipid layer of the cell membrane.

The cobalt(II) complexes:- Complex **(B2)** showed, like with Cu(II), antibacterial activity towards *Escherichia coli*, whilst complex **(B3)** showed the same activity towards *Candida albicans* as the antifungal tested, as indicated by the activity index value of around 1.

The cobalt(III) complexes:- Complexes **(C2)** and **(C3)** were both active against *Staphylococcus aureus* and **(C3)** additionally active against *C. albicans*.

Most of the results are consistent with the antibacterial results in Table 4:6, except that positive results are more pronounced when DMF was used as the solvent for the ligand

and the metal complexes. DMF, by itself in the test medium, was not active against *E. coli*, *Ps. aeruginosa* and *S. aureus*.

4.3.2.2 Tube-dilution method of antibacterial testing (DMF as solvent)

Table 4:8 Antibacterial activity (%Inhibition of bacterial growth) calculated from absorbance readings at 800 nm

Sample	*Ps. aeruginosa*		*E. coli*		*S. aureus*	
	$A_{corrected}$[a]	%I	$A_{corrected}$[a]	%I[b]	$A_{corrected}$	%I[b]
2-OH-*o*VANPN	$\overline{X}$ = 0.216 S = 0.068	27	$\overline{X}$ = 0.001 S = 0.001	100		
Complex **(A1)**	$\overline{X}$ = 0.150 S = 0.006	49				
Complex **(A3)**	$\overline{X}$ = 0.279 S = 0.103	5	$\overline{X}$ = 0.0 S = 0.0	-	$\overline{X}$ = 0.221 S = 0.016	31
Complex **(A4)**	$\overline{X}$ = 0.208 S = 0.026	29	$\overline{X}$ = 0.0 S = 0.0	-	$\overline{X}$ = 0.240 S = 0.105	25
Complex **(B1)**	$\overline{X}$ = 0.181 S = 0.017	39				
Complex **(B2)**	$\overline{X}$ = 0.142 S = 0.032	52	$\overline{X}$ = 0.0 S = 0.0	-		
Complex **(B3)**	$\overline{X}$ = 0.116 S = 0.012	61				
Complex **(C2)**	$\overline{X}$ = 0.079 S = 0.036	73	$\overline{X}$ = 0.0 S = 0.0	-	$\overline{X}$ = 0.419 S = 0.050	0
Complex **(C3)**	$\overline{X}$ = 0.157 S = 0.032	47	$\overline{X}$ = 0.0 S = 0.0	-	$\overline{X}$ = 0.000 S = 0.000	100
$CuCl_2.2H_2O$	$\overline{X}$ = 0.567 S = 0.060	18	$\overline{X}$ = 0.480 S = 0.020	9		
$CoCl_2.6H_2O$	$\overline{X}$ = 0.123 S = 0.049	82	$\overline{X}$ = 0.362 S = 0.009	32		
Control-DMF	$\overline{X}$ = 0.295 S = 0.030	-	$\overline{X}$ = 0.0 S = 0.0	-	$\overline{X}$ = 0.322 S = 0.042	-
Control-water	$\overline{X}$ = 0.695 S = 0.030	-	$\overline{X}$ = 0.533 S = 0.020	-	$\overline{X}$ = 0.385 S = 0.044	-
Ampicillin	$\overline{X}$ = 0.000 S = 0.000	100	$\overline{X}$ = 0.001 S = 0.001	100	$\overline{X}$ = 0.005 S = 0.004	99

a: $A_{corrected} = A_{sample} - A_{sample\text{-}blank}$; sample blank = {sample + solvent (DMF or water)} + nutrient broth

b: %Inhibition of microbial growth. Negative %I was set to 0

Blank cells in Table 4:8 imply that the sample in question was not tested against the bacterial species (column header) based upon a negative outcome during the disk-plate method (section 4.3.2.1) of testing against that particular bacterial species. The absorbance readings for samples, "control-DMF" and "control-water", were used for calculating corrected sample absorbance values (refer to "Calculation of %Inhibition of microbial growth" at the end of section 4.2.2.2). The absorbance readings at 800 nm showed greater growth inhibiting activity of the samples tested compared to those at 600 nm and was therefore reported in Table 4:8. The mean or average ($\bar{x}$ in Table 4:8) is the central value that represents the absorbance readings of three replicates for each sample and is calculated using the formula given below. The standard deviation (s in Table 4:8) is a measure of how close the absorbance readings are to each other in a set of replicates for each sample and was calculated as follows:-

$$\bar{x} = \frac{\sum_{i=1}^{i=n} x}{n}$$

$$s = \sqrt{\frac{\sum_{i=1}^{i=n} (x - \bar{x})^2}{n-1}}$$

In the above formulas, x is the absorbance reading for each replicate and n is the number of replicates for each sample/ control. The smaller the value of s, the closer the absorbance readings are to each other in the set of replicates for each sample and therefore, the higher the precision of the results. A large value of s, relative to $\bar{x}$, indicates a lower precision of the results obtained.

If above 50% inhibition of growth is considered significant, (i) complexes **(B2)**, **(B3)** and **(C2)** have inhibited *Pseudomonas aeruginosa*; (ii) the ligand, 2-OH-*o*VANPN, inhibited *Escherichia coli*; (iii) complex **(C3)** inhibited *Staphylococcus aureus*, and (iv) the control antibiotic, ampicillin, inhibited all three bacterial species tested.

In general, both disk-plate and tube-dilution method worked well for antibacterial activity when dimethylformamide (DMF) was used to dissolve the ligand and the complexes.

4.3.3 Tube-dilution method of antimycotic (*Candida albicans*) testing (DMF as solvent for metal complexes)

Table 4:9 Antimycotic activity (%Inhibition of yeast growth)d from absorbance readings at 600- and 800 nm

Sample	$A_{(corrected)}$[a] 600 nm	800 nm	%I[b]
2-OH-*o*VANPN	$\overline{X}$ = 0.006 S = 0.002	$\overline{X}$ = 0.002 S = 0.000	71
Complex **(A1)**	$\overline{X}$ = 0.004 S = 0.001	$\overline{X}$ = 0.001 S = 0.001	86
Complex **(A3)**	$\overline{X}$ = 0.001 S = 0.001	$\overline{X}$ = 0.000 S = 0.000	100
Complex **(A4)**	$\overline{X}$ = 0.013 S = 0.008	$\overline{X}$ = 0.005 S = 0.005	29
Complex **(B1)**	$\overline{X}$ = 0.000 S = 0.000	$\overline{X}$ = 0.000 S = 0.000	100
Complex **(B2)**	$\overline{X}$ = 0.001 S = 0.001	$\overline{X}$ = 0.005 S = 0.005	29
Complex **(B3)**	$\overline{X}$ = 0.004 S = 0.004	$\overline{X}$ = 0.006 S = 0.005	17
Complex **(C2)**	$\overline{X}$ = 0.020 S = 0.020	$\overline{X}$ = 0.064 S = 0.001	0
Complex **(C3)**	$\overline{X}$ = 0.000 S = 0.000	$\overline{X}$ = 0.000 S = 0.000	100
$CuCl_2.2H_2O$	$\overline{X}$ = 0.453 S = 0.090	$\overline{X}$ = 0.384 S = 0.070	0
$CoCl_2.6H_2O$	$\overline{X}$ = 0.006 S = 0.004	$\overline{X}$ = 0.003 S = 0.002	99
Control-DMF	$\overline{X}$ = 0.008 S = 0.005	$\overline{X}$ = 0.007 S = 0.003	-
Control-water	$\overline{X}$ = 0.364 S = 0.036	$\overline{X}$ = 0.326 S = 0.025	-
Fluconazole	$\overline{X}$ = 0.021 S = 0.002	$\overline{X}$ = 0.016 S = 0.003	95

a: $A_{corrected} = A_{sample} - A_{sample\text{-}blank}$; sample blank = {sample + solvent (DMF or water)} + nutrient broth

$A_{corrected} = A_{control} - A_{control\text{-}blank}$; control blank = solvent (DMF or water) + nutrient broth

b: %Inhibition of microbial growth. Negative %I was set to 0

Some standard deviations (s) values in Table 4:9 are high relative to the absorbance values, but this is normal when dealing with replicates in growing/ culturing microorganisms. DMF (dimethylformamide) was found to be very active against *Candida albicans* as observed by the low absorbance readings of control-DMF. Therefore, each %I that is based on the "control-DMF" absorbance data has large error associated with it; hence, making interpretation of such results largely inconclusive. From Table 4:9 and taking the above into consideration, most of the samples tested were possibly active against *Candida albicans*.

The ligand:- 2-OH-*o*VANPN was found to give positive results against *C. albicans*.

The Cu(II) complexes:- Complexes **(A1)** and **(A3)** were more active against *C. albicans* than the ligand. These results are, as before, explained by Tweedy's theory of chelation (Tweedy, 1964). The other copper complexes were inactive.

The Co(II) complexes:- All of the Co(II) complexes were found to be inactive against the yeast (*C. albicans*), except complex **(B1)**, which gave higher activity than the ligand. The latter's binuclear nature compared to the mononuclear cobalt(II) complexes probably renders it more suitable for antimycotic activity towards the yeast cells because yeast cells and bacterial cells differ in terms of the morphology of the cells. The higher activity compared to the ligand can once again be linked to Tweedy's theory of chelation.

The Co(III) complexes:- Complex **(C3)** was more active against *C. albicans* than 2-OH-*o*VANPN.

Future work in this regard should involve repeating the test with a solvent, for dissolving the ligand and complexes, which has minimal growth inhibiting effect on *Candida albicans*.

An interesting observation made was that *Candida albicans* was dark brown in colour instead of the usual cream colour of the organism, in the presence of the cobalt(III)

complex, **(C3)**. With all other complexes and the ligand, the surrounding test solution was coloured (green, brown or yellow), but the actual organism remained whitish in colour. The brown colour of the organism was possibly due to a chemical interaction, which may have been oxidation-reduction in nature between complex **(C3)** (or Co^{3+}) with *Candida albicans* cell constituents resulting in possible alteration of the physical appearance (colour) and therefore, the absorption characteristics of these yeast cells (A large mass of growth of *C. albicans* was present in the sample tube and was expected to result in a much higher absorbance value than the sample blank, which contained yeast growth, but, instead, for complex **(C3)**, $A_{sample\text{-}blank} > A_{sample}$). Fluconazole was found to be active against *Candida albicans*, but the concentration used for the test may have been too low to show complete growth inhibition.

4.3.4 Tube-dilution method of antifungal testing (DMF as solvent for metal complexes)

The tube dilution method could not be used for studying antifungal activity, as a homogeneous suspension of *Aspergillus niger* was difficult to attain for accurate absorbance readings, despite the fact that the fungus was grown on a rotary shaker at 200 rpm. The heterogeneous nature of the fungal growth therefore resulted in substituting the originally planned PowerWave^{TM} XS Microplate spectrophotometric method of analysis of the fungal growth with the more traditional method of obtaining the dry mass (mg) of cell material from the fungal growth. The latter involved isolation, drying and analytical weighing of the microorganism (*Aspergillus niger*) from the tubes that were originally prepared and incubated for the tube dilution method. The results are reported in Table 4:10.

Table 4:10: Dry mass (mg) of cell material as a measure of antifungal (*A. niger*) activity

"Sample" name	**Number of replicates**	**Mass (mg) of *A. niger***
Water	3	20
DMF	3	17
Fluzol^{TM}IV infusion	4	24
$CuCl_2.2H_2O$	4	46
$CoCl_2.6H_2O$	4	25
2-OH-*o*VANPN	3	18
Complex **(A1)**	2	11
Complex **(A3)**	3	12
Complex **(A4)**	4	8
Complex **(B1)**	4	12
Complex **(B2)**	3	8
Complex **(B3)**	3	16
Complex **(B4)**	4	24
Complex **(C2)**	2	12
Complex **(C3)**	4	20

From these results, the ligand and most of the metal complexes gave lower weights than the control, which imply antifungal activity. The results may be misleading due to the low masses recorded because low masses are associated with large weighing errors. The control (Fluzol^{IV} infusion) was found to be inactive against this particular strain of *Aspergillus niger* used or against the spores (spores are generally highly protected from the environment they are in), and therefore the results can not be properly reported without a positive control. Due to the uncertainties and problems outlined above, the agar infusion method was next attempted for antifungal testing of the samples.

4.3.5 Agar-infusion method of antifungal testing (DMF as solvent for metal complexes)

The average radial growth (mm) of *Aspergillus niger*, which is the average of x and y values on the marked grid for each replicate set of sample/ blank/ control, is represented in Table 4:11. The following metal complexes were omitted from this antifungal test because of a lack of sufficient sample to carry out the test: **(A3)** and **(B1)**. $CuCl_2.2H_2O$ was not included in this method of antifungal testing because it already proved inactive against *Aspergillus niger* when a large mass (Table 4:10) of *Aspergillus niger* grew in its presence.

Table 4:11 Average radial growth (mm) of *Aspergillus niger* recorded daily

	Average radial growth (mm)											
	1	2	4	5	6	7	8	10	11	12	13	14
Day	Control	Fluzol™	Benomyl	DMF	2-OH-*o*VANPN	$CoCl_2.6H_2O$	**(A1)**	**(A4)**	**(B2)**	**(B3)**	**(C2)**	**(C3)**
0	0	0	0	0	0	0	0	0	0	0	0	0
1	8.5	4.5	1.9	3.3	0	11.7	4.6	3.5	3.5	1.3	3	3.7
2	32.5	16.6	2.1	3.9	0	24.7	9.8	5.8	3.7	1.7	4.4	5.3
3	40.2	23	2.1	3.9	0	31.8	16.4	8.4	4	2.9	5.8	6.2
4	48.8	26.7	2.1	5.6	0	48.3	25.8	16.3	5.5	4.7	8.6	9.8
5	58.3	28.9	2.1	7.6	0	56.3	29.4	20.3	6.8	5.3	10.1	11.7

The data in Table 4:11 was used to plot graphs (Figure 4.10) of "Average radial growth (mm)" versus "day number" for each sample, blank, and control tested in the agar-infusion method of antifungal testing against *Aspergillus niger*.

Figure 4.11 Growth rate of *Aspergillus niger*

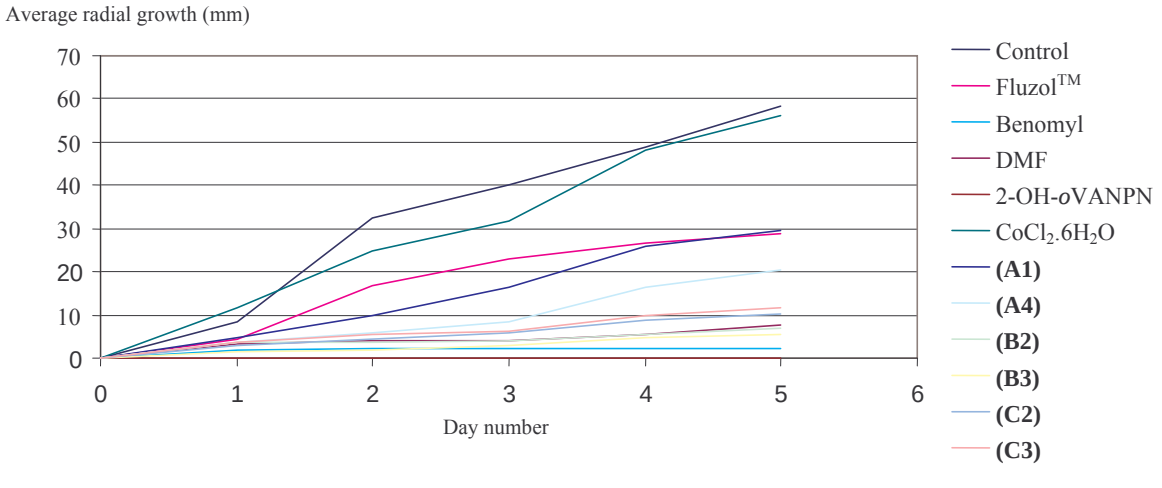

From the above figure (Figure 4.11):-

- All the samples tested, except for the first day in the case of $CoCl_2$, show lower growth rate of *Aspergillus niger* when compared to the control, which contained only nutrient agar and *Aspergillus niger*.
- The ligand, 2-OH-*o*VANPN, lowered the growth rate of the fungus more than all the samples tested and also more than the positive control, benomyl. The structural nature of the ligand must be extremely suitable for the morphology of this fungal species (***A. niger***) in terms of the mechanism of antifungal activity involved. The remarkable antifungal activity probably involves the free OH groups as well as the imine groups (Tümer *et al*., 2007).
- Complexes **(A1)** and **(A4)** lowered the growth rate of the fungus more than DMF, but less than the ligand; hence, implying a positive antifungal result.
- Complexes **(B2)** and **(B3)** lowered the growth rate of the fungus more than DMF, but less than the ligand; hence, implying a positive antifungal result.
- Complexes **(C2)** and **(C3)** lowered the growth rate of the fungus less than the ligand.
- Activity of the synthesized metal complexes is limited to the theory of chelation (Tweedy, 1964) as well as the presence of the imine groups because there are no free hydroxyl groups present on the aromatic ring structure. The apparent lowering of growth rate may have been enhanced by DMF, which is the solvent used to dissolve the sample in order for the dissolved sample to fuse into the nutrient agar. While several of the Schiff base complexes were more effective against *Aspergillus niger* than Fluzol, none proved as effective as the ligand, which had even higher (or equal) activity than Benomyl. Benomyl, an antifungal agent that is no longer used for human antifungal treatment because of toxicity problems, gave zero growth rate – the initial apparent growth for day 1 was most probably due to spreading of the agar that formed part of the inoculum, which was placed at the centre of each replicate plate on day 0.

4.4 CONCLUSIONS

4.4.1 DPPH radical scavenging assay

The ligand, 2-OH-*o*VANPN, as well as the ligand precursor, *o*-vanillin, in the present work was found to have antioxidant (DPPH free radical scavenging) properties. *o*-Vanillin is reported to have suppressed the mutagenesis effects of UV irradiation on *Escherichia coli* (Takahashi *et al*., 1990). When tested on *Escherichia coli*, *o*-vanillin had no genotoxic effect on the DNA of this microorganism (Mikulasova and Bohovicova, 2000). In section 4.3.1, possible hydrolysis of the metal complexes to release the active ligand was given to explain the DPPH antioxidant activity (Table 4:5) of two of the Cu(II) complexes and the Co(III) complexes, **(C2)** and **(C3)**, in the present work.

The positive DPPH radical scavenging results for most of the Co(II) complexes in the present work is in accordance with the literature reports that complexes of *N*,*N*'-bis(salicylidene)ethylenediamine with Co^{2+}, which are similar to Co(II) complexes in the present work, are catalysts for autooxidation of NADH and cytochrome C (Vol'pin *et al*., 1981) and that Co(II) complexes of *N*-alkylsalicyladimine ligands, which are similar to the ligand in the present work, are active for the oxidation of phenol (van Wyk *et al*., 2008).

4.4.2 Antimicrobial testing

The results of the antimicrobial tests employed in the present work are conveniently summarized in Table 4:12. For some microorganisms (*E. coli*, *C. albicans* and *A. niger*) listed in Tables 4:11 and 4:12, the ligand has higher antimicrobial activity than the metal complexes. This remarkable activity of the ligand may arise from the free hydroxyl group(s), which may play an important role in the antimicrobial activity, as well as the presence of the imine group(s) which is vital in elucidating the mechanism of transformation reactions in biological systems (Tümer *et al*., 2007). Tümer and co-workers reported that ligands with two free hydroxyl groups have higher antibacterial

activity than those with only one hydroxyl group (Tümer *et al*., 2007). A similar study showed that having a methoxy group in addition to the free hydroxyl causes an increase in antimicrobial activity.

Table 4:12 A summary of positive results for all the antimicrobial tests employed in the present work

Disk-plate				Tube-dilution				Agar-infusion
E. coli	*Ps. aeruginosa.*	*S. aureus*	*C. albicans*	*E. coli*	*Ps. aeruginosa.*	*S.aureus*	*C. albicans*	*A. niger*
2-OH-*o*VANPN	-	-	2-OH-*o*VANPN	2-OH-*o*VANPN	-	-	2-OH-*o*VANPN	2-OH-*o*VANPN
-	-	-	**(A1)**	-	-	-	**(A1)**	-
(A3)	**(A3)**	-	**(A3)**	-	-	-	**(A3)**	-
-	-	**(A4)**	-	-	-	Not tested	-	-
-	-	-	-	-	-	-	**(B1)**	-
(B2)	-	-	**(B2)**	-	-	-	-	**(B2)**
-	-	-	**(B3)**	-	**(B3)**	-	-	**(B3)**
-	-	-	-	-	**(C2)**	-	-	**(C2)**
-	-	**(C3)**	**(C3)**	-	-	**(C3)**	**(C3)**	**(C3)**

The results in Table 4:12 indicate that complexes **(A3)**, **(B3)** and **(C2)** show activity against the Gram-negative ***Ps. aeruginosa*** and that the ligand, 2-OH-*o*VANPN, does not have any activity. The same trend (Table 4:12) was observed with 2-OH-*o*VANPN, complex **(A4)** and complex **(C3)** against the Gram-positive ***S. aureus***. For activity (Table 4:9) against ***E. coli*** and ***C. albicans*** some complexes show more activity than the ligand (Table 4:9). There is an observed trend here that the metal complexes are more active (toxic) than the corresponding ligand. This trend can be explained by Tweedy's chelation theory (Tweedy, 1964; Karvembu *et al*., 2002 and Tümer *et al*., 2007), which results in permeation of the metal complex through the lipid layer of the microorganism cell membrane. Having entered the microorganism cell, the metal complex or ligand (if hydrolyzed and dissociated from the metal complex) can now bring about a cytotoxic effect, which may ultimately result in stunting cell replication or destruction of the microbial cell. The two Co(II) complexes, **(B2)** and **(B3)**, in the agar-infusion method of antifungal testing (Table 4:12) is in line with literature reports (Vol'pin and Novodarova, 1992) that Co(II) complexes have high antifungal activity. The Cu(II) complexes, **(A1)**

and **(A3)**, were active against *C. albicans* and **(A3)** was active against *E. coli*. This is also in accordance with reports (Golcu *et al*., 2005) that Cu(II) salicylaldimine complexes were found to be active against bacterial species and *Candida* species other than *E. coli* and *C. albicans*.

Since there is no literature available on antimicrobial activities of the ligand (2-OH-*o*VANPN) (or similar compounds) and very little literature available on the metal complexes (or similar compounds) tested in the present work, not much comparison can be made between the antimicrobial results (Table 4:12) in the present work and those found in the literature. Therefore, a brief comparison will be given of the three antimicrobial methods employed in the present work in terms of solvent-, diffusion- and concentrations effects.

Solvent effects:- When comparing the results (Table 4:6) of the disk-plate method when DMF was not the solvent with those (Table 4:7) where DMF was the solvent, positive results are more pronounced when DMF was used as the solvent for the ligand and the metal complexes. The possible effect of DMF is even more enhanced when Sartorius membrane filters, which was thicker and more absorbent, was used instead of Whatman filter paper. This indicates that the solvent plays an important role in these tests, possibly by influencing the integrity of the outer membrane of the microorganism (cell) under consideration and thereby allowing the ligand or the metal complex to enter the microorganism (cell), where it may affect cell constituents (e.g. enzymes involved in the synthesis of proteins or nucleic acids) (Britannica 17, 1990, p517).

Diffusion effect and concentration effect:- The activity of the Schiff base ligand and its corresponding metal complexes increased as the concentration increased because it is a well known fact that concentration plays a vital role in increasing the degree of microbial inhibition. When comparing the results (Table 4:6 and Table 4:7) of the two disk-plate methods, 4.2.2.1.1 with 4.2.2.1.2, it is obvious that there is a concentration effect on antimicrobial activity. Sample concentrations were higher (5- or 10mg. mL^{-1}) in section 4.2.2.1.2 than in 4.2.2.1.1 (1.5 $mg.mL^{-1}$).

More metal complexes were observed to have antimicrobial activity using the disk-plate method when compared to the tube-dilution method (refer to table 4:12). The differences in results for these two methods are due to both a diffusion effect and a concentration effect. During the disk-plate method, the sample-soaked disk (filter/ filter paper) is brought into direct contact with the replicating microorganism on the solid growth medium such that as the sample diffuses (diffusion effect) from the point of application of the disk, the concentration (concentration effect) of sample decreases and therefore the antimicrobial action decreases. During the tube-dilution method, which involves the replicating microorganism and sample solution being diluted (concentration effect) with 3 mL of nutrient broth, the microorganism is not in direct contact with the sample so that the sample has to diffuse (diffusion effect) through the liquid medium to the microorganism where it may bring about antimicrobial action. The effect of diffusion and concentration on antimicrobial activity for these two methods clearly shows in the results displayed in Table 4:12.

Possible hydrolysis of the Schiff base ligand:- As with the DPPH radical scavenging test, positive antimicrobial results for any particular metal complex in Table 4:12 could be attributed to possible hydrolysis of the metal complex to release the Schiff base ligand (2-OH-*o*VANPN), which was found to be highly active in these antimicrobial tests.

Shortcoming in terms of testing the Schiff base ligand precursors:- A major shortcoming with the antibacterial testing in the present work is that the Schiff base ligand precursors, *o*-vanillin and 1,3-diaminopropanol, were not included as test samples as these precursors could easily have been hydrolysis products of the ligand (2-OH-*o*VANPN) in the present work. It would have been interesting to see the outcome of antimicrobial tests for these precursors.

4.5 FUTURE WORK

Based upon the DPPH radical scavenging test results (Table 4:12) in the present work, 2-OH-*o*VANPN and complexes **(A1)**, **(B1)**, **(B2)** and **(B3)** are candidates for cell line testing at the National Cancer Institute (NCI).

The positive antimicrobial results obtained for all the complexes, except for complex **(A2)** and **(B4)** warrant further investigations into potential use as antimicrobial drugs.

The Schiff base precursors, *o*-vanillin and 1,3-diaminopropan-2-ol, should be included as test samples in antimicrobial tests in future work. Wherever DMF, on its own, showed antimicrobial activity, the antimicrobial test should be repeated with another solvent for the metal complexes. Such a solvent should demonstrate no antimicrobial activity towards the microorganisms being employed in such tests.

4.6 REFERENCES

1. Alcamo, I.E. *Fundamentals of Microbiology*. fourth edition. **1994**. The Benjamin/Cummings Publishing Company. Redwood City. 66, 81, 90, 111, 112, 162, 296, 308, 352, 354, 427, 514, 729, 752 and 801.
2. Anderson, J.E.; Goetz, C.M. and McLaughlin, J.L. *Phytochemical Analysis*. **1991**. 2. 107-111.
3. Andrews, J.M. *Journal of Antimicrobial Chemotherapy*. **2001**. 48. 43-7.
4. Behra-Miellet, J.; Calvet, L.; Mory, L.; Muller, C.; Chomarat, M.; Bezian, M.C.; Bland, S.; Juvenin, M.E.; Fosse, T.; Goldstein, F.; Jaulhac, B. and Dubreuil, L. *Anaerobe*. **2003**. 9. 105-11.
5. Benomyl. http://www.speclab.com/ Accessed 2005.
6. Bergenholtz, K.P. and Nielsen, P.V. *Journal of Food Science*. **2006**. 67. 2745-9.
7. Blois, M.S. *Nature*. **1958**. 181. 1199-200.

8. Cavin, A.; Potterat, O.; Wolfender, J-L.; Hostettmann, K. and Dyatmyko, W. *Journal of Natural Products*. **1998**. 61. 1497-1501.
9. Chunhua, C.; Zishen, W. and Zhenhuan, Y. *Synthesis and Reactivity in Inorganic and Metal-Organic Chemistry*. **1993**. 23. 1725-33.
10. Cimanga, K.; Kambu, K.; Tona, L.; Apers, S.; De Bruyne, T.; Hermans, N.; Totte, J., Pieters, L. and Vlietinck, A.J. *Journal of Ethnopharmacology*. **2002**. 79. 213-20.
11. Coyle, B.; McCann, M.; Kavanagh, K.; Devereux, M.; McKee, V.; Kayal, N.; Egan, D.; Deegan, C. and Finn, G.J. *Journal of Inorganic Chemistry*. **2004**. 98. 1361-1366.
12. Dairam, A.; Limson, J.L.; Watkins, G.M.; Antunes, E. and Daya, S. *Journal of Agriculture and Food Chemistry*. **2007**. 55. 1039-44.
13. Daniel, S.; Limson, J.L.; Dairam, A.; Watkins, G.M. and Daya, S. *Journal of Inorganic Biochemistry*. **2004**. 98. 266-75.
14. Daniel, V.P.; Murukan, B.; Kumari, B.S. and Mohanan, K. *Spectrochimica Acta Part A: Molecular and Biomolecular Spectroscopy*. **2008**. 70. 403-10.
15. Dollery, C. *Therapeutic Drugs*. Boobis, A.R.; Burley, D.; Davies, D.M. and Harrison, P.I. (Eds.). Churchill Livingstone. **1991**. A117.
16. Fisch, K.M.; Böhm, V.; Wright, A.D. and König, G.M. *Journal of Natural Products*. **2003**. 66. 968-975.
17. Furones, M.D. *Aquaculture*. **2001**. 196. 1-8.
18. Golcu, A.; Tumer, M.; Demirelli, H. and Wheatley, R.A. *Inorganica Chimica Acta*. **2005**. 358. 1785-97.
19. Goldman, G.H.; da Silva Ferreira, M.E.; dos Reis Marques, E.; Savoldi, M.; Perlin, D.; Park, S.; Martinez, P.C.G.; Goldman, H.S. and Colombo, A.L. *Diagnostic Microbiology and Infectious Disease*. **2004**, 50, 25-32.
20. Gülgür, A.K.; Oya, B.D. and Rahmiye, E. *Turkish Journal of Chemistry*. **2003**. 27. 461-5.
21. Guo, Z. and Sadler, P.J. "*Medicinal Inorganic Chemistry*" In: *Advances in Inorganic Chemistry*. **2000**. Sykes, A.G. (ed.). Academic Press. New York. 183-303.

22. Hay, A-E.; Aumond, M-C.; Mallet, S.; Dumontet, V.; Lituadon, M.; Rondeau, D. and Richomme, P. *Journal of Natural Products*. **2004**. 67. 707-9.
23. Hodnett, E.M. and Dunn, W.J., III. *Journal of Medicinal Chemistry*. **1970**. 13. 768-70.
24. Horn, H.J. *Biometrics*. **1956**. 12. 311-22.
25. Karvembu, R. and Natarajan, K. *Polyhedron*. **2002**. 21. 1721-7.
26. Kitajima, N.; Whang, K.; Moro-oka, Y.; Uchida, A. and Sasada, Y. *J. Chem. Soc. Chem. Comm*. **1986**. 20. 1504-5.
27. Lambert, D.M. and Gallez, B. *Journal of Labelled Compounds and Radiopharmaceuticals*. **1996**. 38. 873-953.
28. Menozzi, G., Merello, L., Fossa, P., Schenone, S., Ranise, A., Mosti, L., Bondavilli, F., Loddo, R., Murgioni, C., Mascia,V., La Colla, P. and Tamburini, E. *Bioorganic & Medicinal Chemistry*. **2004**. 12. 1-31.
29. Meyer, B.N.; Ferrigni, N.R.; Putnam, J.E.; Jacobsen, L.B.; Nichols, D.E. and McLaughlin, J.L. *Journal of Medicinal Plant Research*. **1982**. 45. 31-34.
30. Mikulasova, M.; Bohovicova, I. *Biologia, Bratislava*. **2000**. 55. 229-34.
31. Mohr, J.; Johnson, M.; Cooper, T.; Lewis, J.S. and Ostrosky-Zeichner, L. *Pharmacotherapy*. **2008**. 28. 614-45.
32. Mota, M. de A.; Campos, A.K. and Araújo, J.V. *Brazilian Journal of Microbiology*. **2003**. 34. 157-60.
33. Nallasamy, D.; Periasamy, V. and Karuppannan, W. *Transition Metal Chemistry*. **2001**. 26. 105-9.
34. Özalp-Yaman, Ş; Veli T. Kasumov, V.T. and Önal, A.M. *Polyhedron*. **2005**. 24. 1821-8.
35. Osinsky, S.P.; Levitin, T.; Bubnovskaya, L.; Sigan, A.; Ganusevich, I.; Michailenko, V. and Kovelskaya, T. *6th Internet World Congress for Biomedical Sciences*. **2000**. Inabis Poster #3.
36. Ottino, P. and Duncan, J.R. *Nutrition Research*. **1997**. 17. 661-676.
37. Parejo, I.; Codina, C.; Petrakis, C. and Kefalas, P. *Journal of Pharmacological and Toxicological Methods*. **2000**. 44. 507-12.

38. Parfitt, K. *Martindale: The Complete Drug Reference*. 32nd edition. **1999**. Pharmaceutical Press. U.K. 378.
39. Pelczar, M.J.; Chan, E.C.S. and Krieg, N.R. *Microbiology: Concept and Applications*. **1993**. McGraw-Hill Inc. USA. 578-9.
40. Reddy, P.A.N.; Santra, B.K.; Nethaji, M. and Chakravarty, A.R. *Journal of Inorganic Biochemistry*. **2004**. 98. 377-86.
41. Shivankar, V.S.; Vaidya, R.B.; Dharwadkar, S.R. and Thakkar, N.V. *Synthesis and reactivity in inorganic and metal-organic chemistry.* **2003**. 33. 1597-622.
42. Smith, M.D. and Navilliat, P.L. *Journal of Microbiological Methods*. **1997**. 28. 21-4.
43. Solis, P.N.; Wright, C.W.; Anderson,M.M.; Gupta, M.P. and Phillipson, J.D. *Planta Medical*. **1993**. 59. 120-122.
44. Stanier, R.Y.; Ingraham, J.L.; Wheelis, M.L. and Painter, P.R. *General Microbiology*. Fifth edition. **1987**. Magmillan Education Ltd. London. 186-7.
45. Takahashi, K.; Sekiguchi, M. and Kawazoe, Y. *Mutation Research*. **1990**. 230. 127-34.
46. *The New Encyclopaedia. Britannica*. 15th Edition. **1990**. Encyclopaedia Britannica, Inc., Chicago, Robert P. Gwinn, R.P. (Chairman), Board of Directors:- Norton, P.B.(President); Goetz, P.W. (Editor in Chief): Britannica 17. 517-7.
47. Tümer, M.; Ferhan, D.E. and Bulut, A. *Spectrochimica Acta Part A: Molecular and Biomolecular Spectroscopy*. **2007**. 37. 916-29.
48. Tweedy, B.G. *Phytophatology*. **1964**. 55. 910.
49. van Wyk, J.L.; Mapolie, S.F.; Lennartson, A.; Hakansson, M. and Jagner, S. *Inorganica Chimica Acta*. **2008**. 361. 2094-100.
50. Vlaches, V.; Critchley, A.T. and von Holy, A. *Microbios*. **1996**. 88. 115-23.
51. Vol'pin, M.E.; Novodarova, G.N. and Kolosova, E.M. *Inorganica Chimica Acta*. **1981**. 50. 21-3.
52. Vol'pin, M.E. and Novodarova, G.N. *Journal of Molecular Catalysis*. **1992**. 74.
53. Yam, T.S.; Shah, S. and Hamilton-Miller, J.M.T. *FEMS microbiology letters*. **1997**. 152. 169-74.